MINISTÉRIO DA EDUCAÇÃO
UNIVERSIDADE FEDERAL DO RIO GRANDE DO SUL
ESCOLA DE ENGENHARIA
PROGRAMA DE PÓS-GRADUAÇÃO EM ENGENHARIA DE MINAS, METALÚRGICA
E DE MATERIAIS

MODIFICAÇÃO DE ESTRUTURAS DE CARBONO COM LÍQUIDOS IÔNICOS
IMIDAZÓLIOS PARA COMPÓSITOS MULTIFUNCIONAIS MELHORADOS DE
EPÓXI

BILAL GHAFOOR

Tese para a obtenção do título de Doutor em Engenharia

Porto Alegre

2023

MINISTRY OF EDUCATION
FEDERAL UNIVERSITY OF RIO GRANDE DO SUL
SCHOOL OF ENGINEERING
GRADUATE PROGRAM IN MINING, METALLURGICAL AND MATERIALS
ENGINEERING

MODIFICATION OF CARBON STRUCTURES WITH IMIDAZOLIUM IONIC LIQUIDS FOR ENHANCED MULTIFUNCTIONAL EPOXY COMPOSITES

BILAL GHAFOOR

This work has been carried out at the Department of Materials of the School of Engineering at UFRGS, within the Graduate Program of Mining, Metallurgical and Materials Engineering – PPGE3M as partial requirement for obtaining the title of Doctor of Engineering.

Area of Specialization: **Materials Science and Engineering**

Porto Alegre

2023

This thesis was examined and analyzed adequately for obtaining the title of Doctor of Engineering, in the area of Science and Technology of Materials, and approved in its final form by the Supervisor, Co-supervisor and by the Examining Committee designated by the Graduate Program of Mining, Metallurgical and Materials Engineering Department at the Federal University of Rio Grande do Sul.

Supervisor: **Prof. Dr. Sandro Campos Amico (PPGE3M)**

Co-supervisor: **Prof. Dr. Henri Stephan Schrekker (Institute of Chemistry)**

Examination Committee:

_____

Dr. Bluma Guenther Soares – Universidade Federal do Rio de Janeiro (UFRJ)

_____

Dr.-Ing. Christina Scheffler – Leibniz-Institut für Polymerforschung Dresden

_____

Dr. Raquel Santos Mauler – Universidade Federal do Rio Grande do Sul (UFRGS)

RESEARCH ARTICLES IN INTERNATIONAL JOURNALS

RESEARCH ARTICLE I:

B Ghafoor, HS Schrekker, J Morais, SC Amico, *Surface modification of carbon fiber with imidazolium ionic liquids,* **Composite Interfaces**, p. 915, 2022.
https://doi.org/10.1080/09276440.2022.2029310

RESEARCH ARTICLE II:

B Ghafoor, HS Schrekker, SC Amico, *Multifunctional Characteristics of Carbon Fibers Modified with Imidazolium Ionic Liquids*, **Molecules**, v. 27, p. 7001, 2022.
https://doi.org/10.3390/molecules27207001

RESEARCH ARTICLE III:

B Ghafoor, U Farooq, HS Schrekker, SC Amico, *Thermomechanical properties of imidazolium ionic liquid-modified MWCNT/Carbon fiber/Epoxy hybrid composite laminates*, **Journal of Composite Materials**, v. 0, p. 1, 2023.
https://doi.org/10.1177/00219983231170304

ABSTRACTS IN CONFERENCE PROCEEDINGS

B Ghafoor, HS Schrekker, SC Amico, Spectroscopic Analysis of carbon fiber modified with imidazolium ionic liquids, In: 5th Brazilian Conference on Composite Materials (BCCM), Virtual Conference, 2021.

B Ghafoor, HS Schrekker, SC Amico, Imidazolium ionic liquid for the surface modification of unfinished carbon fiber, In: 6th Brazilian Conference on Composite Materials (BCCM), Tiradentes, Minas Gerais, 2022.

"and that each person will only have what they endeavored towards"

—   Al-Quran-53:39

ACKNOWLEDGEMENTS

RESUMO

A interface em sistemas compósitos de matriz e fibra é um componente chave que influencia suas propriedades e desempenho geral, e a superfície da fibra de carbono (FC) é apolar e leva à incompatibilidade com matrizes epóxidas. Os estudos foram realizados para modificar a superfície de FC com líquidos iônicos (LI) à base de imidazólio. A estratégia foi adotada considerando a superfície de FC recicladas, que são disponibilizadas na forma de fibras sem agentes de acoplamento em sua superfície. Anteriormente, a modificação em geral criava defeitos e introduzia grupos funcionais (-OH, -COOH, -NH, etc.). Nesta pesquisa, a superfície de FC e nanotubos de carbono de paredes múltiplas (MWCNT) foram modificadas com LI. A química estrutural inerente de estruturas baseadas em carbono fornece interação π com a nuvem eletrônica deslocalizada do cátion imidazólio do LI que é utilizado para a modificação. No primeiro estudo, a FC (T300) foi modificada pela aplicação de 10% (p/v) de dois tipos diferentes de LI imidazólio, bis(trifluorometilsulfonil)imida de 1-butil-3-metil imidazólio (hidrofóbico) e cloreto de 1-butil-3-metilimidazólio (hidrofílico). Espectroscopia de infravermelho com transformada de Fourier, espectroscopia Raman, espectroscopia de fotoelétrons de raios-X e microscopia eletrônica de varredura confirmaram a presença de LI na superfície de FC. A molhabilidade de FC tratada com resina epóxi (DGEBA) aumentou significativamente, com uma diminuição do ângulo de contato maior que 15°. A resistência ao cisalhamento interfacial entre a FC modificada e a epóxi aumentou em até 56,5% em relação à FC, sendo comparável às fibras com agentes de acoplamento tradicionais. O segundo estudo focou na otimização da concentração de LI, bis(trifluorometilsulfonil)imida de 1-butil-3-metilimidazólio, cloreto de 1-butil-3-metilimidazólio e cloreto de 1-(2-hidroxietil)-3-metilimidazólio, para tratar a FC e analisar as características multifuncionais. O ângulo de contato para 1% (m/v) de FC tratada com LI e epóxi DGEBA diminuiu em até 35%, acompanhado por um aumento de 91% na resistência ao cisalhamento interfacial e diminuição na resistividade elétrica de 77%. Essas melhorias foram alcançadas com o LI hidroxifuncionalizado, mostrando a sintonização das propriedades de FC por meio do substituinte *N*-imidazólio. No terceiro estudo, NCPM tratados com 1% em peso ou 5% em peso de LI (cloreto de 1-(2-hidroxietil)-3-metilimidazólio) foram aplicados como dispersão em proporções de 0,2 a 2% em massa e de 1 a 3% em massa na matriz epóxi, respectivamente, para obter laminados compósitos híbridos baseados em FC. O laminado híbrido contendo 1% em massa de NCPM modificado com 1% em peso de LI apresentou excelentes propriedades mecânicas e termomecânicas com aumento de 210% e 151% na resistência à flexão e módulo, e apresentou um aumento de 101, 116 e 29% do módulo de armazenamento, módulo de perda e amortecimento, respectivamente. As micrografias eletrônicas de transmissão e varredura mostraram a dispersão e a estrutura de NCPM aprimoradas no compósito com baixa porcentagem de LI, justificando suas propriedades mecânicas aprimoradas. Este estudo demonstrou que a aplicação de uma baixa quantidade de LI disperso é uma abordagem promissora para preparar compósitos híbridos NCPM/CF/epóxi com propriedades aprimoradas. Esta abordagem não-covalente de modificação de estruturas à base de carbono com LI é uma maneira promissora de produzir compósitos de alto desempenho com características multifuncionais.

Palavras-chave: Fibra de carbono, líquido iônico imidazólio, resistência ao cisalhamento interfacial, compósito híbrido, nanotubos de carbono de paredes múltiplas.

ABSTRACT

Interface in fiber-matrix composite systems is a key component influencing the bulk properties and overall performance of composites. Carbon fiber (CF) surface is non-polar in nature and it indicates an incompatible behavior with epoxy matrices. The present research studies were designed to modify the CF surface with imidazolium ionic liquids (IL). The strategy was adopted considering the surface of recycled CF, which are available as fibers without sizing on their surface. Previously, the modification was in general carried out by creating defects, and introducing functional groups (-OH, -COOH, -NH, etc.) at the expense of the inherent surface properties, but in this case has been applied without deteriorating its surface or chemical properties. In this research, CF and multi-walled carbon nanotube (MWCNT) surfaces were modified with IL. An inherent structural chemistry of carbon-based structures allows π-interaction with the delocalized electronic cloud of imidazolium IL cations, which is utilized for the modification. In the first study, CF (T300) was modified by applying 10% w/v of two different imidazolium IL, 1-butyl-3-methylimidazolium bis(trifluoromethylsulfonyl)imide (hydrophobic) and 1-butyl-3-methylimidazolium chloride (hydrophilic). Fourier-transform infrared spectroscopy, Raman spectroscopy, X-ray photoelectron spectroscopy, and scanning electron microscopy confirmed the presence of IL at CF surface. Wettability of the treated CF with epoxy resin significantly increased, with a decrease in contact angle greater than 15°. Interfacial shear strength between the modified CF and epoxy increased up to 56.5% with respect to the unsized CF, being comparable with epoxy sized fibers. The second study was dedicated to optimizing the weight percentage of IL, 1-butyl-3-methylimidazolium bis(trifluoromethylsulfonyl)imide, 1-butyl-3-methylimidazolium chloride, and 1-(2-hydroxyethyl)-3-methylimidazolium chloride, to treat the CF and analyze multifunctional characteristics. The contact angle of optimized 1% w/v IL-treated CF and DGEBA epoxy decreased by up to 35%, accompanied by an increase of 91% in interfacial shear strength and decrease in electrical resistivity of 77%. These enhancements were achieved with the hydroxy-functionalized IL, showing the tunability of CF properties through the *N*-imidazolium substituent. In the third study, MWCNT treated with either 1 wt% or 5 wt% of IL were incorporated as filler in content ranges of 0.2 to 2 wt% and 1 to 3 wt% in epoxy matrix, respectively, to form hybrid composites based on CF. Hybrid composites containing 1 wt% of MWCNT modified with 1 wt% of IL showed excellent mechanical and thermomechanical properties with an increase of 210% and 151% in flexural strength and modulus, and an increase of 101, 116 and 29% in storage modulus, loss modulus and damping, respectively. Transmission and scanning electron micrographs showed the composite enhanced MWCNT dispersion and network at low content of IL, justifying its improved mechanical properties. This study demonstrated that the application of low amount of IL dispersant is a promising approach to prepare MWCNT/CF/epoxy hybrid composites with enhanced properties. This non-covalent approach of modifying carbon-based structures with IL is a promising way to produce high performance composites with multifunctional characteristics.

Keywords: Carbon fiber, imidazolium ionic liquid, interfacial shear strength, hybrid composites, multi-walled carbon nanotubes.

LIST OF FIGURES

LIST OF TABLES

LIST OF ABBREVIATIONS AND SYMBOLS

Abbreviations

CE	Circular economy
CF	Carbon fiber
rCF	Recycled carbon fiber
CVD	Chemical vapor deposition
DGEBA	Diglycidyl ether of bisphenol-A
CFRP	Carbon fiber reinforced polymer composites
CFRC	Carbon fiber reinforced composites
HCFC	Hybrid carbon fiber composites
DMA	Dynamic mechanical analysis
EPD	Electrophoretic deposition
IFSS	Interfacial shear strength
ILSS	interlaminar shear strength
IL	Ionic liquid
MWCNT	Multi-walled carbon nanotubes
SWCNT	Single-walled carbon nanotubes
FTIR	Fourier-transform infrared spectroscopy
NMR	Nuclear magnetic resonance spectroscopy
SEM	Scanning electron microscopy
EDS	Energy-dispersive X-ray spectroscopy
TGA	Thermogravimetric analysis
TLM	Transfer length method
XPS	X-ray photoelectron spectroscopy
XRD	X-ray diffraction

Symbols

$C_2OHMImCl$	1-(2-Hydroxyethyl)-3-methylimidazolium chloride
C_4MImCl	1-Butyl-3-methylimidazolium chloride

$C_4MImNTf_2$	1-Butyl-3-methylimidazolium bis(trifluoromethylsulfonyl)imide
D	Diameter of fiber
d_{fb}	Diameter of fiber bundle
l_e	Length of fiber bundle
E_b	Binding energy
F_{max}	Maximum pullout force
K	Scherrer constant
L_a	Crystallite size in the fiber lateral direction
L_c	Crystallite size in the fiber axial direction
R_c	Contact resistance
S_g	Geometric surface area
T_g	Glass transition temperature
K_d	Adsorption coefficient
ρ_{el}	Electrical resistivity

Greek letters

β	Full width at half maximum
Θ	Bragg's angle
λ	Wavelength
ρ	Fiber density

SUMMARY

1 INTRODUCTION

Carbon fiber (CF) is a high-performance material used in polymer matrices to produce structural and functional composites [1]. These composites are used in various industries like aerospace, defense, sports and leisure, energy, automotive and marine, and have excellent mechanical, thermal, electrical, dynamic-mechanical and chemical properties. The individual components (reinforcement, matrix) and the interface between them determine the properties of CF-epoxy composites. The interfacial bonding strength between CF and epoxy is determined by the type and strength of the chemical bonds formed at the interface [2]. Surface treatment of CF significantly affects the adhesion strength with epoxy by promoting bonding between the fiber and the matrix. Also, the good wetting properties are important to coat the surface of the CF. Poor wetting can result in voids and weak bonding at the interface. The viscosity of the resin can also affect the wetting properties and the ability to fill the gaps among CF. A high cross-linking density of epoxy at the interface region can enhance the chemical bonding between CF and epoxy resin, result in a higher adhesion strength [3].

Multi-walled carbon nanotube (MWCNT) are used as a reinforcing filler in polymer composites due to their exceptional mechanical, electrical, and thermal properties [4]. The adhesion strength of MWCNT depends on the interaction between the surface of MWCNT and the polymer matrix. The dispersion and adhesion quality can affect the mechanical and electrical properties of polymer composites [5]. Poor dispersion can lead to agglomeration of MWCNT, resulting in weak points in the composite structure. Therefore, it is essential to achieve a uniform dispersion of MWCNT in the polymer matrix. Adhesion and dispersion characteristics of the MWCNT can be improved either by functionalization or by using surfactants or dispersing agents. Dispersing agents are molecules that can adsorb on the surface of MWCNT and reduce surface tension between MWCNT and the polymer matrix, improving the wetting properties and dispersion of MWCNT in the polymer [6].

Various methods are used for the surface modification and functionalization of carbon-based structures such as CF and MWCNT, which can be classified as either chemical or physical methods. Chemical methods include acidic treatment using HNO_3, H_2O_2, H_2SO_4 [7], grafting, and electrochemical treatment [8]. Physical methods include plasma treatment [9], gamma irradiation, and plasma treatment [10]. In these methods, the surface of carbon-based structure is altered due

to etching or the formation of functional groups on the surface, which can decrease the inherent strength of the structure, but can increase its compatibility with the polymer matrix [3]. The final strength of the composite depends on the net contribution of both effects. Increasing the roughness of the fiber increases the surface area, and the presence of reactive functional groups promotes stronger chemical bonding. However, these treatments are multi-step procedures, sometimes requiring costly instruments, and strict reaction conditions. Therefore, it is crucial to optimize the treatment procedure to achieve maximum enhancement in strength and desired functional properties of the final composite.

Ionic liquids (IL) have become increasingly important due to their potential for a wide range of applications. Imidazolium-based IL can be applied to modify carbon-based structures, including CF and MWCNT, and their chemical structure allows for strong interactions via secondary bonds. In the case of CF, IL can act as a compatibilizing agent for polymer-based CF composites, providing a balanced interaction with the polymer matrix. For MWCNT, IL can improve compatibility and dispersion characteristics in an epoxy matrix, reducing self-agglomeration. A non-covalent modification approach using π-π interactions can improve the interfacial characteristics of CF and MWCNT in epoxy matrices. The imidazolium cations in the IL can interact with the epoxy groups of the diglycidyl ether of bisphenol-A (DGEBA) resin through hydrogen bonding while anion in the IL can interact through electrostatic interactions leading to improved curing behavior, mechanical properties, and thermal stability of the epoxy resin [11]. This technique can also be applied to produce hybrid composites using IL-modified MWCNT and CF, increasing interfacial area and providing more strength to the composite in the epoxy-dominant region of the composite system. Improved dispersion of MWCNT in this case can delay laminate cracking and delamination, improving resistance to crack growth in CF polymer composites [12].

One of the sustainable development goals defined by the United Nations Member States is to ensure sustainable development and production patterns, with a focus on the use of recycled materials as related to sustainability. Waste is one of the major contributors to climate problems, and finding practical waste management solutions is crucial. This study also addresses this issue by developing a versatile and non-damaging method to modify the surface of recycled CF. Recycled CF has the same chemical structure as virgin CF, but the removal of sizing from its surface during the recycling process limits its compatibility with epoxy matrix. A nondestructive

and efficient modification method can enable successful reuse of recycled CF with improved strength.

Imidazolium-based IL have shown potential in the modification of carbon-based structures with several benefits. First, it improves the surface conductivity of the fiber, making it useful for smart structures [13]. Second, it enhances the interfacial shear strength of the composite, which is an essential property for structural composites [14]. For instance, 1-butyl-3-methylimidazolium chloride IL, in combination with amine functional groups, has been applied to CF, enhancing the interfacial adhesion between the fiber and the matrix [14]. Another study applied 1-ethyl-3-methylimidazolium bis(trifluoromethylsulfonyl)imide on CF using microwave irradiation, producing covalent bonds with IL. In this case, IL was grafted on the CF surface by dipping in IL under microwave irradiation, showing excellent compatibility with the epoxy resin with no apparent effect on the inherent fiber properties [15]. Previously, imidazolium-based IL were applied for the surface modification of CF, which improved interfacial adhesion with epoxy matrix and was comparable to the effect of commercial sizing. The studies were limited to a specific weight percentage of IL as well as type of imidazolium-based IL. This motivated to fill this gap and further explore the IL's potential taking leverage of its chemical structure. Similarly, several studies have reported on modifying multi-walled carbon nanotubes (MWCNT) with imidazolium-based IL for improved dispersion. This non-destructive strategy can be further extended to modify MWCNT for improving dispersion in epoxy and producing CF-based hybrid composites [16, 17].

Based on previous studies, the hypothesis of the present research is to improve the interfacial performance of epoxy-based CF composites by modifying the surface of unfinished CF and MWCNT using imidazolium-based IL. Three different IL were applied to modify CF without sizing: 1-butyl-3-methyl imidazolium bis(trifluoromethylsulfonyl)imide (hydrophobic), 1-butyl-3-methylimidazolium chloride (hydrophilic), and 1-(2-hydroxyethyl)-3-methylimidazolium chloride (hydrophilic). In all cases, the anion (Cl, NTf$_2$) provided interaction with carbon-based structures, while the primary interaction occurred through the imidazolium cation of IL. Study 1 aimed to apply the IL, 1-butyl-3-methyl imidazolium bis(trifluoromethylsulfonyl)imide and 1-butyl-3-methylimidazolium chloride in percentage (10 wt%) considering the previously used in literature. Study 2 expanded the work by considering more factors, such as a lower content of IL and the polar functional group of the alkyl chain of the imidazolium ring. Three IL were used: 1-butyl-3-methyl imidazolium bis(trifluoromethylsulfonyl)imide (hydrophobic), 1-butyl-3-

methylimidazolium chloride (hydrophilic), and 1-(2-hydroxyethyl)-3-methylimidazolium chloride (hydrophilic). The study also analyzed the electrical conductivity and stability of IL on CF surfaces. In Study 3, IL-modified MWCNT were applied in the manufacturing of CF epoxy hybrid composites, and their effect on the overall composite properties was analyzed. 1-butyl-3-methylimidazolium chloride (hydrophilic) at two percentages (1 wt% and 5 wt%) was used to modify MWCNT. **Figure 1** provides a summary of the overall study, giving an abstract overview.
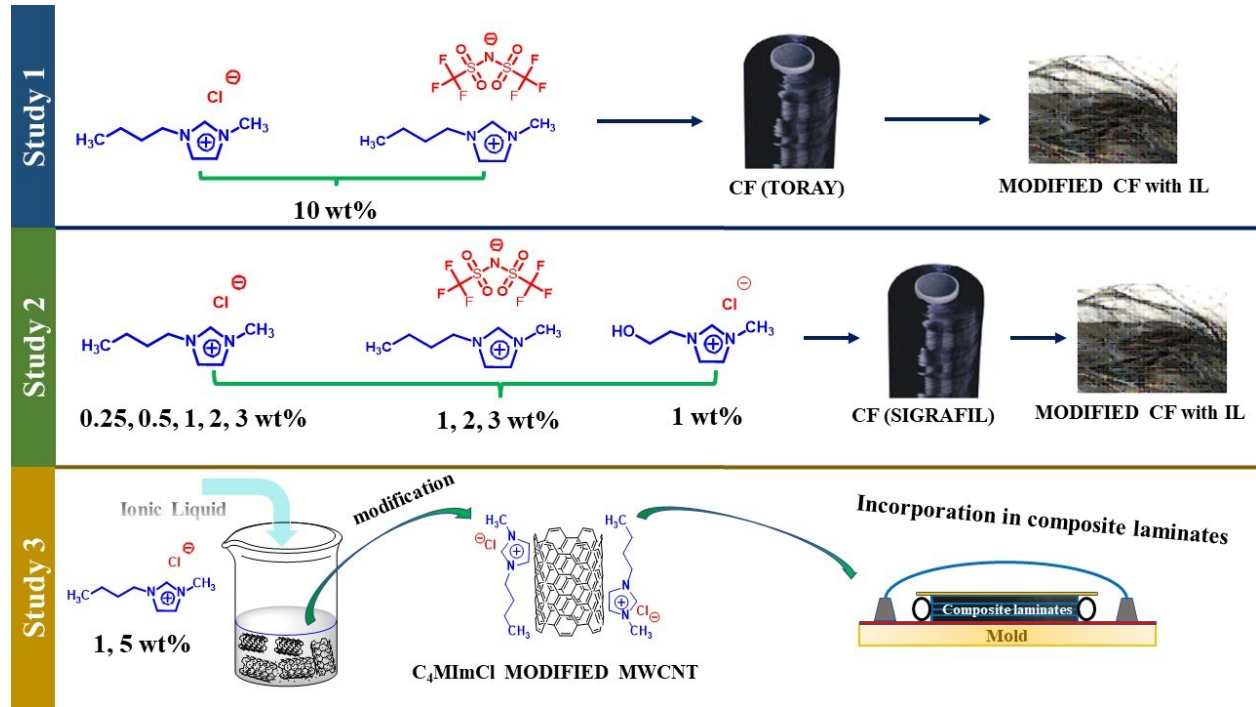

Figure 1 – Overview of the pursued research strategies.

2   OBJECTIVES

To modify the surface of unfinished CF (emulating recycled CF) and MWCNT with imidazolium-based IL to improve interfacial performance of epoxy-based CF composites via non-destructive functionalization.

The specific objectives are to:

- Establish the potential of IL 1-butyl-3-methyl imidazolium bis(trifluoromethylsulfonyl)imide (hydrophobic), 1-butyl-3-methylimidazolium chloride (hydrophilic) and 1-(2-hydroxyethyl)-3-methylimidazolium chloride (hydrophilic) to improve the interfacial shear strength with epoxy resin.
- Determine the optimum w/v concentration of IL for the treatment of unfinished CF.
- Investigate the improvement in interfacial shear strength of CF epoxy.
- Study the effect of IL on the electrical properties of CF surface.
- Examine the dispersion of MWCNT modified with imidazolium-based IL in epoxy matrix.
- Investigate the mechanical and thermomechanical properties of IL-modified MWCNT hybrid composites.

3 LITERATURE REVIEW

3.1 CARBON FIBERS

Carbon fiber (CF) typically contains over 92 wt% carbon, with around 7% nitrogen and 1% oxygen exhibiting excellent thermal, mechanical, and electrical properties. Polyacrylonitrile (PAN) is the most commonly used precursor for commercial CF synthesis, but the conversion process from PAN to CF is only around 50% efficient. Both the precursor and conversion process influence the final properties of CF. Moreover, the microstructure of CF is influenced by the precursor characteristics and processing conditions [18].

CF is produced in the form of fabric, tow, or random distribution after manufacturing. A single tow of commercial CF can contain thousands of fibers (12K, 24K, 50K), with fiber diameters typically ranging from ~5-10 μm. CF obtained directly after the manufacturing process has inert surface characteristics, and its final properties are more dependent on crystallinity, molecular orientation, and carbon content. CF is categorized into three types based on heat treatment: type I (graphitization temperature at or above 2000 °C), type II (graphitization temperature at 1500 °C), and type III (graphitization temperature at 1000 °C) [19]. The strength and modulus of CF depend on the graphitization temperature, with type I CF being high modulus fibers and type III CF being high strength fibers. PAN-based CF typically has a tensile modulus ranging from 200 to 350 GPa, tensile strength ranging from 3-7 GPa, compressive strength up to 3 GPa, electrical conductivity less than 10^5 S/m, and thermal conductivity less than 14 W/mK. The modulus of PAN-based CF can be further improved to 500-600 GPa by graphitization at temperatures above 2000 °C [20].

3.1.1 PROPERTIES

The microstructure of CF depends on the precursor and processing conditions used to manufacture the fiber, as discussed above. The quality of CF can be defined by the size and orientation of graphite crystals, interlayer stacking of graphite layers, microvoids, and other defects. Various models in the literature explain the characteristic microstructure of CF and its relationship with the precursor and end properties [21]. One model proposes that CF has graphite

layers aligned parallel to the fiber direction but stacked randomly in the transverse direction. In the transverse direction, microdomains separated by microvoids, while in the longitudinal direction, regions are separated by zones of extensive bending and twisting of the basal layers. The relationship between the orientation of graphite crystallites, crystal size (L_a), and stack size (L_c) in PAN suggests that crystallites closer to the fiber axis have larger L_c. TEM studies show the existence of a wrinkled ribbon structure in PAN-based CF, and a 3-D model was proposed to demonstrate the microdomains. In high-strength PAN-based CF, there are interlayer links between the graphite sheets and amorphous carbon. In high-modulus PAN-based CF, the stacking of graphitic sheets is in high order and oriented along the fiber axis [20].

CF are composed of layers of carbon atoms that are arranged in a hexagonal pattern resembling graphite, as illustrated in **Figure 2**. The planar structure of CF can be either turbostratic, graphitic or a hybrid of both, depending on the precursor used during synthesis. When the crystalline structure is graphitic, the layer planes are stacked parallel to each other in a regular fashion. The atoms in each plane are arranged parallel to each other and covalently bonded through sp^2 bonding, while the interaction between the sheets is relatively weak van der Waals forces [22]. However, the fundamental structural unit of many CF comprises a stack of layers with a turbostratic structure. In this case, the parallel graphene sheets are stacked in an irregular manner, folded, tilted, or split. Studies have indicated that the presence of sp^3 bonding and irregular stacking can increase d-spacing to 0.344 nm. Van der Waals forces are present in the transverse plane direction, as shown in **Figure 2a**. The PAN precursor generally promotes the formation of a turbostratic structure in CF, making it the most crucial factor in determining the end properties [20].

CF with graphitic crystallites and turbostratically layered basal planes exhibit non-polar characteristics. The strong covalent bonding between carbon atoms in CF results in high mechanical strength and modulus along the longitudinal axis of the fiber. However, achieving very high strength and modulus simultaneously is difficult. Typically, increasing the carbonization temperature enhances the degree of crystallinity of the graphitic-type layers, leading to increased modulus [23]. However, higher crystallinity also increases the sensitivity of the fibers to flaws, which can decrease the strength of the material. The high-strength PAN-based CF types have interlayer links between graphite sheets and amorphous carbon, which results in a suitable microstructure among the graphite crystallites to form connections among the graphite sheets and

crystallites. This allows all the graphite structure to be active upon applied stress on the CF. Conversely, in high-modulus PAN-based CF type, the graphite sheets stack in high order and are oriented along the fiber axis, reducing deformation upon applied stress on the CF. During stabilization, carbonization, and graphitization of PAN precursor fibers, the oxygen, nitrogen, and hydrogen atoms are excluded, which typically results in voids in the resulting CF [18].
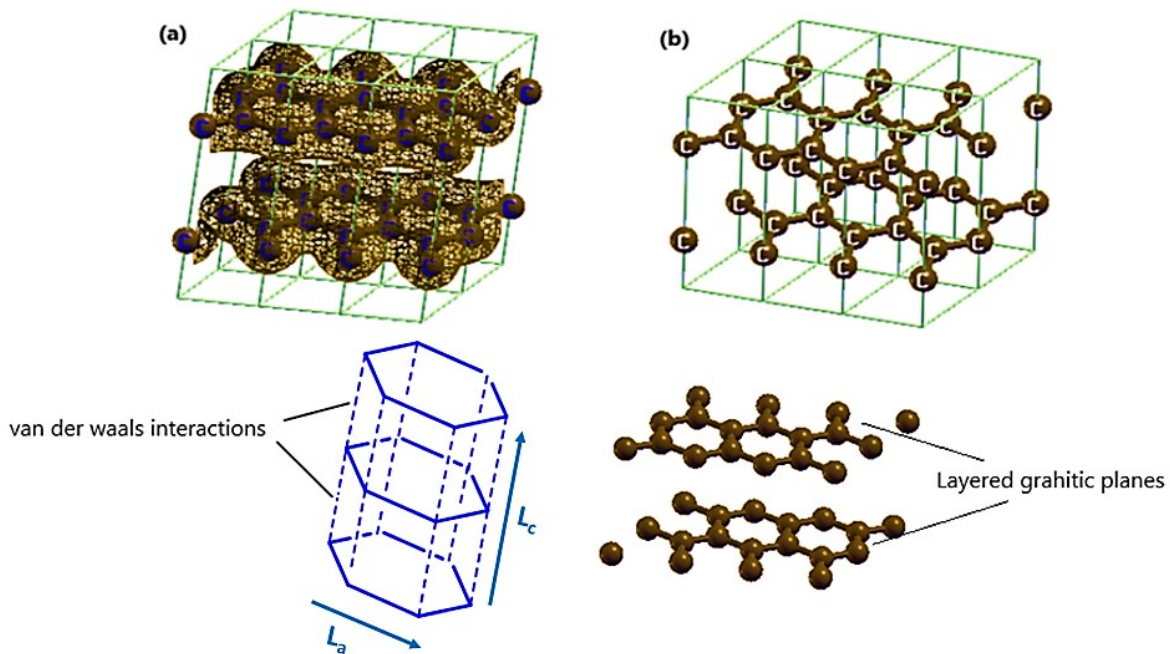

Figure 2 - Representation of building blocks of CF: (a) molecular surface, (b) unit cell.

CF possesses a distinctive black or dark grey color and is often sought after for its aesthetic appeal as well as its functional properties. Its density typically falls within the range of 1.7-2.0 g/cm^3, making it an excellent material for weight-sensitive applications. Its high strength-to-weight ratio and stiffness provide resistance to bending and deformation under loading. The high modulus of CF is attributable to its highly crystalline plane with covalent bonds oriented in the fiber direction, whereas strength primarily depends on the crystallinity and the presence of defects in the structure. Due to weak van der Waals forces between graphene layers and its fibrillar structure, CF exhibits low compressive strength [19]. CF has a low thermal conductivity, making it an excellent insulator that can reduce heat transfer in certain applications. Its coefficient of thermal expansion is -1 × 10^{-6}/K in the axial direction and 10 × 10^{-6}/K in the radial direction due to the highly crystalline arrangement in the fiber direction, making it suitable for use in extreme thermal

circumstances. This low coefficient of thermal expansion also makes it a suitable material for applications where dimensional stability is critical. While the electrical conductivity of CF is good, it cannot match metals such as copper or aluminum. However, the small diameter of CF imparts specific characteristics, with a large surface area that could enhance surface reactivity. Moreover, it has good corrosion resistance, making it an excellent material for use in marine or other corrosive environments [23].

3.1.2   LIFE CYCLE

The life cycle analysis assesses the environmental impact of CF throughout its entire lifespan. In accordance with the United Nations policies, adopting a life cycle approach that prioritizes resource efficiency and environmental waste management is crucial. Therefore, evaluating the sustainability of CF has a significant impact on the concept of a circular economy (CE). The CE concept pertains to wastes that are recycled and converted into resources, either through a technological feedback mechanism or a natural ecosystem feedback mechanism, with a focus on maintaining a constant stock of resources or increasing it over time [24].

CE has gained increased attention in recent years as a means to advance efficiently towards sustainable consumption and production patterns and contribute to achieving sustainable development goals. Coherent application in the development, adoption, and implementation of CE is necessary to progress more effectively and efficiently towards environmental sustainability [25].

Ensuring the continued utilization of resources is crucial for maximizing their utility. This objective can be attained through recycling, which can occur either within the economy via interlinked industrial sectors, or through natural ecosystem processes. This may necessitate extending the lifespan of products to minimize the need for recycling waste activities. Although recycling CF using mechanical, chemical, or thermal methods demands significant capital investment, a high recovery rate of fibers from composite waste helps to reduce its environmental impact [26].

A comprehensive analysis of recycling methods serves as the foundation for life cycle assessment methods such as cradle-to-grave and cradle-to-cradle analysis. To assess the life cycle of CF, three critical indicators of life cycle assessment are human toxicity, global warming potential, and acidification. The global warming potential indicator is used to measure the direct impact of associated environmental change and recycling costs [27].

The scientific community and composite industry have started incorporating recycling techniques to recover fibers, and government policies are encouraging the adoption of a life-cycle approach for waste fibers through recycling. The most sustainable way to manage the accumulating composite waste is by recycling fibers as an alternative to virgin fibers and reusing them in the form of composite materials [26]. The recycling and reuse of CF not only mitigates the waste of CF composites but also provides a fiber raw material that can be utilized in the production of new composite products [28].

There are two types of CF waste: one is produced at the end of a component's life cycle, while the other is produced during the manufacturing of composites, accounting for around 40% of all CF waste. In both cases, recycled CF has a different apparent structure; it is typically shorter in length and has different mechanical properties compared to virgin CF. Closed-loop recycling processes can enable efficient usage of recycled CF in the future. The concept of the circular economy ensures the reuse of CF at the end of its life cycle by recycling composites, as shown in **Figure 3**. The production of CF requires a high amount of energy, while obtaining recycled CF requires only 10-30% of the total energy required for virgin CF (which ranges from 198-595 MJ/kg) [24, 26].

The surface characteristics of recycled CF are distinct from those of virgin CF whereas the chemical structure of the recycled CF is same as that of virgin CF. The fibrillar structure of the fiber is difficult to observe and there may be binder residues on the surface of the virgin fiber. The recycled CF has a smoother surface and a specific orientation to the fiber axis, unlike virgin CF. Raman studies indicate a decrease in the I_D/I_G ratio, which suggests an increase in the degree of graphitization of the CF. Surface oxidation and sizing also affect the surface characteristics. During recycling, the surface functional groups on the oxidized CF decompose and create surface defects on the fiber, which can reduce its tensile strength [29, 30]. Furthermore, the recycled CF may have a defective surface without sizing, which can cause weak interaction between fiber and matrix, leading to fiber pull-out and composite delamination. Improving the fiber-matrix adhesion is critical to establishing strong interactions and efficient load transfer through the interface [31].

Figure 3 - Circular economy implementation by recycling loop for CF.

3.2 CARBON FIBER-MATRIX COMPOSITES

3.2.1 INTERFACE

The combination of the physical and chemical properties of the fiber and matrix produces mechanical properties that cannot be achieved individually. Due to the difference in their chemical nature, an interface appears between them. The interface is a boundary region between the two materials that occupies only a few atomic layers. Due to the presence of different components at the interface, its properties differ significantly from those of the bulk materials. This interface region is crucial in maintaining the bond and transferring the load from the matrix to the fiber. Therefore, the study of the interface as a critical component is a major focus of interest in composites. However, understanding the interface is not easy due to its unique composition and properties, which are mainly governed by the chemical/morphological nature and physical/thermodynamic compatibility between the components. Considerable work has been done regarding the influence of the interface on the fracture mechanics characteristics of composites. Thus, there is a need to understand the structure-property relationship at the interface

region. The qualitative design of the interface can be accomplished by using various chemical-physical and thermodynamic-mechanical principles [32, 33].

Interface has unique physical and mechanical properties different from those of fiber and matrix. The contact surface combined with the near-region of finite volume is termed as interphase (**Figure 4**). The chemical, physical, and mechanical properties vary either continuous or in stepwise manner between those of bulk fiber and matrix [34]. In other words, the interphase exists from some point on the fiber through the actual interface into the matrix, embracing all the volume altered during fabrication process from the original fiber and matrix material. Interfacial area in composite material is a design parameter determined by the geometric surface area of the fiber. The equation for calculating the geometric surface area S_g is given as:

$$S_g = 4\,\rho^{-1}\,D^{-1} \tag{1}$$

where ρ and D are the fiber density and diameter, respectively. The rugosity factor of CF can be calculated by the ratio of specific surface area and the geometric area which generally lies between 1 to 50 [32].

Carbon exists in various forms, such as coke, char, carbon black, synthetic graphite, glassy carbon, fibers, and filaments, and they all contain more than 90% carbon. These materials have a common basic lamellar structure consisting of polycondensed hexagonal rings. The surface of these materials inherently contains various defects such as vacancies, dislocations, edges, and steps, which create "prismatic planes" or the "active surface area." To study the surface characteristics of carbon, two approaches are considered. The first approach is based on the principles of solid-state chemistry, which considers carbon to have a crystalline ordering. The second approach is based on surface organic groups, which explain the surface properties of carbon as a less-ordered structure. In the solid-state chemistry approach, the defects in the aromatic basal planes are considered an "active site" of the carbon surface. The carbon atoms located at grain boundaries are more reactive than those at basal planes. The active surface area of CF depends on its structural properties and thermal history. The approach of organic surface groups depends on the nature and functionality of oxygen complexes chemisorbed on carbon atom edges, in addition to other atoms such as hydrogen, nitrogen, and sulfur. PAN-based CF contains nitrogen, which

forms nitrile groups on the surface and contributes to its surface properties through bipolar interactions [35].
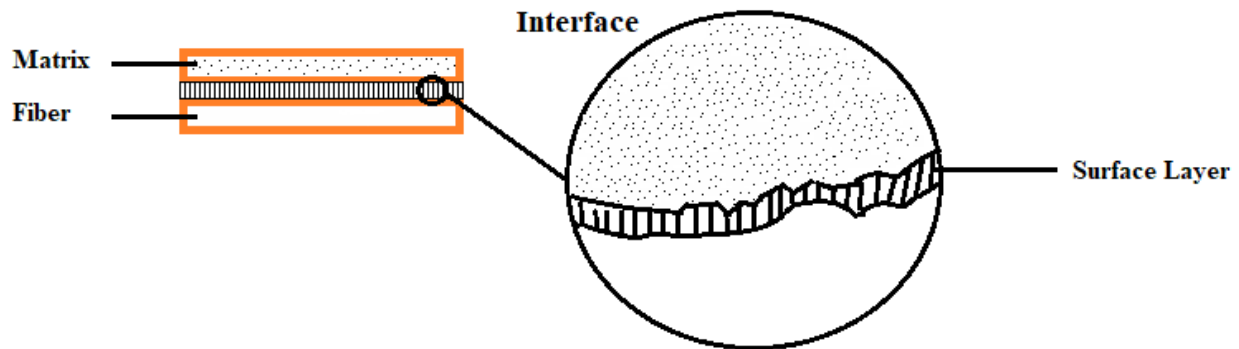

Figure 4 - Components of three-dimensional interphase.

The surface structure of CF plays a vital role in its wetting behavior with the polymer matrix, and consequently, its adhesion. In a fiber-matrix composite system, the degree of adhesion at the interface is crucial for the mechanical behavior, owing to the presence of physical or secondary interactions such as van der Waals attractions. This interaction can be categorized as physical interaction due to mechanical interlocking and the chemical bonding interaction. Increase in the physical interaction due to mechanical interlocking can be achieved by increasing the roughness of the CF surface [36]. The increase in roughness on the CF surface increases the surfaces available for bonding between the fiber and the epoxy. However, a high increase in the surface roughness of the fiber can create stress concentration areas leading to the premature failure of the composite. In case of CF composite, high roughness can lead to localized stresses at the fiber-matrix interface, resulting in the formation of micro-cracks or delamination. This can possibly weaken the composite material and reduce the overall mechanical properties of composite. Therefore, an optimum level of roughness to avoid stress concentration and premature failure of the composite materials is always essential. Moreover, increase in the roughness increase the surface area that leads to a stronger interfacial adhesion, resulting to an improved load transfer between the fiber and the matrix. Improved interfacial adhesion can reduce the probability of interfacial debonding or delamination, leading to a more reliable and durable composite material. However, a very high roughness of CF can lead to poor wetting characteristic of the fiber by the epoxy that can form voids between the fiber and the matrix, reducing the contact area between

them [37]. Therefore, it is essential to maintain an optimum level of roughness to ensure proper wetting of the fiber with the matrix. Furthermore, an increase in the roughness of the CF surface enhances the moisture absorption behavior of the composite [38]. Therefore, surface treatments are inevitably applied to CF to modify their surface properties or enhance their surface free energy, alter roughness, thereby achieving suitable wetting and a robust composite system [3].

Surface properties of carbon materials in general and CF in particular are strongly influenced by the presence of functional groups on the surface. It has been observed from experimental studies that basal planes of CF (untreated) have least (~ 0) contribution to the polar component and the total surface energy is only from its dispersive component. Noticeably, the polar component also increases and, in some cases, becomes the major contributing component in the total surface energy of CF. After treatment, its surface energy becomes much higher than epoxy ($\gamma^s = 40$ mJ m^{-2}), which increases wettability. The other factor of importance is the lowering of surface energy due to adsorbed species on the surface [39, 40].

To make an interfacial bond between CF and polymer matrix, the key parameter to consider is the wetting characteristic of CF with matrix. The attraction between fiber and matrix can be understood by the attraction that arises from the quantum-mechanical effect of the valence electrons present in the constituents as a free gas. Wetting of matrix on fiber is followed by bonding which involves short-range interactions of electrons which develops at atomic scale. Thermodynamic work of adhesion of a liquid on a solid can be expressed by Dupre equation:

$$\text{Work of adhesion } (W_A) = \gamma_1 + \gamma_2 - \gamma_{12} \qquad (2)$$

Wetting is dependent on two key factors: contact angle and viscosity. Wetting behavior of the liquid droplet on solid surfaces can be determined by the Young's equation:

$$\gamma_{sv} = \gamma_{sl} + \gamma_{lv} \cos\Theta \qquad (3)$$

Surface free energy between solid and vapor (γ_{sv}), surface free energy between solid and liquid (γ_{sl}) and surface free energy between liquid and vapor γ_{lv} define Θ, the contact angle of liquid-vapor interface as shown in **Figure 5**. For non-wetting surface condition, contact angle is

(> 90º), for wetting (< 90º), and for spreading (~ 0º). Lower contact angle between the liquid and the solid indicates higher wetting of the solid [34, 41].
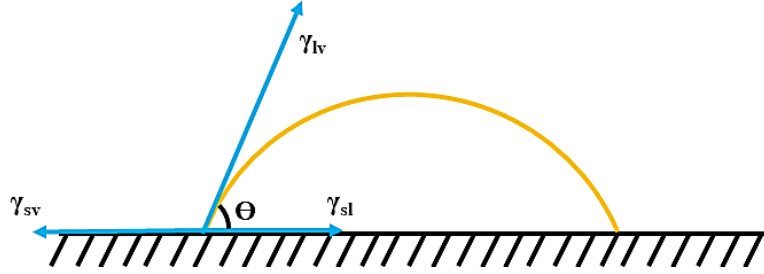

Figure 5 - Contact angle and surface energy of a liquid drop on solid surface [34].

Combining Equation 2 and 3, leads to the Young-Dupre Equation:

$$W_A = \gamma_{lv} (1 + \cos\Theta) \tag{4}$$

With this equation, it can be estimated that the higher work of adhesion determines strong interactions between matrix and fiber. It can be calculated by measuring the surface energy and contact angle. Introduction of spreading pressure, which is the adsorption of vapors in equilibrium, which reduces the surface free energy of the solid as given by:

$$\pi_s = \gamma_s - \gamma_{sv} \tag{5}$$

where subscript s is the hypothetical case of solid in contact in vacuum. To more readily estimate the work of adhesion, Young- Dupree equation can be modified to:

$$W_A = \gamma_{lv} (1 + \cos\Theta) + \pi_s \tag{6}$$

The equation above mainly describes the thermodynamic behavior between fiber and matrix. Practically, the composite system consists of large number of fibers with small diameter fibers and its adhesion with the resin is dependent on the infiltration process and a small gap can arise capillary pressure which can alter the surface energy of the system [38, 42].

Measurement of the contact angle for wettability of fiber surface of the order of 10 μm in diameter requires a sophisticated approach. A simple and direct method of contact angle measurement proposed by Carrol in 1976, called the "droplet aspect ratio method" can be applied to measure the initial contact angle. The liquid droplet on a monofilament (fiber) is assumed to form a symmetrical droplet about its axis as shown in **Figure 6**. Neglecting the effect of gravity, the droplet shape can be defined by the following expression:

$$L = 2[a\, F(\Phi, \kappa) + n\, E\,(\Phi, \kappa)] \tag{7}$$

where $L = \frac{l}{x_1}$, $n = \frac{x_2}{x_1}$, $a = \frac{x_2 \cos\Theta - x_1}{x_2 - x_1 \cos\Theta}$, $\kappa = \sqrt{1 - (a/n)^2}$ and $\Phi = \sin^{-1}\frac{\sqrt{(n^2-1)}}{\sqrt{(n^2-a^2)}}$. $F(\Phi, \kappa)$ and nE (Φ, κ) are the elliptical integrals. Θ can be calculated by measuring the relative dimensions of the droplet, x_1 and x_2.
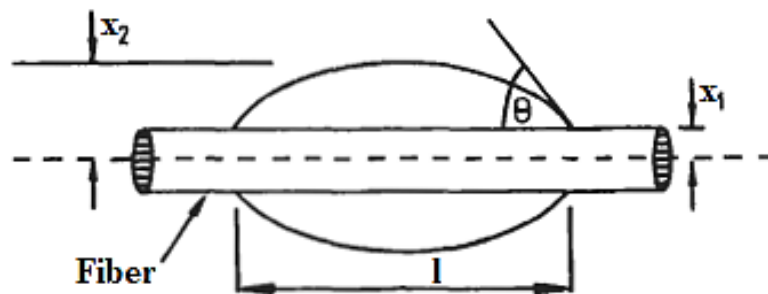

Figure 6 - Epoxy droplet on a cylindrical shape monofilament to measure contact angle [34].

3.2.2 FIBER SURFACE TREATMENTS

Surface treatments can significantly impact the physical, chemical, and morphological properties of the fiber surface. Such modifications result in improved composite properties with enhanced fiber surface area, chemical bonding, and adhesion between the fiber and matrix. Commonly employed surface treatment methods include acid oxidation, plasma treatment, rare earth treatment, and gamma irradiation [21]. These treatments function by removing weak boundary layers, such as contaminant species or gas molecules physically adsorbed onto the fiber surface, entangling the polymer matrix with the molecular network of the polymer coating on the

fiber, increasing interlocking at the fiber-matrix interface through surface roughness, and creating additional active sites to promote chemical bonding with the polymer matrix [43]. Below are some of the detailed treatment methods.

3.2.2.1 OXIDATIVE TREATMENT

Oxidation treatment adds acidic functional groups on CF surface. The effectiveness of treatment in improving the surface properties depends on the concentration of oxidative medium, treatment time and temperature as well as the fiber itself. Generally, oxidation is achieved with gases (by air, oxygen, ozone, etc.) or liquids (by nitric acid, hydrochloric acid, etc.). It has been evidenced that the tensile strength of fiber generally decreases with the oxidation time and that the surface of fibers is pitted and fragmented. The surface area of CF after oxidation increases compared to virgin fibers. Roughness and oxygen concentration increase which enhances adhesion. Oxidation treatment introduces various functional groups (–O–C–, –C=O, –O–C=O) on the CF surface, which increases total surface energy and polarity and thus, enhance the wettability of CF with the polymer matrix [8].

Electrochemical oxidation of CF in ammonium oxalate solution improves adhesion strength in 8.6% and tensile strength in 16.6% due to the removal of weak carbonaceous layer and refinement of graphitic crystallites in the sheath region [8]. CF treated with O_3 introduced carboxyl groups on CF surface which enhanced the interfacial strength by 60% with polyamide 6 matrix [44]. In another study, the oxidative treatment in the presence of H_2SO_4, $KClO_3$ and silane coupling agent improved the interfacial strength by 47.2% with phenolic matrix. It also improved chemical activity at the surface, oxygen content, surface area as well as roughness [45]. A combined oxidative treatment and sizing on CF reduced tensile strength in up to 16%, and increased interfacial shear strength with epoxy matrix in 12.35% [3]. CF oxidized with strong oxidant $K_2S_2O_8$ in the presence of a catalyst $AgNO_3$ introduced carboxyl and hydroxyl functional groups. It preserved the tensile strength and surface morphology, improved oxygen concentration and IFSS with epoxy matrix up to 62.5% [46]. In another study, a maximum of 45% increase in IFSS with polyaryletherketone has been achieved by electrochemical oxidation of CF [47].

3.2.2.2 PLASMA TREATMENT

CF surface treatment is performed in an electrically conducting medium consisting of electrons, positively charged ions and neutral atoms. The purpose of plasma surface treatment of fibers is to modify the chemical and physical structures on their surface, altering fiber matrix adhesion strength. The mechanisms activated by plasma treatment are removal of surface contaminants, enhanced degree of mechanical keying due to surface roughness, increased surface energy, and deposition of functional groups on fiber surface [48]. With oxygen plasma, reactivity between fiber surface and matrix takes place due to the presence of functional groups like COOH, -C-OH and =C=O groups. Microscopy analysis showed striations, micropitting and roughness on the fiber surface which is proportional to surface area with oxygen plasma etching. Active species in the plasma gas aggressively attack the defect rich or the edge carbon site which increases surface area. Increase in the time of plasma treatment increases the amount of oxygen content on CF, and the presence of polar components, etching and deeper crevices on fiber. A small reduction in tensile strength occurs due to plasma treatment and Raman analysis showed a slight distortion in graphitic structure of CF after treatment. CF treated with plasma improved interfacial strength up in 29.7% with polypropylene matrix due to the increase in hydroxyl groups on the fiber surface [49]. He/O_2 atmospheric plasma of carbon fiber increased oxygen-containing functional groups and IFSS with polyimide matrix in up to 21% [50]. Treatment of CF with oxygen plasma introduced oxygen functional groups, increased roughness and enhanced interfacial strength with epoxy up to 21% [51]. CF treated with helium plasma for 1 min improved interfacial strength with epoxy in up to 27.9% [52].

3.2.2.3 GAMMA TREATMENT

Fibers are exposed to high energy gamma irradiation which introduces roughness as well as chemical functional groups such as carbonyl at the fiber surface. It also increases roughness due to radiation. In the presence of nitrate solution, oxygen groups are generated due to gamma irradiation and increased amount of oxygen containing functional groups on fiber surface strengthen the chemical bonding [53]. CF irradiated in oxygen atmosphere and ambient temperature affected the crystal lattice by displacing atoms within the lattice or electronic excitation. The electrons stripped from the atoms believed to cause dimensional change in CF and

create active sites at the surface bounded with functional groups with 69% increase in oxygen content after gamma-ray radiation. Fibers showed the presence of carboxyl group and hydroxyl group and increased ratio carbon/oxygen as confirmed by XPS. Degree of roughness is also increased by lower absorbed dose and Raman spectroscopy confirmed the slight distortion in graphitic structure possibly indicated by the increased I_D/I_G ratio. Gamma treatment improved adhesive wear resistance and the interfacial strength in up to 60% with polyetherimide matrix at absorbed dose of 300 kGy, whereas, tensile strength reduced in 18% [10]. CF treated with gamma irradiation increased the roughness of the fiber surface, the O/C ratio, the amount of oxygen functional groups, as well as interfacial strength with epoxy matrix up to 29.5% at 250 kGy [54]. In another study, gamma irradiation increased the CF modulus due to the increase in graphitization character which also increases density at high radiation doses [53].

3.2.2.4   RARE EARTH TREATMENT

The chemical activity of rare earth elements allows adsorption on the fiber surface and promotes chemical bonding due to increased reactive functional groups. It increases compatibility with the polymer matrix and in turn increases adhesion. A high effective nuclear charge and a strong ability to attract a structure with delocalized electrons of rare earth elements provide a mechanism of modification of CF.   The treatment of CF in alcoholic solution of $LaCl_3$ has shown an increase in surface roughness and surface area with the increased content of –C–OH, –C–O–C–, bridged structure, C=O and –COOR. Also, Raman spectroscopy showed an increase in the disorder structure of CF due to the treatment with rare earth elements. CF treatment with $LaCl_3$ solution improved tensile strength, elongation as well as bending strength of the composite with polytetrafluoroethylene matrix in 16% [55]. Treated CF with alcoholic solution of $LaCl_3$ (0.3 wt%) improved the O/C ratio up to 38.4%, showing an improvement in oxygen concentration [56]. CF treatment with praseodymium nitrate solution, increased roughness and oxygen containing groups and praseodymium element on the surface. An improvement of interfacial adhesion with epoxy matrix in 15.8% was obtained [57]. Another study showed the formation of disorder surface due to rare earth treatment which was confirmed by Raman spectroscopy. CF surface was found rougher and surface crystallinity was reduced. An improvement of 13.1% in interfacial strength with an epoxy matrix has been achieved [58]. Also, 61% increase in interfacial strength has been observed with the treatment of carbon fiber with rare earth salt (YbF_3). The treatment introduced

changes in surface topography of fibers and inclusion of oxygenated functional groups such as ether, carbonyl and carboxyl [59].

3.2.2.5 SOLUTION SIZING

Commercial CF are always coated with a thin film of sizing consisting of a polymer solution or emulsion and assistant components. Generally, 0.5 to 1.5% of the sizing material is applied on the surface of fiber to provide protection from damage, for strand integrity, and to improve adhesion and composite processability. Coupling agent is added in sizing to create covalently bonded oxy-carbonated functional groups at the CF surface that promote chemical interactions with the matrix polymer. Weight average molecular weight of the sizing also influences the interfacial properties, and if it is low, it creates a soft interface region while if it is high, there is lower compatibility with matrix and more susceptibility to fiber/matrix debonding [60].

Commercial sizing is mainly based on bifunctional epoxy resin, usually DGEBA, with other components. In one of the studies, a slight difference is observed for interlaminar shear strength of composites treated with 0.7 wt% of tetraglycidyldiaminodiphenylmethane (TGDDM) and diglycidylether of bis-phenol-A (DGEBA) compared with commercial sized fibers [61]. A modified polyacrylate sizing (added organosilicone and fluoropolymer) caused an improvement of 14.2% in interlaminar shear strength. Sizing applied by aqueous dip coating of vinyl ester resin emulsion synthesized by phase inversion emulsification reduced the surface energy of the fibers and increased ILSS in 20.7% [60]. Latent curing of epoxy sizing based on ethylenediamine with butylacrylate improved ILSS of CF/epoxy composites in 10% with improved interface toughness. The drawback of sizing is that sometimes interdiffusion of fiber sizing and polymer matrix results in a formation of a weak interphase region that limits interfacial strength [39].

3.2.3 EFFECT OF SURFACE TREATMENT ON INTERFACIAL ADHESION

The surface treatment of CF is critical in achieving strong interfacial adhesion with the polymer matrix in composite materials. Adhesion refers to the attraction between different atoms or molecules, while cohesion refers to the attraction between the same type of atoms or molecules.

Strong adhesion at the interface requires more energy to cause separation and can be categorized based on physical, chemical, and/or mechanical bonding processes [62].

While chemical bonding is generally preferred over physical bonding forces, the latter still plays an important role in achieving strong interfacial adhesion between the fiber and polymer matrix in composite materials. To improve physical adhesion, it is essential to create a clean and rough surface, which increases the surface area and enhances wetting and bonding characteristics. Additionally, the surface free energy of the fiber is crucial for achieving good adhesion, as it represents the active available atoms on the surface. Chemical bonding mechanisms, such as covalent, ionic, and in some cases chelation bonding, are also important for achieving strong adhesion. However, the theoretical bond densities in chemical bonding are often quite small and are overshadowed by the contribution of mechanical bonding [2].

Various approaches can be adopted to achieve good adhesion, such as the use of organo-silane coupling agents and creating rough surfaces. Rough surfaces promote mechanical bonding and can be characterized at different levels, including macro-mechanical retention, micro-mechanical retention, and nano-interdigitation [63]. Additionally, nano-interdigitation occurs when adhesive monomers diffuse into existing polymer phases, polymerize, and become molecularly intertwined with existing molecules [10]. Permeability is another parameter that influences adhesion at the interface, and determining parameters such as the permeability coefficient can help predict the contributions of diffusion bonding.

Overall, the surface treatments applied to carbon fiber (CF) surfaces significantly improve the mechanical properties of high-performance polymeric composites. However, controlling the fiber/matrix interfacial properties remains a major task. Sometimes, a 'multi-scale' coating consisting of nano-particles, carbon nanotubes, and graphene modifications is applied to the CF surface using techniques such as electrophoretic deposition (EPD), chemical vapor deposition (CVD), and dip coating. The efficacy of fiber/matrix adhesion at the interface depends on the simultaneous action of various parameters that entail physical adsorption and chemical interaction [21].

Most conventional carbon fiber (CF) treatment methods improve fiber/matrix interfacial strength, but often at the expense of a significant loss in fiber strength. This is because these methods can create pits and flaws on the fiber surface, which act as stress concentration points for

crack initiation and propagation. Therefore, it is essential to balance physical and chemical means of enhancing adhesion to achieve optimal composite properties [64, 65].

3.3   TREATMENT OF CARBON-BASED STRUCTURES WITH IONIC LIQUIDS

Ionic liquids (IL) are a class of compound that consist of ions and exist in liquid state below 100 °C [66]. They have unique physical and chemical properties such as non-toxicity, low vapor pressure, high chemical and thermal stability, and high ionic conductivity, which makes them suitable candidates to develop advanced functional materials. These ILs are very promising also in terms of environmental perspectives [67-69].

IL are basically formed by the combination of cations and anions. In task specific ionic liquids, cations and anions are combined according to the desired properties required for a certain application. The most common cations are: imidazolium, ammonium, pyridinium, pyrrolidinium whereas the anions associated can be any one of Cl^-, $[BF_4]^-$, $[PF_6]^-$, Br^-, or organic-based such as trifluoromethylsulfonate, bis (trifluoromethyl) sulfonyl imide. ILs are being used in a wide range of applications, e.g., electrodes preparation [70-76], energy storage [77], anti-wear and antioxidant [78]. Liquid crystalline properties can also be induced in IL which adds new function and superior properties [79].

3.3.1   TREATMENT OF CARBON FIBERS

The inert nature of CF is made reactive by its modification with an external agent which increases its adhesion with a polymer matrix. Imidazolium-based IL can be applied for the modification of CF where it can provide benefits in several ways. First of all, it will improve the surface conductivity of the fiber which will be beneficial for its application in smart structures [13]. Secondly, it will improve the interfacial shear strength of the composite [14]. With IL treatment, CF chemical structure will not be affected, retaining its tensile strength and modulus. Cation shows stronger attraction when placed above the π-electron-system of carbon materials whereas the anions provide attraction to hydrogenated edges due to electrostatic charge distribution. 1-Butyl-3-methylimidazolium chloride IL applied to CF enhanced the interfacial adhesion between the fiber and the matrix [14]. It is worthwhile to note that coating with only IL

improved the interfacial shear strength up to 106% compared to unmodified CF epoxy composite with the synergistic effect of the surface chemistry and IL with the epoxy matrix (**Figure 7**).

Various other modification methods were also applied with and without functionalization of epoxy sized and unsized CF. And various used imidazolium-based IL with different combination of cations and anions [14]. In one study, 1-ethyl-3-methylimidazolium bis(trifluoromethylsulfonyl)imide has been applied on CF by microwave irradiation forming covalent bonds with IL. IL in this case was grafted on the surface of CF by dipping in IL under microwave irradiation. This functionalization showed an excellent compatibility with the epoxy resin with no apparent effect on the inherent fiber properties. Efficient grafting on the surface of fiber increased the crosslinks with the epoxy matrix. With this modification, 28% increase in interfacial adhesion was achieved compared to untreated CF. It is also expected that Tf_2N which is non-polar in nature has strong attraction with carbon surface [15]. These studies provide a strong basis to apply more ILs with imidazolium cation, different anions (hydrophobic or hydrophilic) and alkyl chains with different functional groups for the modification of CF/recycled CF.
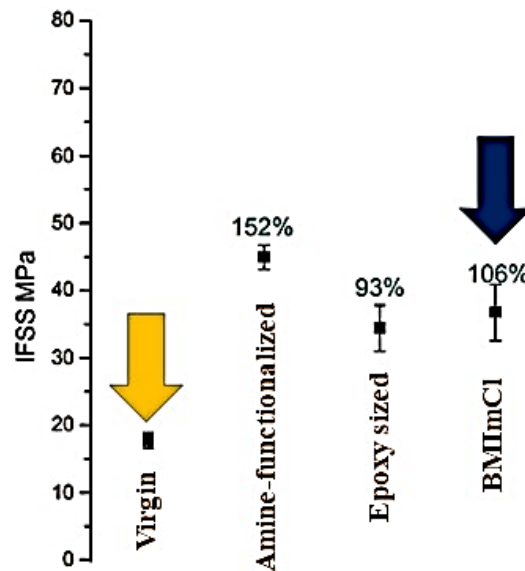

Figure 7 - Interfacial shear strength of CF and treated CF in epoxy resin [14].

3.3.2 TREATMENT OF CARBON-BASED NANOSTRUCTURES

IL can be used for the modification of carbon-based structures in general. The most widely used ILs for that are based on imidazolium cation. Broadly, there are two ways to accomplish that:

(i) covalent bonding in which a primary bond forms between the imidazolium ring and the carbon on the hexagonal structure as shown in **Figure 8**, (ii) attachment of IL with the graphite structure via non-covalent forces such as hydrogen bonding, π–π stacking, electrostatic forces and van der Waals forces. The second way is quite efficient and more practical [80, 81]. In one of the studies [82], graphene was covalently functionalized with 1-butyl-3-aminopropyl imidazolium chloride. The bonding is possible since the structure of graphene has sp^2 – hybridized carbon atom with p-electronic architecture. It has an additional advantage over chemical methods that it avoids the disruption of π-electronic conjugation of CNT [83].

The microscopic interaction between graphene and IL can be explained by short-range interactions involving delocalized electronic cloud of IL cation and carbon nanomaterials and by long-range dispersion interactions. Fedorov and Lynden-Bell have proposed the mechanisms by molecular dynamics simulation of the formation of an interfacial layer between neutral graphene and 1,3-dimethyimidazolium chloride. Vibrational spectroscopy and contact angle measurements suggest a significant interaction of the alkyl chains of the cation with graphene, which are extended parallel to the surface. The imidazolium ring slightly tilted to the surface plane of graphene enabling π–π interactions between imidazolium ring and the surface [72, 84].

The crosslinked IL consisted of the mono cationic IL, 1-vinyl-3-butylimidazolium bis(trifluoromethanesulfonyl)imide as the monomer and the dicationic 1,12-di(3-vinylimidazolium) dodecane bis(trifluoromethanesulfonyl)imide as the IL crosslinker, were also applied for CNT modification to promote covalent bonding. Despite the advantages, the covalent poly IL functionalization of CNT has drawbacks since it is time consuming and the chemical treatment employed can disrupt their π-conjugation, causing destabilization of the structure, change in electrical and mechanical properties, surface defects and CNT shortening [85].
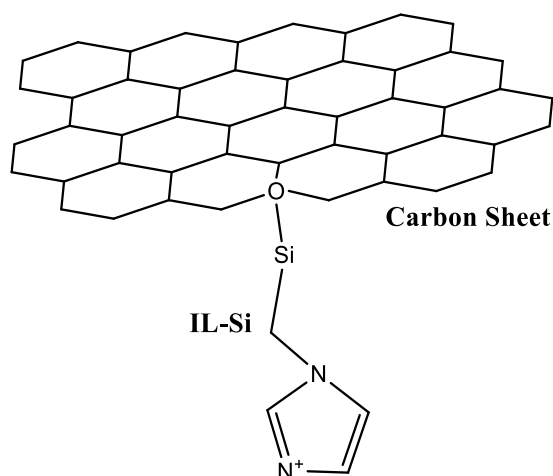
Figure 8 - Possible covalent bond/link of imidazolium IL with CF [86].

The non-covalent functionalization of carbon-based nanostructures (MWCNT, SWCNT, graphene) has been reported for use in various applications. Some of the imidazolium IL with applications from literature are explained below with structures listed in **Table 1**. In one of the studies, 5 to 15 phr of 1-butyl-3-methyl-imidazolium tetrafluoroborate was used for the non-covalent functionalization of MWCNT. MWCNT was then added as filler in epoxy and enhanced dispersion, electrical and thermomechanical properties were achieved. The dispersion was attributed to cation-π interactions between the surface of CNT and the imidazolium ions [87].

An effective strategy to improve conductivity and thermal properties was to incorporate 1-(3-aminopropyl)-3-methylimidazolium bromide and 1-(3-aminopropyl)-2-methyl-3-butylimidazole modified MWCNT in poly(etheretherketone). This system provided good dimensional stability and considerable interfacial interactions [88]. An improvement in dispersion was achieved in styrene-butadiene rubber by applying 1-decyl 3-methyl imidazolium chloride as a coupling agent for MWCNT. The resultant composite showed improved electrical and mechanical properties [89]. 1-Ethyl-3-methylimidazolium tosylate has been applied as a modification agent of MWCNT and resulted in increased viscosity when MWCNT are well-dispersed and the bonding can be disrupted by an increase in temperature to weaken hydrogen and electrostatic interactions [90]. 1-Butyl-3-methyl imidazolium chloride was used for the disentanglement of CNT bundles based on the dispersing and lubricating characteristics of the IL. The high local shear increases the spaces among CNT and the IL adsorption further enlarges the space which lead to separation of CNTs. The adsorption is enhanced due to π-stacking of the

hexagonal structure of carbon atoms on the surface and in case of 1-butyl-3-methyl imidazolium chloride, imidazolium rings having chloride anions, interaction via π-π electron bonding promotes dispersion in epoxy matrix [16].
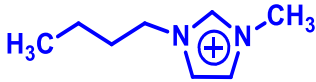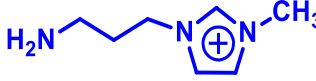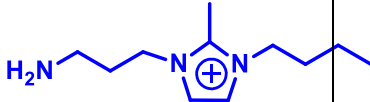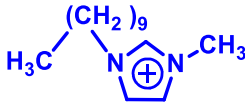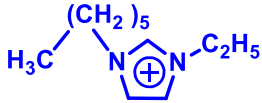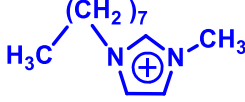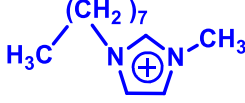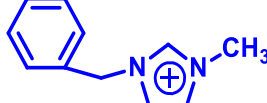
Ionanofluids, a class of heat transfer fluids, have been prepared by dispersing MWCNT in various imidazolium IL. 1-butyl-3-methyl imidazolium bis(trifluoromethanesulfonyl)imide containing MWCNT successfully enhanced thermal conductivity in 26% at 3 wt% content. The interaction between ionic liquids ions and dispersed MWCNT plays an important role for the enhancement of the thermal conductivity of ionanofluids [91]. Amine-terminated IL was applied for the modification of MWCNT incorporated in epoxy to produce thermal management material for high power applications improving thermal conductivity of epoxy in up to ~211% [92]. The 1-hexyl-3-methylimidazolium tetrafluoroborate with different concentration of cation and anion adsorbed on carbon nanotubes was used to improve thermoelectrical properties. The amphoteric doping of carbon nanotubes with imidazolium IL has been done with different CNT surface states. The increased number of anionic surfactants induced negatively charged surfaces, whereas the imidazolium cation induced favorable p-doping to optimize thermoelectric power factors. In this case, a high performance the produced flexible carbon nanotube film thermoelectric generator exhibited enhanced p-type thermoelectric power factor of up to 762 $\mu W\ m^{-1}\ K^{-2}$ [93].
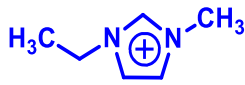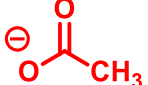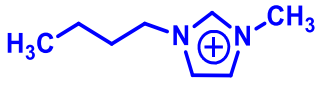
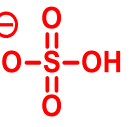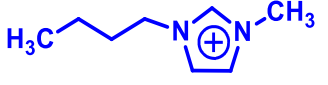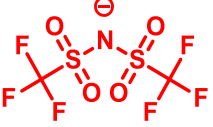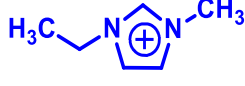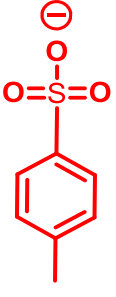Thermoelectric properties of polypropylene-based nanocomposites have been studied for 1-allyl-3-methyl-imidazolium chloride, 1-methyl-3-octylimidazolium tetrafluoroborate, 1-methyl-3-octylimidazolium chloride, and 1-allyl-3-methylimidazolium dicyanamide modified SWCNT. The highest Seebeck coefficients achieved were +49.3 $\mu V/K$ for *p*-type composites and −27.6 $\mu V/K$ for *n*-type composites, and the type of IL is decisive in whether *p*- or *n*-type thermoelectric behavior is achieved [94]. The conductivity and electromagnetic shielding effectiveness can be modulated by improving the dispersion of the conductive fillers. Also, the heterogeneous interface plays an important role in absorbing electromagnetic radiations due to dipoles formation. The addition of 1-benzyl-3-methylimidazolium chloride modified MWCNT in styrene-butadiene rubber exhibited a stable high dielectric constant and AC conductivity in the wide frequency range due to the fine dispersion and the formation of a three-dimensional continuous network of MWCNT in the matrix, improving electromagnetic shielding effectiveness up to 35.06 dB [95].

In biomedical application, 1-ethyl-3-methylimidazolium acetate and 1-butyl-3-methylimidazolium hydrogen sulfate was applied for the modification of MWCNT to make

nanocomposite with polyetheretherketone. An improvement of 37% in elastic modulus of the nanocomposite was achieved with 1 wt% IL modification [96].

Table 1 – Imidazolium-based IL used for the modification of carbon-based nanostructures.

Cation	Anion	Ionic liquid	Ref
	$\ominus$ BF_4	1-butyl-3-methylimidazolium tetrafluoroborate	79
	$\ominus$ Br	1-(3-aminopropyl)-3-methylimidazolium bromide	80,81
	$\ominus$ Br	1-(3-aminopropyl)-2-methyl-3-butylimidazole	80
	$\ominus$ Cl	1-decyl-3-methylimidazolium chloride	82
	$\ominus$ BF_4	1-hexyl-3-ethylimidazolium tetrafluoroborate	83
	$\ominus$ Cl	1-allyl-3-methyl-imidazolium chloride	84
	$\ominus$ BF_4	1-methyl-3-octylimidazolium tetrafluoroborate	84
	$\ominus$ Cl	1-methyl-3-octylimidazolium chloride	84
	$N\equiv C\underset{N}{\overset{\ominus}{\diagup}}C\equiv N$	1-allyl-3-methylimidazolium dicyanamide	84
	$\ominus$ Cl	1-benzyl-3-methylimidazolium chloride	85

		1-ethyl-3-methylimidazolium acetate	86
		1-butyl-3-methylimidazolium hydrogen sulfate	86
		1-butyl-3-methyl imidazolium bis(trifluoromethanesulfonyl)imide	87
		1-ethyl-3-methylimidazolium tosylate	88

3.4   HYBRID COMPOSITES WITH MWCNT

Hybrid composites are a class of composites consisting of three components, such as the introduction of a nanofiller in a CF composite. These laminates are of great interest due to the significant property improvements in the epoxy region of the laminates. Generally, matrix properties dominate composite performance in the thickness direction, and the interlaminar region's performance depends on the epoxy's properties, which may decrease in-plane laminate properties [97].

There are two approaches to producing hybrid composites based on carbon fiber and epoxy. One approach involves depositing a nanofiller on the surface of carbon fiber and then impregnating it with an epoxy matrix. The nanofiller can be deposited on the fiber surface using techniques such as chemical functionalization, electrospray, or chemical vapor deposition. The second approach involves dispersing the nanofiller in the epoxy and then using it to impregnate the carbon fabric. The presence of a third phase contributes to the strength of composites at the interfacial region and provides a more effective load distribution. Additionally, modification of the interfacial behavior

with the nanofiller significantly impacts the mechanical behavior of the composite. A more homogeneous dispersion produces a composite with good mechanical properties in the transverse direction [97]. In case of CNT as a filler, the self-interaction of nanofiller is high due to its chemical structure and high aspect ratio. This gives rise to the problem of dispersion in epoxy and even after mechanical dispersion there is a possibility of re-agglomeration of CNT. This reduces the viable amount of CNT in a composite and also the threshold value for maximum increase in electrical and mechanical properties [4].

Various methods are in practice to disperse CNT and produce hybrid laminates. MWCNT dispersed in epoxy matrix with probe sonication improved 28% interlaminar shear strength by effectively sharing the stress from matrix to the CF [12]. Improvement in toughness and flexural strength has also been achieved by dispersing MWCNT under rotation in ultrasonic treatment at 60°C [98]. The interlaminar shear strength of unidirectional laminates are improved by incorporating plasma treated MWCNT in epoxy which provided better dispersion and distribution, improving the resistance to crack propagation in epoxy [99].

Various mechanical mixing approaches for the dispersion of CNT in epoxy have been tried, including ultrasound, mechanical stirring, roller machine, gears machine, and combined ultrasound and high-speed stirring. Among these techniques, ultrasonic treatment combined with high-speed stirring was found to be an efficient method [100]. In another study, an increase of 19% in interlaminar shear strength was achieved through mechanical mixing at 55°C in a controlled environment [101]. Incorporating hydroxyl-functionalized multi-walled carbon nanotubes (MWCNTs) (1%) in epoxy using a three-roll mill at different contents reduced agglomeration and increased flexural strength by 11.94% [102]. Additionally, recent studies have reported on the modification of MWCNTs with imidazolium-based ionic liquids and their improved dispersion in epoxy matrices [16, 70, 87, 103]. Therefore, this method is considered very promising [104].

4 RESEARCH ARTICLE - I

Taylor & Francis
Taylor & Francis Group

Check for updates

Surface modification of carbon fiber with imidazolium ionic liquids

Bilal Ghafoor [a], Henri Stephan Schrekker [b], Jonder Morais [c]
and Sandro Campos Amico [a]

aPPGE3M, Federal University of Rio Grande Do Sul, Porto Alegre/RS, Brazil; bLaboratory of Technological Processes and Catalysis, Institute of Chemistry, Federal University of Rio Grande Do Sul, Porto Alegre/RS, Brazil; cInstitute of Physics, Federal University of Rio Grande Do Sul, Porto Alegre/RS, Brazil

ABSTRACT

Carbon fiber composites are high-performance materials commonly used in advanced applications and their performance is highly dependent on the fiber-matrix interfacial interaction. The non-polar carbon fiber surface may be modified via different techniques to improve adhesion with the polymer matrix. In this work, non-covalent surface modification of carbon fiber has been carried out using two different imidazolium ionic liquids, 1-n-butyl-3-methyl imidazolium bis(trifluoromethylsulfonyl) imide (hydrophobic) and 1-n-butyl-3-methylimidazolium chloride (hydrophilic). The treatment was performed by immersing the fiber into 10 wt. % methanolic ionic liquid solution for 10 min. Treated fibers were characterized using Fourier-transform infrared spectroscopy, Raman spectroscopy and X-ray photoelectron spectroscopy confirmed the presence of ionic liquid on the carbon fiber surface. Surface morphology of treated fibers analyzed by scanning electron microscopy showed ionic liquid moieties. Wettability of the treated carbon fiber with epoxy resin significantly increased, with a decrease in contact angle greater than 15°. Interfacial shear strength between the modified carbon fiber and epoxy increased up to 56.5% with respect to the unsized carbon fiber, being comparable with epoxy-sized fibers. Thus, the proposed surface modification has the potential to improve the interfacial performance of carbon fiber polymer composites.
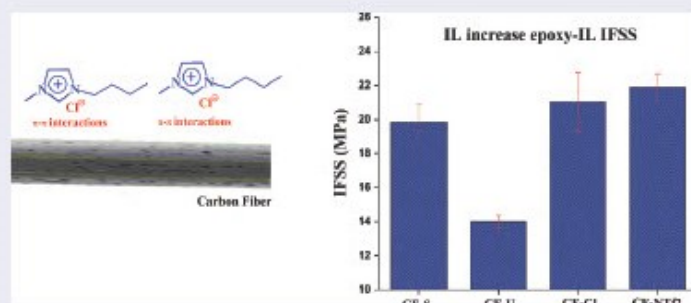
1. Introduction

Surface treatment of carbon fiber (CF) is an interesting area of research due to its importance to enable high-performance structural applications. The CF surface is inherently chemically inert, non-polar and highly stable, limiting its interaction with polymer matrices and the resulting interlaminar shear strength of CF-reinforced composites. Improved interfacial properties promote efficient load transfer from the matrix to the fiber by shear ultimately improving the mechanical properties.

One of the most widely used treatments is the use of an epoxy-based polymer sizing, which produce an interphase region with stronger interactions [1,2]. This increases stress transfer to the fiber by providing an alternative way for the crack to proceed into the matrix. Nevertheless, several treatments have been studied to improve the referred interaction including physical methods, which increase roughness and provide mechanical interlocking, or wet chemical processes sometimes introducing chemical functional groups [3]. The various methods attempt to increase the interfacial shear strength (IFSS), interlaminar shear strength (ILSS) and toughness of fiber matrix composites [4], but most of them are complex or unsuitable for large-scale implementation [5], or have a detrimental effect on the CF strength [5,6]. The surface and microstructural characteristics of the fibers altered due to these treatments directly influence the overall mechanical properties of the composite [7]. Methods such as oxidation, plasma deposition and irradiation grafting [6] create defects, increase the oxygen content or introduce chemical bonds at the CF surface [8,9]. Other recent techniques include electrophoretic deposition and microwave- plasma enhanced chemical vapor deposition. These techniques were also employed to deposit carbon nanotubes on the fiber surface, producing a transition layer at the fiber/matrix interface to enhance IFSS of the composite [10–13].

In this context, alternative treatment methods are still demanded, and the use of ionic liquids (IL) may be a promising approach. IL are salts that exist in the liquid state at 100 ℃ [14,15], being considered designer materials since their properties can be altered via changes in their chemical structure, in both anion and cation, for a particular application. Such IL can interact with non-ionic compounds by a combination of ion-dipole and dipole–dipole forces, hydrogen bonds, π-π interactions and dispersion forces. In the case of imidazolium IL, the electron poor aromatic imidazolium ring favors their interaction with aromatic carbonaceous fillers (fullerenes, graphene and carbon nanotubes) via π-π stacking [16]. These fillers with non-covalently attached imidazolium IL have a more active surface for interaction with polymer matrices [17]. Since this surface functionalization does not modify the original filler microstructure, this approach is also of interest for polymer composites with CF [18].

In this work, non-covalent surface modification of CF has been carried out using two different imidazolium IL, 1-*n*-butyl-3-methyl imidazolium bis-(trifluoromethylsulfonyl) imide (hydrophobic) and 1-*n*-butyl-3-methylimidazolium chloride (hydrophilic). The chosen IL have distinct hydrophobic nature, varying the

adsorption on the CF surface due to a weak ion pair association. The comparison of both the hydrophobic and hydrophilic behavior of IL will provide a better understanding in terms of interfacial shear strength between CF and epoxy.

2. Experimental

Intermediate modulus CF (modulus = 230 GPa; density = 1.76 g/cm³; filament diameter = 7 μm) roving (T300) with 1% epoxy sizing from Toray was used. 1-*n*-Butyl-3-methylimidazolium bis(trifluoromethanesulfonyl) imide, $C_4MImNTf_2$, ≥95% purity and 1-*n*-butyl-3-methyl imidazolium chloride, C_4MImCl, ≥ 95% purity, were acquired from Sigma-Aldrich. Acetone (99.5% purity) and methanol (99.5% purity) were purchased from Sigma-Aldrich. DGEBA epoxy resin (AR260) was used for contact angle measurements and fiber pull out testing.

As-received CF (designated as **CF-S**) yarns were washed with acetone for the removal of sizing. The yarns were cut (12 cm length), placed in a beaker containing 50 mL of acetone for 25 min followed by manual stirring for 3–4 min. The CF yarns were squeeze dried followed by heating in an oven with air-circulation for 30 min at 30 °C to remove excess solvent. This sample was designated as **CF-U** and conditioned in a desiccator. Some **CF-U** fibers were then treated by immersion in methanolic 10% (w/v) IL solution (50 mL) for 10 min at room temperature. Afterwards, the samples were removed and dried in a vacuum oven for 30 min at 50 °C. The CF treated with $C_4MImNTf_2$ and C_4MImCl were designated as **CF-NTf₂** and **CF-Cl**, respectively. To study the presence of IL on the CF surface, IL-treated CF samples (with **BMImCl** and **BMImNTf₂**) were placed in a Soxhlet apparatus to perform the extraction process with methanol for 5 h. After the extraction process the samples were dried in vacuum oven at 60 °C for 60 min. The weight of the samples was measured before and after the extraction process in dried condition until gaining a constant weight.

Fourier-transform infrared spectroscopy was performed in a Perkin-Elmer equipment, model Spectrum-GX, in the 500–3500 cm^{-1} range with 116 scans at a constant spectral resolution of 6 cm^{-1}. Raman spectroscopy was performed in a Horiba apparatus, model Lab Ram, equipped with a helium-neon laser at an excitation wavelength of 632 nm.

X-ray photoelectron spectroscopy (XPS) (Model: VG ESCALAB MkII) analysis was performed using an Al-K$_\alpha$ (1486.6 eV) X-ray source and a SPECS PHOIBOS 150 hemispherical electron analyzers at 15 eV pass energy. In the XPS analysis, no charge neutralization was used. The samples were fixed onto the sample holder using a conductive carbon tape (5 × 5 mm²), where a bundle of fibers of the same size were carefully placed and aligned to cover the entire tape on the sample holder. The samples size was around 8 × 6 mm². A conventional X-ray source was used and therefore a large area was radiated, basically the whole sample. The analyzer spot size was set to 6 mm diameter and aligned at the center of the samples, monitoring this whole area in each analysis. The spectra were analyzed using the CasaXPS software with a charging correction setting the adventitious C1s component at 284.5 eV binding energy (E_b) and

32

a Shirley background. The value 284.5 eV used for referencing in this study is the value indicated in the Perkin Elmer XPS Handbook [19]. The fitting procedure also addressed the peaks line shape considering a 30% asymmetry.

Scanning electron microscopy was carried out in a JSM 6060 electron microscope at an operating voltage of 5 kV. Samples were gold-coated, and images were acquired in secondary electron imaging mode. Contact angle evaluation of epoxy droplets on single CF were performed aided by a Carl Zeiss axio Lab optical microscope. The obtained images were processed with the Image J software. Contact angle was calculated by the method of droplets geometry in cylindrical filaments generally referred to as Carrol method and Wagner method [19,20].

To calculate interfacial shear strength (IFSS) of the unmodified and modified CF, fiber tow pull-out test was performed in a universal testing machine (Emic/Instron 23–5D). Samples were prepared by placing the tow in a perpendicular position in relation to a block of epoxy (DGEBA) cured in a silicon mold. Ten samples of each type were tested at a strain rate of 2 mm/min. Finally, the IFSS was calculated by the following equation:

$$IFSS = F_{max} / \pi.d_{fb}.l_e$$

where F_{max} is the maximum pull-out force value, and d_{fb} (2.43–2.89 mm) and l_e (3.43–3.57 mm) are the diameter and the length of the fiber tow embedded in epoxy. Both values were measured with a digital caliper (accuracy = 0.0125 mm). Images of the fiber tow before and after pull-out have been taken aided by a digital microscope (image resolution 1920 × 1080) and an optical microscope (Carl Zeiss axio Lab A).

3. Results and discussion

The increase in the effectiveness of fiber surface modification demands enhanced fiber interaction with the modifying agent. The overall purpose of the CF surface CF surface treatment is to protect the CF surface, and to improve fiber adhesion with matrix. IL as a modifying agent may be beneficial by introducing a plasticizing effect around the fiber used with epoxy matrices [21]. Figure 1 shows the expected π-π bond stacking between the ILs's imidazolium ring and CF (sp^2 hybridized carbon

Carbon Fiber
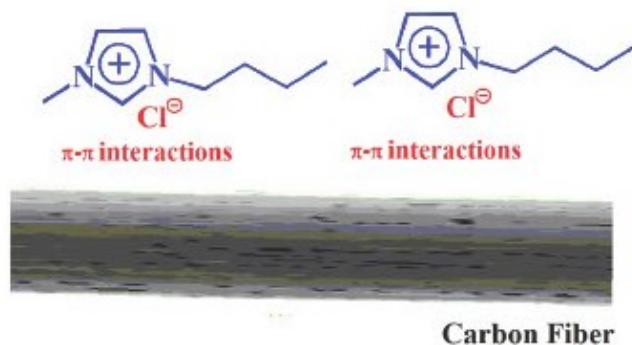
Figure 1. Interaction of IL with CF.

33

atoms) surface. That kind of interaction is expected to keep the IL adsorbed on the CF surface and at the same time will provide improved intermolecular interactions with epoxy matrix [22,23].

Figure 2a shows the FTIR spectra obtained for CF-S, CF-U, $C_4MImNTf_2$ and CF-NTf_2. Comparison of CF-S and CF-U spectra shows that the epoxy finish was largely removed after washing with acetone since no peaks related to the sizing are observed in the latter [24]. The characteristic peaks of $C_4MImNTf_2$ at 2879–3157 cm^{-1}, 1300–1500 cm^{-1} and 1000–1150 cm^{-1} confirm its presence on the surface of CF-NTf_2. The characteristic peaks of C_4MImCl at 2868–3059 cm^{-1}, 1563 cm^{-1}, 1453 cm^{-1} and 1170 cm^{-1} also confirm its presence on the surface of CF-Cl, as shown in Figure 2b [16,25].

Weight gain measurements have been performed to identify the amount of IL on the fiber surface after treatment. For the C_4MImCl treatment, a weight gain of 58.6% was observed whereas, for $C_4MImNTf_2$, a weight gain of 61.0% was observed. The C_4

Figure 2. FTIR-ATR transmittance spectra for: (a) CF-S, CF-U, $C_4MImNTf_2$ and CF-NTf_2; (b) CF-U, C_4MImCl and CF-Cl.

34

MImCl and **C₄MImNTf₂** on the CF surface will provide good compatibility to allow stronger interfacial interaction with polymer matrices *e.g.*, epoxy, which will improve strength of the polymer matrix composite [21]. Moreover, the Soxhlet extraction performed 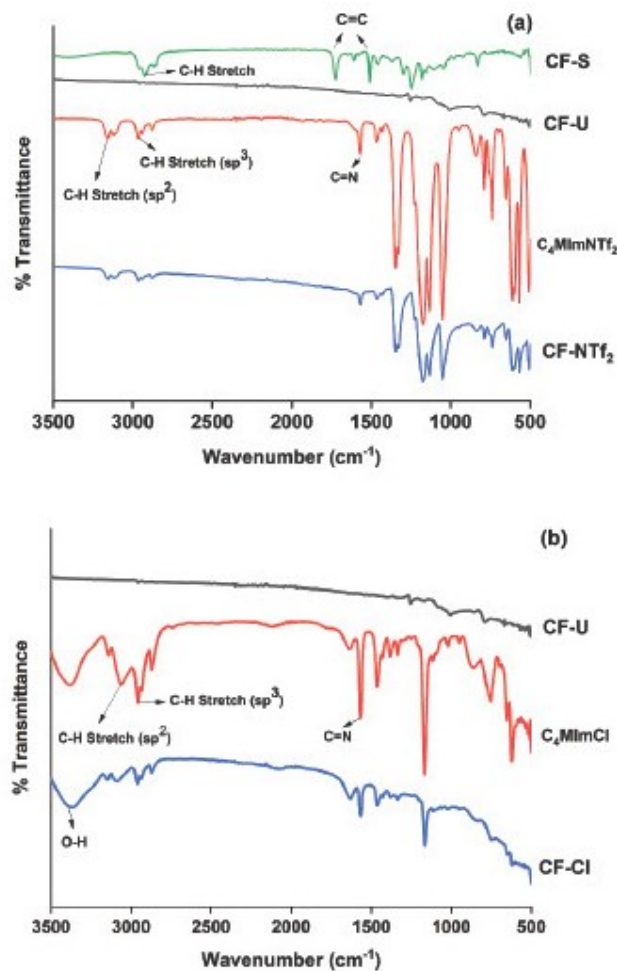for IL modified CF showed weight loss that corresponds to the extraction of IL from the CF surface. It also shows a greater ionic association of ILs with methanol as compared to CF. Afterwards, the IL was recovered from the methanol that confirmed its presence on CF surface.

Raman shift spectra of CF-U treated with IL are shown in Figure 3. The characteristic CF bands are the D-band at 1345 cm^{-1}, associated with the disordered graphite structure, and the G-band at 1578 cm^{-1}, related to the ordered hexagonal carbon–carbon bond structure of CF [24,26]. CF with IL on its surface (**C₄MImNTf₂** or **C₄MImCl**) showed a decrease in intensity of the D- and G-bands, although the I_D/I_G ratio did not change significantly, being 1.08 (**CF-U**), 1.17 (**CF-NTf₂**) and 1.03 (**CF-Cl**) which indicates an unaffected CF structure. This confirms the chemical and morphological stability of the CF structure for the employed surface functionalization procedure [24]. Interestingly, the presence of IL on the CF surface induced strains that produced an upshift of 4 cm^{-1}, perhaps due to stronger CF-IL interactions [27].

Figure 4 displays the C1s region of the XPS spectra for **CF-S**, **CF-U**, **CF-NTf₂** and **CF-Cl**. Four distinct carbon chemical states were identified at their surfaces: C-C (284.5 eV), C-O or C-N (286.0 eV), -CONH- (287.5 eV) and C-F bonds (292.3 eV). Table 1 shows the composition investigated with a large spot size for each sample to obtain average compositions. The graphitic nature of the carbon is clearly noticeable for sample **CF-S** (Figure 4) where a shake-up feature appears in the C1s due to the π-π* character. The desizing process was successful in concentrating C-C bonds at the fiber surface, as observed when comparing the results for **CF-S** and **CF-U**. Besides, the XPS analysis corroborated the presence of IL on the surface of the treated fibers (**CF-NTf₂** and **CF-Cl** samples) by the enhancement in the C-N chemical component. Particularly for the former the presence of C-F bonds was quite evident [28].
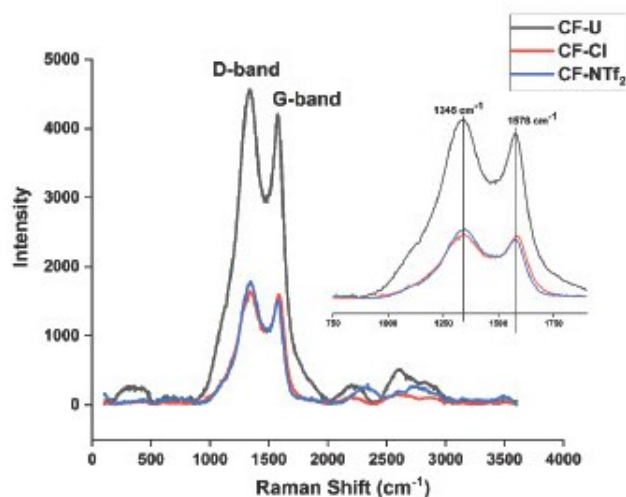
Figure 3. Raman shift spectra of CF before and after treatment with the ILs.
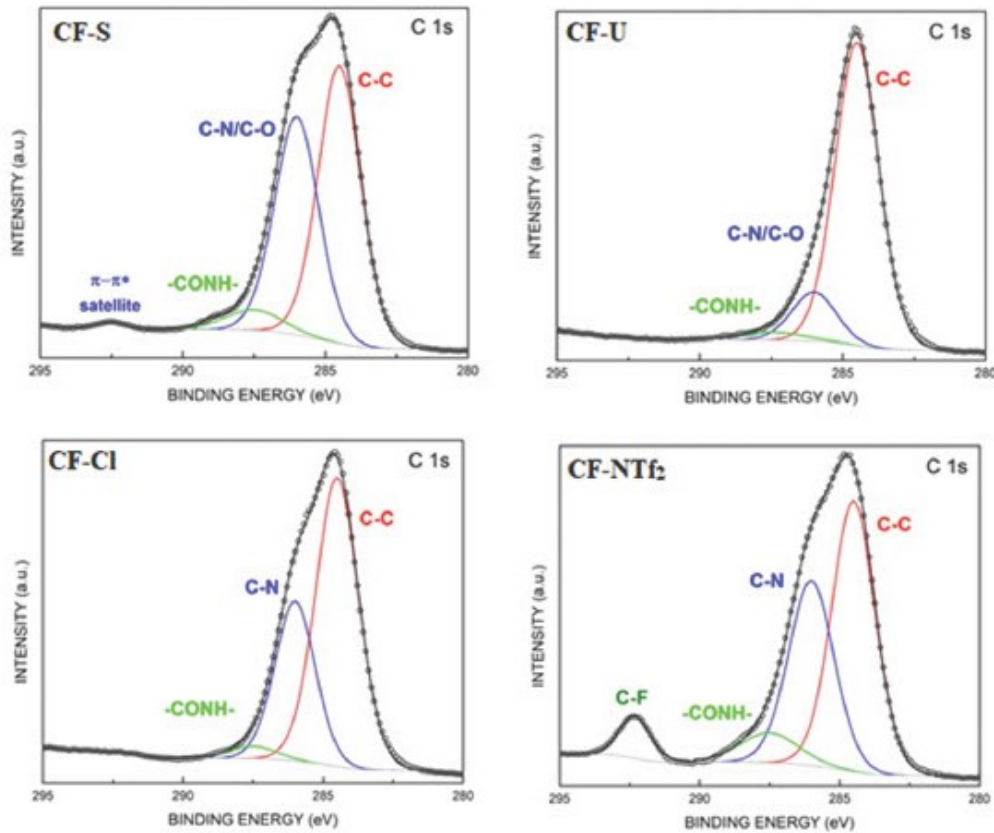
Figure 4. XPS spectra of the C1s region for: (a) **CF-S**, (b) **CF-U**, (c) **CF-Cl**, and (d) **CF-NTf₂**.

Table 1. Apparent surface composition [%] of the CF samples as determined from the XPS survey spectra.

Sample	C	O	N	F	Cl
CF-S	72.0	24.7	3.3		
CF-U	78.1	19.1	2.3	0.5	
CF-NTf₂	57.8	23.3	7.7	11.2	-
CF-Cl	75.7	10.0	8.7	-	5.6

Figure 5 shows the micrographs of **CF-U** and the IL-functionalized CF (**CF-NTf₂** and **CF-Cl**). The difference in the micrographs is evident, a smooth neutral surface without imperfections for the desized CF and some adsorbed particles on the surface of CF for **CF-NTf₂** and **CF-Cl**. However, contrary to many other surface functionalization methods, SEM micrographs of IL-treated CF taken at different magnifications do not indicate any detrimental effect on fiber integrity (absence of structural defects) which is expected to enable stronger polymer-based composites. Also, the imidazolium-based IL offered a unique way of attachment with the CF surface through π-π bond stacking. The presence of IL on the surface is beneficial since it provides protection and many sites for mechanical entanglement at the interface, and also by enabling intermolecular forces.

36
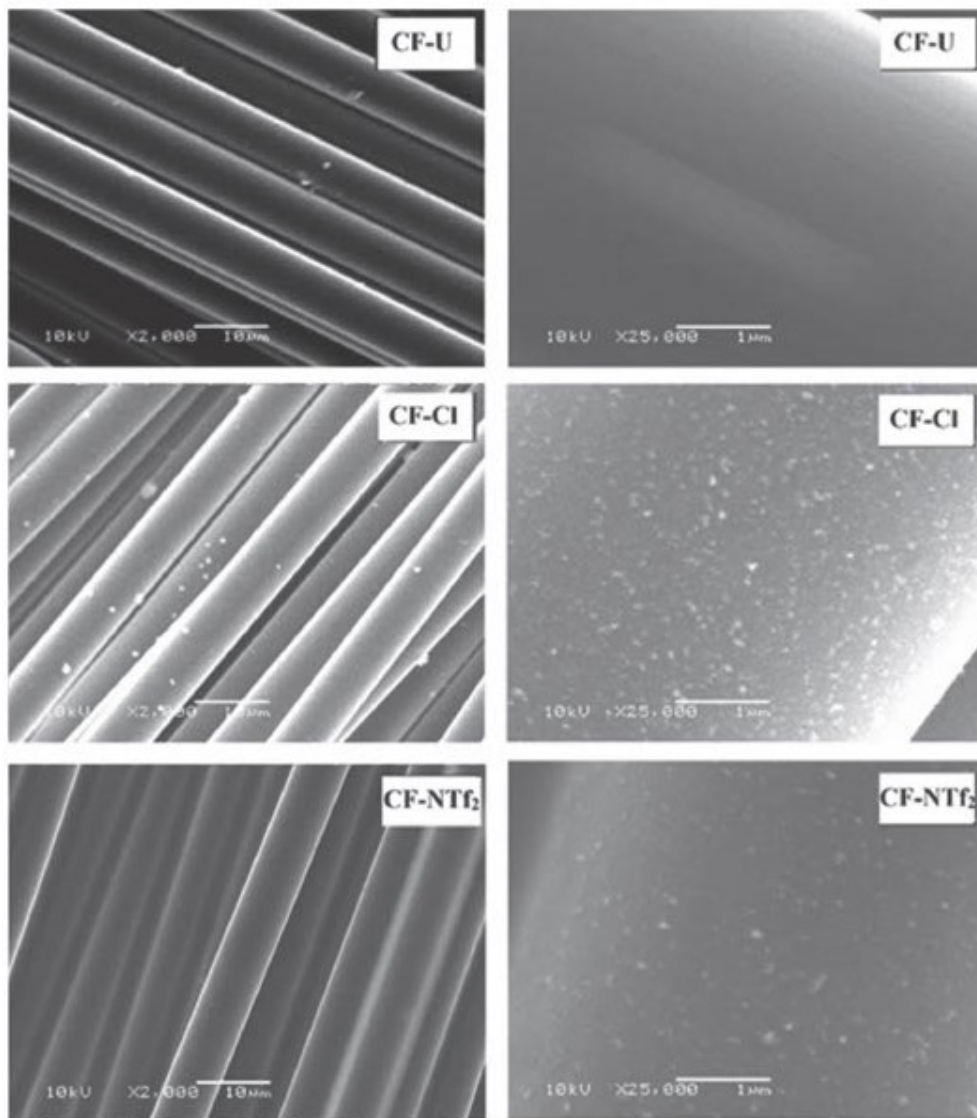
Figure 5. SEM micrographs of **CF-U, CF- Cl,** and **CF- NTf$_2$** at magnification of 2000× (left column, scale bar = 10 μm) and 25,000× (right column, scale bar = 1 μm).

The influence of the IL treatment on the wettability of CF was determined by contact angle measurements of epoxy resin on CF, whose results are shown in Figure 6. The mean contact angle of CF-U was calculated as 31.5°. The untreated carbon fiber has a surface tension close to 40 mJ.m^{-2} [29], whereas polymeric resins, such as epoxy, have a surface tension in the range of 35–45 mJ.m^{-2}. Due to a similar surface energy, suitable wetting of the fiber by epoxy is not expected. The ion-pair formation constant (K_{IP}) is an important parameter to define the association of oppositely charged ions in IL quantitatively. This K_{IP} value is directly related to the adsorption coefficient (K_d) characteristics of
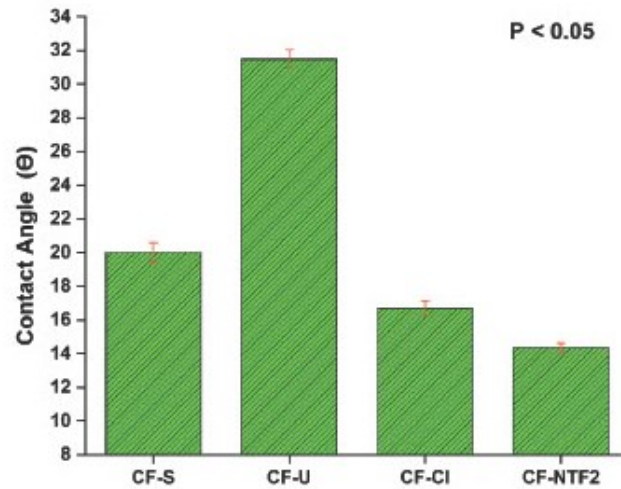
Figure 6. Contact angles of epoxy resin on **CF-U, CF-S, CF-Cl** and **CF-NTf2** fibers.

IL. A strong binding energy between the imidazolium-based cation and NTf$_2$ leads to a strong ion pair association which leads to higher adsorption of IL onto a carbon-based structure [30].

After the IL treatment, the contact angle decreased to 14–16° what is a clear indication of the increase in surface energy of the CF. This decreased contact angle corresponds to increased wettability, enhancing secondary interactions such as van der Waals attraction and hydrogen bond force at the interface. Since the decrease was similar for both IL anions, with different hydrophilic/hydrophobic character, the anion and the imidazolium ring were most likely involved in the interaction with the CF surface. In this case, the *N-n*-butyl side-chain of the imidazolium cation would be available to interact with epoxy in a composite.
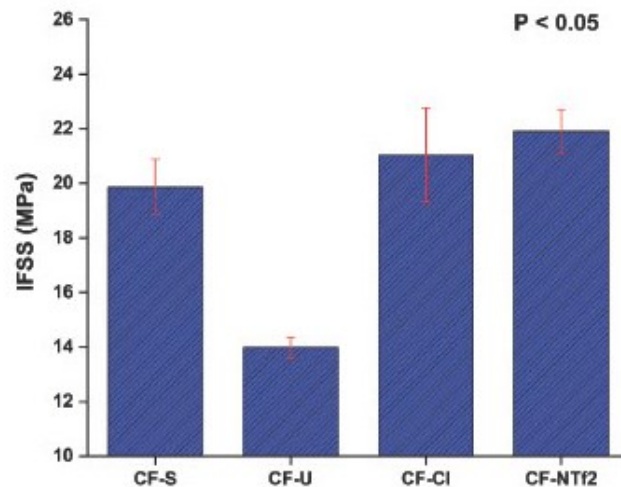
Figure 7. IFSS value of **CF-U, CF-S, CF-Cl, CF-NTf2.**
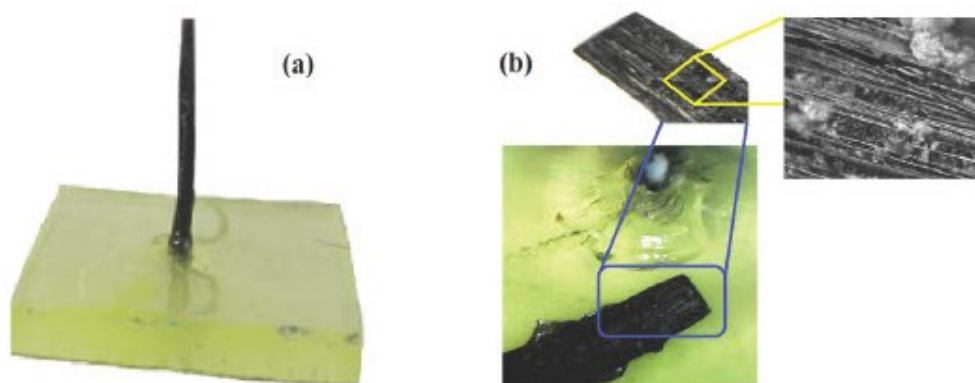
Figure 8. Fiber pull-out sample: (a) before pull-out; (b) after pull-out.

Fiber pull-out tests were carried out to evaluate the interfacial shear strength (IFSS) between CF and epoxy resin, and the results are presented in Figure 7. The load–displacement curves (Figure S1 in the supplementary material) show that the load increased mostly linear until a peak value was reached, and the carbon fiber tow started being pulled out from the epoxy block. Moreover, these results are in good agreement with the contact angle measurements that showed a decrease in contact angle with IL [31].

The values of IFSS of commercially sized CF, C_4MImCl modified CF (**CF-Cl**) and $C_4MImNTf_2$ modified CF (**CF-NTf₂**) were 19.67 MPa, 21.02 MPa and 21.90 MPa, all above 13.98 MPa found for the unsized CF, as expected. That represented an IFSS increase of 40.7%, 50.3% and 56.5% in IFSS, respectively. The increase in IFSS due to IL modification is similar as that reported in another study for carbon fiber treatment [21]. Furthermore, the IFSS values of the IL-treated CF were slightly higher than that of the commercially sized CF.

The chemical characteristic influenced the corresponding mechanical strength parameters at the interface between fibers CF and polymer [32]. At the interface region, the association of cation and anion of IL influence the absorbability. The imidazolium ring with hydrophobic anion serves as a strong scaffold that promotes adhesion on CF surface. The interfacial bond strength formed as a result, is sufficient for the load to be transferred from the matrix to the fibers, being comparable with the fiber having an epoxy sizing. The improved behavior in terms of adhesion strength is expected due to its hydrophobic nature. The presence of water molecules reduce inter-ionic interactions in Cl anion-based IL can be a limiting factor for effective interfacial properties with epoxy whereas the hydrophobic behavior of NTF_2 anion in IL avoids that limitation. This behavior is also interesting in terms of defining toughening characteristics such as debonding and premature fiber pull-out which are generally affected in strong interfaces [33]. Indeed, IL may act as a plasticizer at the interface, making the system more ductile and promoting elastic deformation by creating shear tolerant fiber-matrix adhesion [32,34].

The fracture behavior at the interface zone of the pulled-out fiber sample is shown in Figure 8. The phenomena of debonding along the full embedded length in the matrix and breakage of the fiber happened due to the shear forces. Significant

sliding friction at the interface region due to matrix and the interface region in the form of multiple cracks with serrated debonding aspects increases the energy absorption leading to toughening of composite [35]. Certainly, this enhanced energy dissipation mechanism is the contributing factor for the increased strength at the interface region.

4. Conclusions

In this study, a practical route for the surface functionalization of CF with imidazolium IL has been demonstrated. Functionalization occurred without chemical or structural modification of the CF. The presence of IL on the CF surface improved CF wettability and the IFSS with epoxy, which is beneficial for making high strength polymer composites. This work may be a guideline for the use of imidazolium IL for the modification of the CF surface and this lab-scale study for CF treatment can be easily integrated into an industrial process.

Acknowledgments

Disclosure statement

The author(s) declare no conflict of interest.

ORCID

Bilal Ghafoor http://orcid.org/0000-0001-8232-9624
Henri Stephan Schrekker http://orcid.org/0000-0002-8173-3841
Jonder Morais http://orcid.org/0000-0002-4143-1208
Sandro Campos Amico http://orcid.org/0000-0003-4873-2238

References

[1] Zhang X, Fan X, Yan C, et al. Interfacial microstructure and properties of carbon fiber composites modified with graphene oxide. Appl Mater Interfaces. 2012;4(3):1543–1552.
[2] Sager R, Klein P, Lagoudas D, et al. Effect of carbon nanotubes on the interfacial shear strength of T650 carbon fiber in an epoxy matrix. Compos Sci Technol. 2009;69(7–8):898–904.
[3] Rahmani H, Ashori A, Varnaseri Njpf AT. Surface modification of carbon fiber for improving the interfacial adhesion between carbon fiber and polymer matrix. Polym Adv Technol. 2016;27(6):805–811.
[4] Zhang C, Pei X, Xu Z, et al. Performance of composites via multiple interface engineering techniques: plasma etching, UV-induced grafting and nanotube deposition. Mater Today Commun. 2020;22:100723.
[5] Corujeira Gallo S, Charitidis C, Dong H, et al. Surface functionalization of carbon fibers with active screen plasma. Journal of Vacuum Science & Technology A: Vacuum, Surfaces, and Films. 2017;35(2):021404.

[6] Tiwari S, Bijwe JJPT. Surface treatment of carbon fibers-a review. Procedia Manuf. 2014;14:505–512.

[7] Shan M, Wang H, Xu Z, et al. Synergetic improvement of mechanical properties and surface activities in γ-irradiated carbon fibers revealed by radial positioning spectroscopy and mechanical model. Anal Methods. 2018;10(5):496–503.

[8] Xu Z, Chen L, Huang Y, et al. Wettability of carbon fibers modified by acrylic acid and interface properties of carbon fiber/epoxy. Eur Polym J. 2008;44(2):494–503.

[9] Liu L, Wang H, Zhao L, et al. In situ characterization of surface-layer structure evolution in γ-irradiated carbon fibers by X-ray photoelectron spectroscopy combined with argon-ion sputtering. Polym Compos. 2019;40(S1):E832–E834.

[10] Sui X, Shi J, Yao H, et al. Interfacial and fatigue-resistant synergetic enhancement of carbon fiber/epoxy hierarchical composites via an electrophoresis deposited carbon nanotube-toughened transition layer. Compos Part A: Appl Sci Manuf. 2017;92:134–144.

[11] Yao H, Sui X, Zhao Z, et al. Optimization of interfacial microstructure and mechanical properties of carbon fiber/epoxy composites via carbon nanotube sizing. Appl Surf Sci. 2015;347:583–590.

[12] Zhao Z, Teng K, Li N, et al. Mechanical, thermal and interfacial performances of carbon fiber reinforced composites flavored by carbon nanotube in matrix/interface. Compos Struct. 2017;159:761–772.

[13] Zhang C, Liu L, Xu Z, et al. Improvement for interface adhesion of epoxy/carbon fibers endowed with carbon nanotubes via microwave plasma-enhanced chemical vapor deposition. Polym Compos. 2018;39(S2):E1262–E1268.

[14] Ferguson JL, Holbrey JD, Ng S, et al. A greener, halide-free approach to ionic liquid synthesis. Pure Appl Chem. 2011;84(3):723–744.

[15] Corley CA, Iacono ST. Recycling of 1, 2-Dimethyl-3-propylimidazolium bis (trifluoromethylsulfonyl) imide ionic liquid by stacked cation and anion exchange adsorption-desorption. Separations. 2019;6(2):29.

[16] França JM, de Castro CAN, Pádua AA. Molecular interactions and thermal transport in ionic liquids with carbon nanomaterials. Phys Chem Chem Phys. 2017;19(26):17075–17087.

[17] Yang Y-K, He C-E, Peng R-G, et al. Non-covalently modified graphene sheets by imidazolium ionic liquids for multifunctional polymer nanocomposites. J Mater Chem. 2012;22(12):5666–5675.

[18] Mahltig B, Kyosev Y. Inorganic and composite fibers: production, properties, and applications. Cambridge: Woodhead Publishing; 2018.

[19] Moraes CV, Schrekker HS, Amico SC. Surface treatment of Kevlar® polyaramid fibers with imidazolium-based ionic liquids. Adv Mater -Tech Connect Br. 2017: 245–249.

[20] Livi S, Duchet-Rumeau J, Gérard JF, et al. Polymers and ionic liquids: a successful wedding. Macromol Chem Phys. 2015;216(4):359–368.

[21] Eyckens DJ, Servinis L, Scheffler C, et al. Synergistic interfacial effects of ionic liquids as sizing agents and surface modified carbon fibers. J Mater Chem A. 2018;6(10):4504–4514.

[22] Pensado AS, Malberg F, Gomes MC, et al. Interactions and structure of ionic liquids on graphene and carbon nanotubes surfaces. RSC Adv. 2014;4(35):18017–18024.

[23] Fonseca E, Da Silva VD, Klitzke JS, et al. Imidazolium ionic liquids as fracture toughening agents in DGEBA-TETA epoxy resin. Polym Test. 2020;87:106556.

[24] Li J, Su S, Zhou L, et al. Carbon nanowalls grown by microwave plasma enhanced chemical vapor deposition during the carbonization of polyacrylonitrile fibers. Adv Mater. 2013;113(2):024313.

[25] Wang J, Chu H, Yjan L. Why single-walled carbon nanotubes can be dispersed in imidazolium-based ionic liquids. ACS Nano. 2008;2(12)2540–2546.

[26] Ager IIIJW, Veirs DK, Shamir J, et al. Laser heating effects in the characterization of carbon fibers by Raman spectroscopy. J Appl Phys. 1990;68(7):3598–3608.

[27] Washer G, Blum F. Developing Raman spectroscopy for the nondestructive testing of carbon fiber composites. Mater Eval. 2011;69(10):1219–1226.

[28] Moulder JF. Handbook of X-ray photoelectron spectroscopy. Eden Prairie, Perkin-Elmer Corp. Phys Elect. 1995;230–232.

[29] Zheng Y, Chen L, Wang X, et al. Modification of renewable cardanol onto carbon fiber for the improved interfacial properties of advanced polymer composites. Polymers. 2020;12(1):45.

[30] Liu M, Zhu L, Zhang X, et al. Insight into the role of ion-pairing in the adsorption of imidazolium derivative-based ionic liquids by activated carbon. Sci Total Environ. 2020;743:140644.

[31] Kasahara S, Koyanagi J, Mori K, et al. Evaluation of interface properties of carbon fiber/resin using the full atomistic model considering the electric charge state. Adv Compos Mater. 2021;30(2):164–175.

[32] Jiang Y, Jjci W. Enhancement of interface strength of carbon fiber/epoxy resin composites filled with low-dimensional materials. Compos Interfaces. 2021;28(3):273–286.

[33] Li X, Yang Z, Zhao Y, et al. Excellent interfacial structural integrity of pre-oxidized carbon fiber-reinforced carbon-carbon composites. Compos Interfaces. 2021;1–14. DOI:10.1080/09276440.2021.1943141.

[34] Kumar P, Prakash P, Ramya K, et al. Probing translational and rotational dynamics in hydrophilic/hydrophobic anion based imidazolium ionic liquid–water mixtures. Soft Matter. 2018;14(29):6109–6118.

[35] Hernandez DA, Soufen CA, Orlandi MO. Carbon fiber reinforced polymer and epoxy adhesive tensile test failure analysis using scanning electron microscopy. Mater Res. 2017;20(4):951–961.

SURFACE MODIFICATION OF CARBON FIBER WITH IMIDAZOLIUM IONIC LIQUIDS

Bilal Ghafoor[a], Henri Stephan Schrekker[b], Jonder Morais[c], Sandro Campos Amico[a]

[a]PPGE3M, Federal University of Rio Grande do Sul, Porto Alegre/RS, 91501-970, Brazil

bilalghafoorist@hotmail.com, amico@ufrgs.br

[b]Laboratory of Technological Processes and Catalysis, Institute of Chemistry, Federal University of Rio Grande do Sul, Porto Alegre/RS, 91501-970, Brazil

henri.schrekker@ufrgs.br

[c]Institute of Physics, Federal University of Rio Grande do Sul, Porto Alegre/RS, 91501-970, Brazil
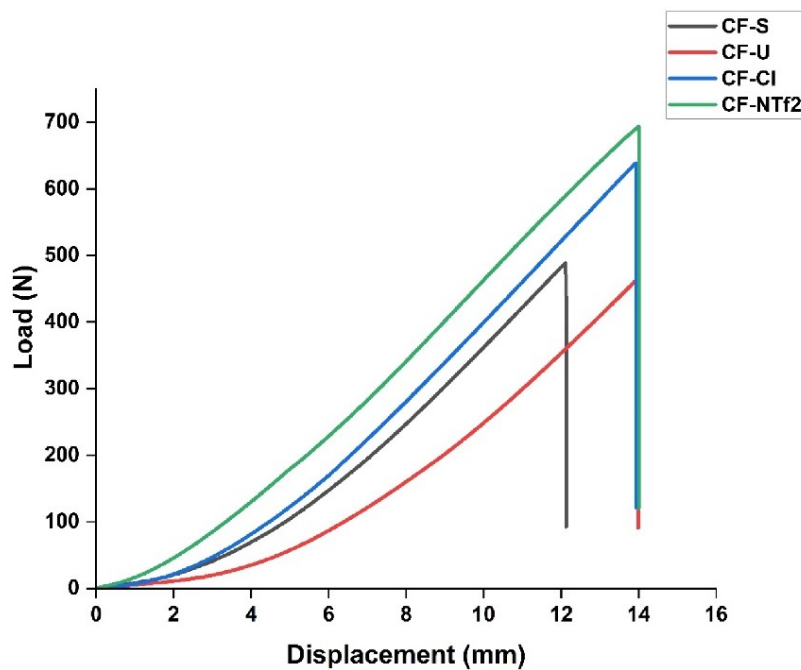
jonder@if.ufrgs.br

Supplementary Material

Figure S1- Load-displacement curve of **CF-S, CF-U, CF-Cl, CF- NTf₂**

Article

Multifunctional Characteristics of Carbon Fibers Modified with Imidazolium Ionic Liquids

Bilal Ghafoor [1] , Henri Stephan Schrekker [2] and Sandro Campos Amico [1],*

[1] PPGE3M, Federal University of Rio Grande do Sul, Porto Alegre 91501-970, RS, Brazil
[2] Laboratory of Technological Processes and Catalysis, Institute of Chemistry, Federal University of Rio Grande do Sul, Porto Alegre 91501-970, RS, Brazil
*   Correspondence: amico@ufrgs.br

Abstract: A multifunctional designing approach is of great importance for advanced composite applications. This study assessed the use of ionic liquids (ILs) to modify the surface of carbon fiber (CF) and impart multifunctional characteristics to it. For that, ethanolic solutions of different ILs, 1-butyl-3-methylimidazolium bis(trifluoromethylsulfonyl)imide, 1-butyl-3-methylimidazolium chloride and 1-(2-hydroxyethyl)-3-methylimidazolium chloride, at different concentrations, were used to treat the CF. Fourier-transform infrared spectroscopy confirmed the presence of IL on the CF surface. The contact angle for 1% w/v IL-treated CF and DGEBA epoxy decreased by up to 35%, corresponding to an increase in surface energy of fiber, accompanied by an increase of 91% in interfacial shear strength. These enhancements were achieved with the hydroxy-functionalized IL, showing the tunability of CF properties through the N-imidazolium substituent. An increase in crystallite size along the basal plane was also found due to the ordering of the graphitic structure on the surface. Moreover, there was a decrease in electrical resistivity of 77%. In all, the imidazolium ILs were considered a promising approach to induce multifunctional characteristics, namely enhanced interfacial strength and electrical conductivity, to unsized CF, which can also be beneficial for recycled fibers without deteriorating their inherent surface properties.

Keywords: task-specific ionic liquid; carbon fiber recycling; electrical resistivity; interfacial bonding; epoxy

1. Introduction

A considerable effort to increase the use of more sustainable materials in various fields is of prime interest. The neoteric sense of ionic liquids (ILs) can be understood by multiple aspects like low flammability, neglectable volatility and high thermal stability, providing safe and robust alternatives to traditional organic solvents. The importance of ILs in terms of design flexibility is impressive, including structural changes in the IL's cation, anion, alkyl chain and functional group. Factors like size and asymmetry of their ions contribute to complex interactions, including dipole–dipole, dipole-induced dipole, dispersion and hydrogen bonding. The structural and chemical characteristics of ILs and their interactions with the liquid–solid interface are a result of these complex Coulombic and intermolecular interactions [1].

Imidazolium ILs, in particular, have good transport properties and high charge carrier capacities and ionic mobilities [2]. Their surface activity is mainly dependent on the molecular structure, i.e., cation, anion, N-alkyl chain length and functional group. Their interactions are predominantly of ion-ion (cation-anion) and hydrogen bonding nature (anion-imidazolium cation C_2-hydrogen) [3]. Coulomb forces are dominant, and the imidazolium cation provides multiple sites for the anion interaction, which is possible from above and below the imidazolium ring as the preferable and thermodynamically stable site. The imidazolium ring C_2-hydrogen has an acidic character that favors hydrogen bonding with an anion through in-plane conformation [4].

Currently, the ILs have been mostly associated with electrochemical, chemical and, to some extent, optical applications [5], and not much with structural composite materials. Carbon fiber reinforced polymer composites (CFRP) are being used in an ever-growing number of applications in aerospace, automotive, energy and other sectors due to excellent specific strength and functional characteristics. As a side-effect, an ever larger amount of CFRP waste is being discarded at the end of the component life [6].

Different recycling methods for CFRP are being developed to mitigate the impact, including thermal (e.g., pyrolysis, fluidized bed recycling), chemical (e.g., solvolysis, hydrolysis) and electrochemical routes [7–12]. Indeed, recycling is a difficult process for composites prepared with thermoset polymer matrices, and the resulting recovered fibers commonly have short lengths and hence low aspect ratios. Nevertheless, many sectors have plans for the use of recycled carbon fibers (rCF) as in urban air mobility, utility poles to trench covers, engine cradles [13], fuel cells [14], wind turbine blades [15], and cementitious mortar to increase mechanical properties [16].

The recycling process also modifies the surface characteristics of carbon fibers since it removes the sizing used to increase compatibility and interfacial adhesion between rCF and the polymer matrix. This has a direct impact on the mechanical properties of the future recycled CFRP [17]. In some cases, rCF without any further surface modification is applied for producing composites [18,19], whereas some studies focused on the treatment of rCF with nitric acid and a coupling agent [20–23], plasma [17], superheated steam [14], steam/air [24], and polymer sizing [25], which are expected to partly recover the reinforcing potential of the original fiber.

The microcrystalline structure of CF consists of layers of sp^2 hybridized carbon atoms arranged in a regular hexagonal pattern similar to graphite structure arranged parallel to each other in a regular pattern having atom in plane covalently bonded atoms and van der Waals forces in the transverse direction of the plane. Highly delocalized π-electrons are evident from graphene layers aligned parallel to the fiber axis, and they have a strong influence on the surface properties of carbon fiber. The overall morphology of rCF remains the same, and the changes are observed as increased surface defects, reduced lateral crystallite size, and decreased surface oxygen concentration that might decrease the interfacial shear strength (IFSS) with a polymer [26]. rCF from supercritical methanol has a reduced tensile strength of 9% and an IFSS of 20% due to the removal of some functional groups [27], rCF from an electrochemical method retained 80% of the tensile strength with no change of oxygenated groups on the fiber surface but with a loss in crystallinity [28], and rCF from pyrolysis showed poorer mechanical properties due to the presence of residue on the surface, although the surface morphology remained the same [29].

In a previous study of our group, 10% w/v of IL was used to treat CF, focusing on the effect of hydrophilic and hydrophobic anions [30]. The successful non-covalent modification of unsized carbon fiber in a mild treatment with ILs has opened new alternatives for the CF treatment without harming its inherent properties. An increase in surface free energy, a decrease in contact angle and an enhanced compatibility with the epoxy matrix in terms of interfacial shear strength were observed. Other reports on the functionalization of CF with IL include the use of 10 wt% of a single IL, 1-butyl-methylimidazolium chloride, as a sizing agent for CF, in which an improved CF/epoxy adhesion strength has been reported [31]. Another study assessed the CF-functionalization with concentrated 1-ethyl-3-methylimidazolium bis(trifluoromethylsulfonyl)imide under microwave irradiation at 50 °C and reported an improvement in CF/epoxy interfacial shear strength [32]. The current study follows on that research, addressing issues like the optimization of the IL concentration (from 0.25% to 3% w/v) and the effect of different functional groups of the *N*-alkyl side chain of the cation on the surface interactions on the microcrystalline structure of CF, and also assessing the treatment effect on electrical resistivity, focusing on multifunctional characteristics (Figure 1).
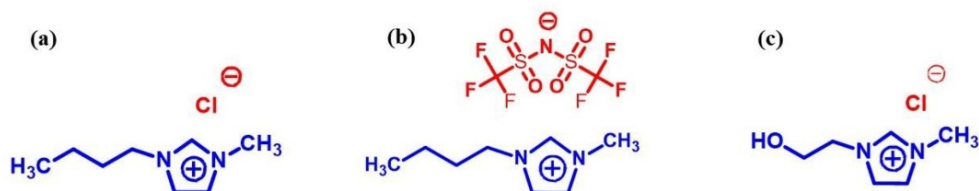
Figure 1. Chemical structures of IL studied: (**a**) C_4MImCl, (**b**) C_4MImNTf$_2$, (**c**) C_2OHMImCl.

2. Experiment

2.1. Materials

Commercially available carbon fiber roving (modulus = 280 GPa; tensile strength = 4.8 GPa; density = 1.78 g/cm^3; filament diameter = 6.6 µm) (SIGRAFIL C T50-4.8/280-UN) without sizing was selected as the base material to emulate a rCF. 1-butyl-3-methylimidazolium bis(trifluoromethanesulfonyl)imide (C_4MImNTf$_2$; purity > 99%; water content of 500 ppm; liquid) and 1-butyl-3-methyl imidazolium chloride (C_4MImCl; purity > 98%; water content < 1%; solid) were acquired from Sigma-Aldrich. The 1-(2-hydroxyethyl)-3-methylimidazolium chloride (C_2OHMImCl; purity > 98%; solid) was synthesized, and its ^{1}H NMR spectrum (shown as Figure S3 in Supplementary Materials), and characterization data were in agreement with those reported [33] Anhydrous ethanol (99.5% purity) was purchased from Sigma-Aldrich. DGEBA epoxy resin (AR260) and hardener (AH260) purchased from e-composites (Brazil) were used for contact angle measurements and to produce samples for pull-out testing.

2.2. Fiber Treatment Process

As-received CF (designated as CF) roving was cut (12 cm length), placed in a beaker containing 50 mL of ethanol for 10 min, followed by manual stirring for 4–5 min. The treated CF roving was squeeze dried followed by heating in an oven with air circulation for 30–45 min at 60 °C to remove excess solvent. CF were then treated by immersion in an ethanolic IL solution (50 mL), at different concentrations, for 10 min at room temperature. Afterwards, the samples were removed and dried in a vacuum oven for 30 min at 60 °C. The CF treated with C_4MImCl, C_4MImNTf$_2$ and C_2OHMImCl were designated as CF-Cl, CF-NTf$_2$ and CF-OH, respectively. CF was washed with ethanol (designated as CF-W) to measure its interfacial strength and to establish differences due to the ethanol treatment on CF. This is the same procedure followed in our previous study [30].

2.3. Characterization Techniques

Fourier-transform infrared spectroscopy was performed with Nicolet 6700 equipment in the 750–3500 cm^{-1} range with 120 scans at a constant spectral resolution of 4 cm^{-1} in ATR mode using a germanium crystal. Scanning electron microscopy was carried out in a Carl Zeiss EVO MA10 electron microscope operating at 10 kV, with a tungsten filament current of 2.004 A, a probe current of 20 pA and a working distance of 5.5 mm. Samples were gold-coated, and images were acquired in secondary electron imaging mode. The characteristic X-ray detector (EDS) was used for elemental composition analysis and compositional mapping of the CF samples. The thermal stability of the samples (minimum 10 mg each) was determined using TA instruments (TGA Q50) in the 30 °C to 700 °C range, at a heating rate of 10 °C/min under a nitrogen atmosphere.

The electrical properties of single carbon fibers were measured by the transfer length method (TLM) according to the procedure described in [34]. A single fiber was placed onto a laboratory glass slide, and electrical contacts were made with small droplets of colloidal silver paste (60 ± 1% Ag, sheet resistance: 0.02–0.05 Ω mm^2 (25 µm)). The two-terminal resistance (R) between the contacts separated by an increasing distance was measured with a multimeter (MD-6200). Then, R was plotted against the distance between the electrical

contacts and, by linear fitting, the contact resistance (R_c) was calculated from the y-intercept and the electrical resistivity (ρ_{el}) from the slope, based on Equation (1). Two samples of each CF were tested, and an average value was reported.

$$R = \left(\rho_{el} A^{-1} \right) \cdot L + R_c \tag{1}$$

where A is the CF cross-section (equal to 38.5 μm^2).

Carbon fiber X-ray diffraction analysis was performed by first grinding it to powder form with a mortar. The grounded fiber was transferred to a glass substrate, ensuring the initial zero angle for analysis in a Rigaku equipment, model Ultima V (Cu K_α radiation with 0.1541 nm). XRD signals were collected in a 2θ range from 10° to 60° with a step size of 0.05° in a continuous scanning mode operating at 40 kV and 17 mA. The Scherrer equation (Equation (2)) was used to estimate the crystallite size.

$$L_a = \frac{K\lambda}{\beta Cos\theta} \tag{2}$$

where K is the Scherrer constant, λ is the wavelength, β is the full width at half maximum (FWHM) corresponding to the physical broadening of the fibers, and θ is the Bragg's angle.

Contact angle evaluation of epoxy droplets on single CF monofilaments, generally referred to as the Carroll method and Wagner method, was performed aided by a Carl Zeiss axio Lab A optical microscope. The obtained images were processed with the Image J software. To measure interfacial shear strength (*IFSS*), fiber roving pull-out tests were performed on a universal testing machine (Emic/Instron 23-5D). The samples were prepared by placing the bundle in a perpendicular position in relation to a block of epoxy cured in a silicon mold. Ten samples of each type were tested at a strain rate of 1 mm/min. The load curves were initially linear during the test when the fiber–matrix interface remained intact. The actual pull-out of the fiber bundle from the matrix takes place when the shear forces exceed the critical (peak) load, which is used in Equation (3) to calculate the *IFSS* [34].

$$IFSS = \frac{F_{max}}{\pi \cdot d_{fb} \cdot l_e} \tag{3}$$

where F_{max} is the maximum pull-out force, and d_{fb} (2.17–2.93 mm) and l_e (3.15–3.88 mm) are the diameter and length of the fiber bundle embedded in epoxy, which were measured with a digital caliper (accuracy = 0.0125 mm).

3. Results and Discussion

3.1. Interfacial Shear Strength

The pull-out test was used to identify the most promising concentrations of IL since it is an effective and suitable method to evaluate a critical feature of composites, the fiber–matrix interfacial bonding characteristics. Load-displacement pull-out curves are given as supplementary data (Figure S1). The carbon fiber-epoxy matrix IFSS results are compiled in Figure 2, showing the values obtained with CF, CF-W, CF-Cl, CF-NTf$_2$, and CF-OH. The pristine CF had an IFSS of 20.08 MPa, which is quite comparable to the value reported in literature for a fiber bundle pullout test of unsized CF and epoxy [35]. Regarding the chosen method for carbon fiber treatment, the effect of ethanol washing (CF versus CF-W) was verified and found to be negligible. Initially, to get an optimized IL content for the surface treatment of CF, various percentages (1, 2 and 3% *w/v*) were studied with the ILs C$_4$MImCl and C$_4$MImNTf$_2$. For both ILs, CF treated with 1% *w/v* of IL (CF-1Cl and CF-1NTf$_2$) produced the most enhanced effect on IFSS. Lower contents of C$_4$MImCl (0.25% and 0.50% *w/v*) were also tested for the surface modification of CF, but the content of 1% *w/v* IL was the optimum and most effective in terms of property improvement. From this outcome, the detailed study was designed to study the effect of 1% *w/v* of IL on the surface properties of CF.
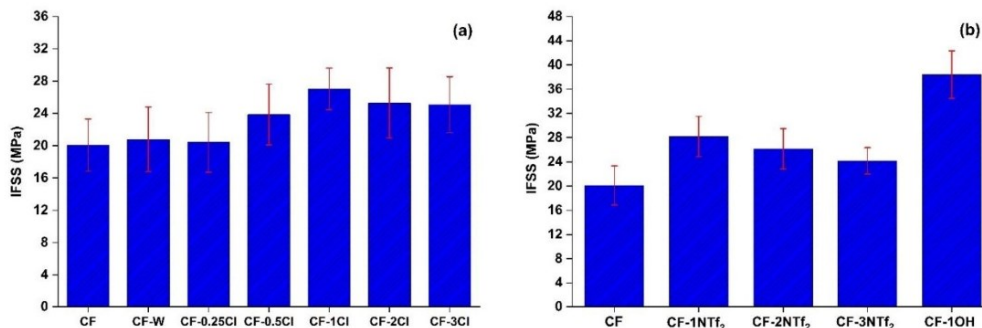
Figure 2. Interfacial shear strength of (**a**) CF, CF-W and CF-Cl (at different concentrations); and (**b**) CF, CF-NTf$_2$ (at different concentrations) and CF-1OH.

Apart from the contact angle, various other factors like increased crosslinking of the epoxy matrix and microcrystalline morphology impact the interfacial properties significantly [36,37]. In this work, that effect can be initially assessed based on the effectiveness of π-bridging between carbon fiber and IL influencing bonding at the interface and also the reactive characteristics of ILs during the curing reaction of epoxy, contributing to its interfacial strength [38]. The interfacial strength is further influenced by the presence of a specific anion and a functional group in the imidazolium *N*-alkyl side chain. The presence of a nucleophilic functional group, OH, enhanced interaction of the fiber with the matrix, most likely due to its ability to react with epoxide groups (Figure 2) [39]. This increased the IFSS value to a maximum of 38.38 MPa with CF-1OH, which is the same effect as the treatment with aqueous ammonia and oxidation of carbon fiber [34,40,41].

The alkyl side chain on the imidazolium cation, on the other hand, has its own significance, as it has low interionic interactions, which allows a more uniform distribution over the CF surface with less agglomeration [38]. The enhanced contribution of side alkyl chains at a low percentage of ionic liquid provided a more balanced approach towards the modification process in terms of imparting plasticity and elastic deformation in order to distribute shear stress gradient along the interface, achieving a toughened composite. A stronger interface bonding would also improve the aging resistance and conduction properties of the rCF composite [42]. This lab scale treatment was chosen considering the possibility of its easy adoption for large scale processes, which can be utilized for the modification of recycled CF that is generally available as random fibers.

3.2. Wettability

To further analyze the effect of IL on wettability and interfacial properties between CF and epoxy, contact angle values were obtained for CF treated with the different ILs at the optimized IL content of 1% *w*/*v*. The values of contact angle are presented in Figure 3, showing the average contact angle between CF and the epoxy of 29.5°, which corresponds to poor wettability due to the inert fiber surface. After its treatment with IL, a 27.6%, 30.7% and 34.9% decrease was observed for CF-1Cl, CF-1NTF$_2$ and CF-1OH, respectively, indicating enhanced compatibility [43]. This also indicates that the chemical nature of the fiber surface was modified, although only 1% *w*/*v* of IL was used. The maximum decrease in contact angle shown by CF-1OH could be due to the presence of a functional group with polar characteristics that might enhance its surface polarity compared to the other samples, enabling dipole-dipole interactions and hydrogen bonding. Indeed, better compatibility between epoxy and CF from the lower contact angle due to high surface activity and functionality favors chemical and physical interlocking, contributing to the interfacial adhesion in the composite [44], helping to justify the previous IFSS results.
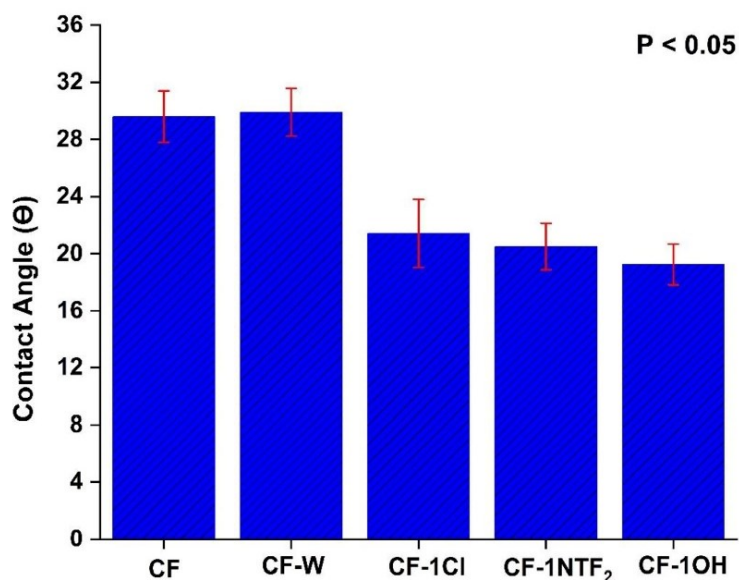
Figure 3. Contact angles of epoxy resin: CF, CF-1Cl, CF-1NTf$_2$ and CF-1OH.

The morphological analysis of the interfacial pull-out region of the samples carried-out to assess epoxy retention and its interaction with the fiber surface is shown in Figure 4. Large break gaps and debonded interfaces due to the shear forces can be seen on CF. The micrograph of CF, without sizing, shows large gaps that could result from relatively weak interface bonding strength and stress transfer efficiency. Clearly, a dense matrix layer was still there after the pull-out for CF-1Cl, CF-1NTf$_2$ and CF-1OH, which resulted from a relatively stronger interaction with the fiber. The serrated bonding aspects were also evident at the surface of IL-modified samples, suggesting increased energy absorption leading to composite toughening [34].

3.3. Surface Analysis

After the modification of CF with IL, a weight gain was observed, being 10.94%, 9.34% and 7.38% for CF-1Cl, CF-1NTf$_2$ and CF-1OH, respectively. In addition, among all the studied concentrations, the increase in weight was maximum for CF-Cl with only 1% *w/v* of IL, suggesting an optimized amount of IL on the fiber surface that triggered a change in surface properties. Figure 5 shows the FTIR-ATR transmittance spectra of CF, CF-1Cl, CF-1NTf$_2$ and CF-1OH, and the transmittance peaks of the studied ILs are detailed as supplementary material (Tables S1–S3) to aid in the discussion. The CF spectrum shows a straight line with no transmittance peak due to the absence of any functional group on the CF surface. After the surface treatments with 1% *w/v* of IL, various transmittance peaks associated with IL were observed. In the spectrum of CF-1NTf$_2$, peaks due to aromatic stretching of the imidazolium ring can be seen at 3121 cm^{-1} and 3158 cm^{-1}. Specific peaks related to NTf$_2$ appeared at 1349 cm^{-1} (O–S–O, stretching) and 1056 cm^{-1} (S-N-S, stretching), and there are other peaks at 2878 cm^{-1}, 2941 cm^{-1} and 2968 cm^{-1} that belong to C-H (stretching) of the linear alkyl chain attached to the imidazolium ring. The peak present at 1571 cm^{-1} is due to the bending of C-N in the aromatic ring [45–47].
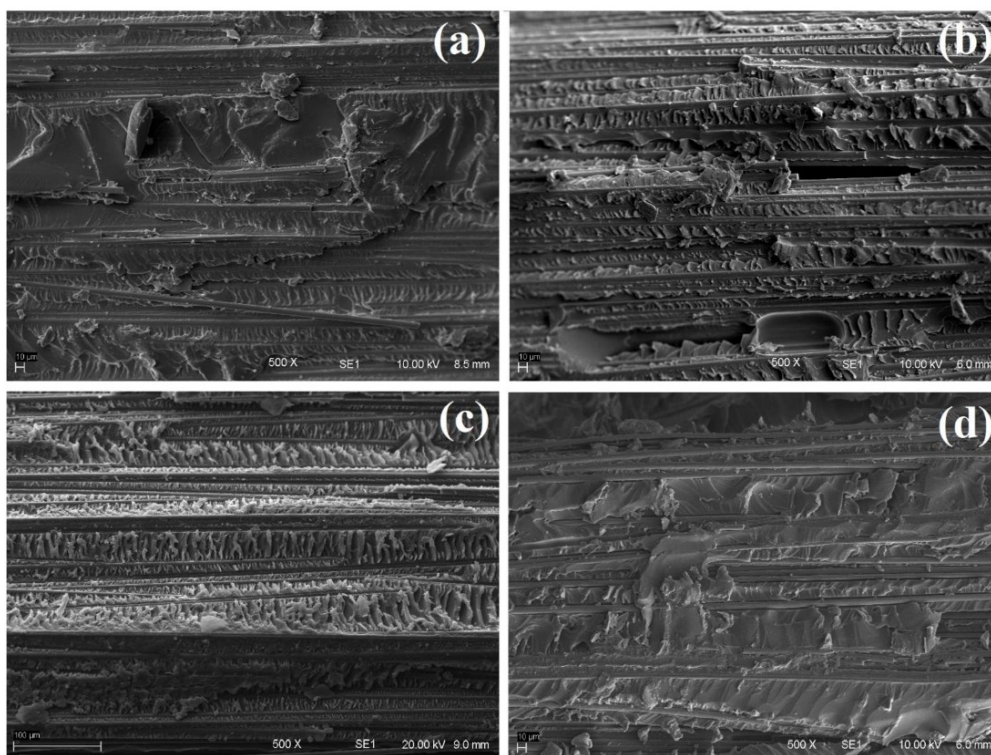
Figure 4. SEM micrographs of the interfacial pull-out region of the samples: (**a**) CF, (**b**) CF-1Cl, (**c**) CF-1NTf$_2$ and (**d**) CF-1OH.
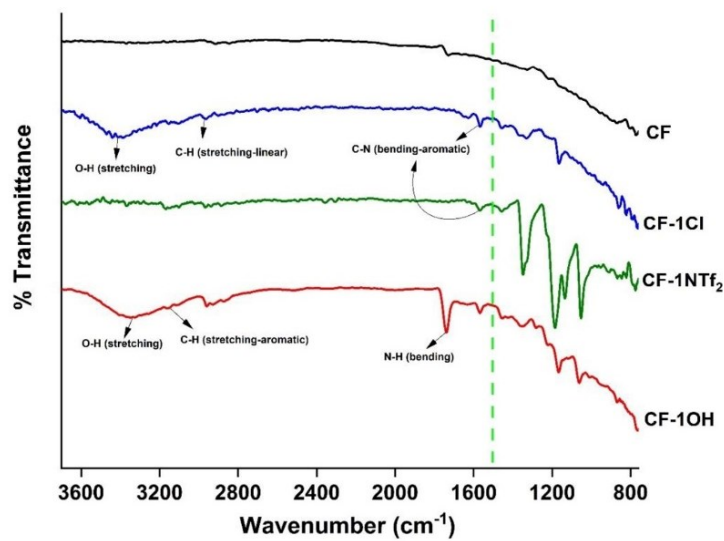

Figure 5. FTIR-ATR transmittance spectra for the studied CF samples.

For CF-1Cl, in addition to the peaks (2973 cm^{-1}, 2870 cm^{-1}, 1600 cm^{-1}) corresponding to the imidazolium ring and linear carbon chain, a broad peak at around 3200 cm^{-1} is present, which corresponds to the OH stretching. A broad peak for OH reveals hydrogen bonding corresponding to the water molecule [5]. For $C_2OHMImCl$, the peak at 1340 cm^{-1} is due to the bending vibration of the OH functional group, whereas the peak at 3316 cm^{-1} is due to OH stretching, indicating its hydrophilic nature. The attachment of IL to the CF surface suggests a favorable interaction between them, which may arise from the delocalized electronic cloud of the IL's imidazolium ring and sp^2 hybridized carbon atoms in the hexagonal structure of CF [48].

The surface morphology of CF samples analyzed with SEM micrographs is shown in Figure 6. The facile way adopted to modify the CF with ILs produced a significant change on its surface. The micrographs show a smooth surface containing carbon fiber having some inherently available oxygen as shown in EDS. The presence of IL can be observed as a dispersed phase of nanostructured particles attached and uniformly distributed over the surface of the CF without affecting its surface topography in CF-1Cl, CF-1NTf$_2$ and CF-1OH. Careful observation shows that the morphology of the surface of IL-treated CF was different. C_4MImCl was present on the surface as small irregular-shaped particles and even as some aggregates. $C_4MImNTf_2$ was present on the surface as a layered type of structure, whereas $C_2OHMImCl$ appeared as a circular particle, comparatively larger than the others.

Elemental analysis of the carbon fiber surfaces showed the presence of specific elements belonging to the ILs used. The compositional maps showed chlorine for CF-1Cl, sulfur and fluorine for CF-1NTf$_2$, and chlorine for CF-1OH, in addition to carbon and oxygen, being distinguishable characteristics to affirm the presence of the corresponding ILs on the CF surface. The attachment of IL to CF may be possible due to π-π bond stacking, and this is the only apparent mechanism that can provide interaction [30]. Flexibly, present on the surface of carbon fiber, its molecular component will provide a bonding mechanism with the epoxy matrix.

An X-ray diffraction analysis was carried out to investigate the effect of IL on the crystallite size and microstrains of CF. The crystallite size is basically the mean size of coherent-scattering regions in a specified direction of CF. The XRD spectra of the fibers show two discernible peaks, one at $2\theta = 43.9°$, corresponding to the 002 plane that is perpendicular to the graphite layers (perpendicular to the fiber axis), and one at $2\theta = 24.8°$, representing the 100 planes along the graphite layers. The crystallites are mainly oriented along the fiber axis and the 002 plane basically reflects its turbostratic structure.

The average crystallite size (L_c) in the direction of the 002 plane is within 2.07–1.89 nm and the crystallite size (L_a) along the 100 plane is within 1.87–1.94 nm. Both the crystallite size and microstrain have been calculated from FWHM and by using Scherrer's equation. A broad peak belonging to the 002 plane is observed for CF, whereas the broadening is reduced for CF-1Cl, CF-1NTf$_2$ and CF-1OH, as shown in Figure 7. The crystallite size calculated for CF along L_c and L_a is 2.04 nm and 1.87 nm, respectively. The crystallite size (L_c) was reduced for CF-1Cl, CF-1NTf$_2$ and CF-1OH, whereas a slight increase in L_a can be seen compared to CF. This improved microstructure behavior of CF due to IL means increased surface area of the graphitic structure along basal planes. The alignment of the hexagonal graphitic structure along the basal plane has the potential to enhance the electrical and mechanical properties at the fiber surface. Better ordering of the graphitic microstructure in both directions has contributed to the decrease in strain values [43,49]. An increased crystallite size (L_a) decreased the strain between the layers of carbon atoms and both of these effects have resulted in a broadening of the peak depicting a more relaxed microstructure [50].
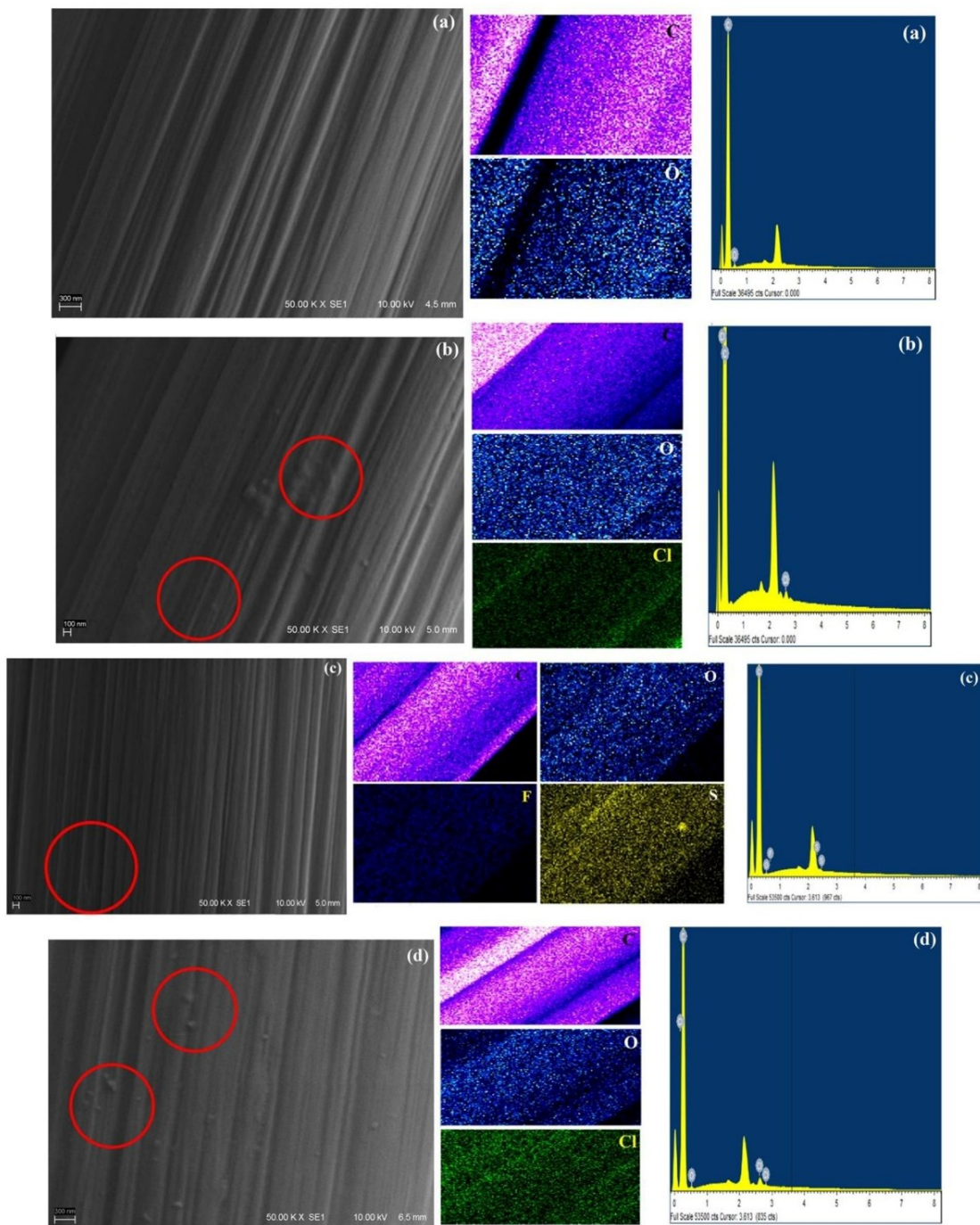
51

Figure 6. SEM micrographs, elemental maps and EDS spectrum of the samples: (**a**) CF, (**b**) CF-1Cl, (**c**) CF-1NTf$_2$ and (**d**) CF-1OH.
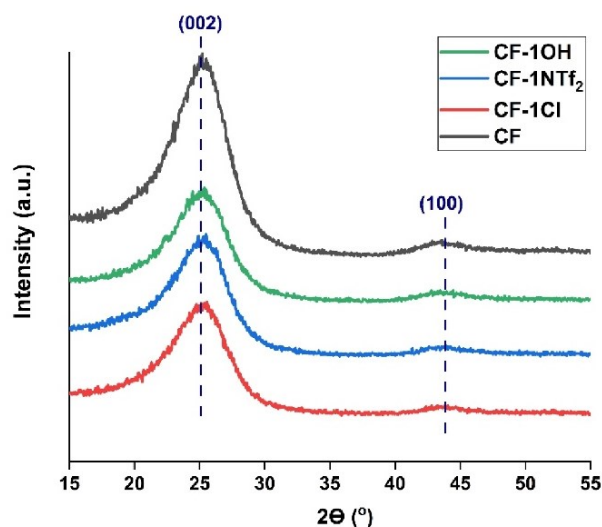
Figure 7. XRD spectrum of the studied samples and zoomed-in view of the 002 peak.

3.4. Electrical Properties

Carbon fiber-based composites are suited for multifunctional applications due to their inherent electrical and mechanical properties, and it was a primary objective of this study to increase CF electrical conductivity. The obtained values of electrical resistivity and contact resistance are shown in Table 1, being 11.30 μAm and 325 Ω for the carbon fiber, with 29% lower than the manufacturer's value (SIGRAFIL C T50-4.8/280-UN), which is acceptable for comparison purposes [51].

Table 1. Electrical resistivity and contact resistance of the CF samples.

	Resistivity (μAm)	Contact Resistance (Ω)
CF	11.30 ± 0.14	325
CF-1Cl	8.39 ± 3.68	244
CF-1NTF$_2$	3.33 ± 0.64	297
CF-1OH	2.84 ± 0.28	284

After IL treatment, the CF electrical resistivity was reduced, which can be explained by analyzing the constituents (cation, anion, alkyl side chain, functional group) of the ILs, being attributed to a more ordered structure long-range ion pair distribution on the fiber surface [52]. It is worthwhile to discuss the different characteristics of the hydroxyl functional group (OH) on the alkyl side chain, where the presence of polar groups enhances the surface polarizability in the presence of an electrical field due to an uneven distribution of charges. The polarity of the functional group (OH greater than CH_3) influences the overall electrical transport mechanism of the IL [51].

The contribution of ILs towards conductivity can be explained by considering the electron conduction dominancy over the ion contribution in the dry state. Primarily, the use of imidazolium cation showed its good charge carrying ability, which is more effective in the parallel direction of the imidazolium ring than in the perpendicular direction. The reduced electrical resistivity of CF-1NTF$_2$ compared to CF-1Cl is due to its presence as a layered structure on a planar surface, influencing the differential capacitance inside the layers [53]. In the case of NTf$_2$, the anion has a greater ability to diffuse and form multiple H-bonds via oxygen atoms in addition to having a strong delocalized negative charge,

which reduces the hydrogen bonding with cation and contributes to charge carrying for electrical conduction [54]. The low percentage of IL (1% w/v) in the present case, provides reduced ion pairing or aggregation, which increases the number of available charge carriers and its mobility. Compared to CF-1Cl and CF-1OH, the reduced electrical resistivity of CF-1OH is due to better packing with smaller anion and polar nature from the presence of the OH group [2,55].

The thermal stability of CF and IL-modified CF has been determined by thermogravimetric analysis (Figure 8). CF is thermally stable up to 600 °C, and the thermal stability of IL-modified CF is mainly dependent on the thermal stability of the particular IL [56]. Initially, loss of water has been observed in CF treated with chloride ILs. The onset temperature of degradation of CF-1NTF$_2$ is higher compared to that of CF-1Cl and CF-1OH, which can be attributed to the anion. Overall, the IL-treatment provided CF with thermal stabilities that are high enough for common CF/epoxy composite applications.
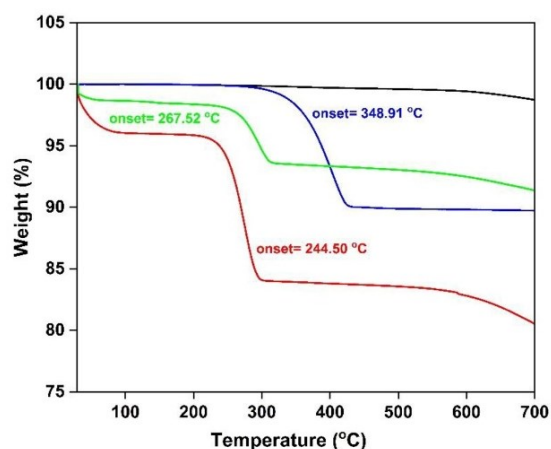
Figure 8. TG results for CF (black), CF-1Cl (red), CF-1NTf$_2$ (blue) and CF-1OH (green).

4. Conclusions

A procedure for the surface treatment of CF has been developed, in which an optimized concentration of 1% w/v IL was identified. A large increase in the IFSS between CF and epoxy was obtained with the IL 1-(2-hydroxyethyl)-3-methylimidazolium chloride, showing potential use for advanced composites. Enhanced electrical conductivity on the fiber surface was also obtained, allowing the design of composites with more electrically conductive interfaces. The obtained characteristics provide an opportunity to use carbon fiber, including recycled carbon fiber, in wider multifunctional applications.

References

1. Kar, M.; Plechkova, N.V.; Seddon, K.R.; Pringle, J.M.; MacFarlane, D.R. Ionic liquids–further progress on the fundamental issues. *Aust. J. Chem.* **2018**, *72*, 3–10. [CrossRef]
2. Kowsari, M.; Alavi, S.; Ashrafizaadeh, M.; Najafi, B. Molecular dynamics simulation of imidazolium-based ionic liquids. II. Transport coefficients. *J. Chem. Phys.* **2009**, *130*, 014703. [CrossRef] [PubMed]
3. Cao, H.; Hu, Y.; Xu, W.; Wang, Y.; Guo, X. Recent progress in the assembly behavior of imidazolium-based ionic liquid surfactants. *J. Mol. Liq.* **2020**, *319*, 114354. [CrossRef]
4. Izgorodina, E.I.; MacFarlane, D.R. Nature of hydrogen bonding in charged hydrogen-bonded complexes and imidazolium-based ionic liquids. *J. Phys. Chem. B* **2011**, *115*, 14659–14667. [CrossRef] [PubMed]
5. Chen, K.; Xu, W.; Ding, Y.; Xue, P.; Sheng, P.; Qiao, H.; Wang, S.; Yu, Y. Mechanical and thermal properties of all-wood biocomposites through controllable dissolution of cellulose with ionic liquid. *Polymers* **2020**, *12*, 361. [CrossRef]
6. May, D.; Goergen, C.; Friedrich, K. Multifunctionality of polymer composites based on recycled carbon fibers: A review. *Adv. Ind. Eng. Polym. Res.* **2021**, *4*, 70–81. [CrossRef]
7. Abdou, T.R.; Junior, A.B.; Espinosa, D.C.R.; Tenório, J.A.S. Recycling of polymeric composites from industrial waste by pyrolysis: Deep evaluation for carbon fibers reuse. *Waste Manag.* **2021**, *120*, 1–9. [CrossRef]
8. Wang, Y.; Jin, B.; Ye, D.; Liu, Z. Fully recyclable carbon fiber reinforced vanillin-based epoxy vitrimers. *Eur. Polym. J.* **2022**, *162*, 110927. [CrossRef]
9. Pimenta, S.; Pinho, S.T. The effect of recycling on the mechanical response of carbon fibres and their composites. *Compos. Struct.* **2012**, *94*, 3669–3684. [CrossRef]
10. Boulanghien, M.; R'Mili, M.; Bernhart, G.; Berthet, F.; Soudais, Y. Mechanical characterization of carbon fibres recycled by steam thermolysis: A statistical approach. *Adv. Mater. Sci. Eng.* **2018**, *2018*, 8630232. [CrossRef]
11. Henry, L.; Schneller, A.; Doerfler, J.; Mueller, W.M.; Aymonier, C.; Horn, S. Semi-continuous flow recycling method for carbon fibre reinforced thermoset polymers by near-and supercritical solvolysis. *Polym. Degrad. Stab.* **2016**, *133*, 264–274. [CrossRef]
12. Song, W.; Magid, A.; Li, D.; Lee, K.-Y. Application of recycled carbon-fibre-reinforced polymers as reinforcement for epoxy foams. *J. Environ. Manag.* **2020**, *269*, 110766. [CrossRef] [PubMed]
13. Fonseca, J.H.; Han, G.; Quagliato, L.; Kim, Y.; Choi, J.; Keum, T.; Kim, S.; Kim, N.; Lee, H. Design and numerical evaluation of recycled-carbon-fiber-reinforced polymer/metal hybrid engine cradle concepts. *Int. J. Mech. Sci.* **2019**, *163*, 105115. [CrossRef]
14. Cai, G.; Wada, M.; Ohsawa, I.; Kitaoka, S.; Takahashi, J. Interfacial adhesion of recycled carbon fibers to polypropylene resin: Effect of superheated steam on the surface chemical state of carbon fiber. *Compos. Part A Appl. Sci. Manuf.* **2019**, *120*, 33–40. [CrossRef]
15. Upadhyayula, V.K.; Gadhamshetty, V.; Athanassiadis, D.; Tysklind, M.; Meng, F.; Pan, Q.; Cullen, J.M.; Yacout, D.M. Wind Turbine Blades Using Recycled Carbon Fibers: An Environmental Assessment. *Environ. Sci. Technol.* **2022**, *56*, 1267–1277. [CrossRef] [PubMed]
16. Wang, Y.; Zhang, S.; Luo, D.; Shi, X. Effect of chemically modified recycled carbon fiber composite on the mechanical properties of cementitious mortar. *Compos. Part B Eng.* **2019**, *173*, 106853. [CrossRef]
17. Lee, H.; Ohsawa, I.; Takahashi, J. Effect of plasma surface treatment of recycled carbon fiber on carbon fiber-reinforced plastics (CFRP) interfacial properties. *Appl. Surf. Sci.* **2015**, *328*, 241–246. [CrossRef]
18. Jiang, G.; Pickering, S.; Walker, G.; Wong, K.; Rudd, C. Surface characterisation of carbon fibre recycled using fluidised bed. *Appl. Surf. Sci.* **2008**, *254*, 2588–2593. [CrossRef]
19. Jiang, G.Z.; Pickering, S.J. Recycled Carbon Fibres: Contact Angles and Interfacial Bonding with Thermoset Resins. In *Materials Science Forum*. 2012, pp. 255–261. Available online: https://www.scientific.net/MSF.714.255 (accessed on 30 August 2022).
20. Feng, N.; Wang, X.; Wu, D. Surface modification of recycled carbon fiber and its reinforcement effect on nylon 6 composites: Mechanical properties, morphology and crystallization behaviors. *Curr. Appl. Phys.* **2013**, *13*, 2038–2050. [CrossRef]
21. Pakdel, E.; Wang, J.; Varley, R.; Wang, X. Recycled carbon fiber nonwoven functionalized with fluorine-free superhydrophobic PDMS/ZIF-8 coating for efficient oil-water separation. *J. Environ. Chem. Eng.* **2021**, *9*, 106329. [CrossRef]
22. Wong, K.; Mohammed, D.S.; Pickering, S.; Brooks, R. Effect of coupling agents on reinforcing potential of recycled carbon fibre for polypropylene composite. *Compos. Sci. Technol.* **2012**, *72*, 835–844. [CrossRef]
23. Burn, D.; Harper, L.T.; Johnson, M.; Warrior, N.; Nagel, U.; Yang, L.; Thomason, J. The usability of recycled carbon fibres in short fibre thermoplastics: Interfacial properties. *J. Mater. Sci.* **2016**, *51*, 7699–7715. [CrossRef]

24. Kim, K.-W.; Lee, H.-M.; An, J.-H.; Chung, D.-C.; An, K.-H.; Kim, B.-J. Recycling and characterization of carbon fibers from carbon fiber reinforced epoxy matrix composites by a novel super-heated-steam method. *J. Environ. Manag.* **2017**, *203*, 872–879. [CrossRef]

25. Palola, S.; Laurikainen, P.; García-Arrieta, S.; Goikuria Astorkia, E.; Sarlin, E. Towards Sustainable Composite Manufacturing with Recycled Carbon Fiber Reinforced Thermoplastic Composites. *Polymers* **2022**, *14*, 1098. [CrossRef] [PubMed]

26. Van de Werken, N.; Reese, M.S.; Taha, M.R.; Tehrani, M. Investigating the effects of fiber surface treatment and alignment on mechanical properties of recycled carbon fiber composites. *Compos. Part A Appl. Sci. Manuf.* **2019**, *119*, 38–47. [CrossRef]

27. Okajima, I.; Hiramatsu, M.; Shimamura, Y.; Awaya, T.; Sako, T. Chemical recycling of carbon fiber reinforced plastic using supercritical methanol. *J. Supercrit. Fluids* **2014**, *91*, 68–76. [CrossRef]

28. Sun, H.; Guo, G.; Memon, S.A.; Xu, W.; Zhang, Q.; Zhu, J.-H.; Xing, F. Recycling of carbon fibers from carbon fiber reinforced polymer using electrochemical method. *Compos. Part A Appl. Sci. Manuf.* **2015**, *78*, 10–17. [CrossRef]

29. Alves, S.M.C.; da Silva, F.S.; Donadon, M.V.; Garcia, R.R.; Corat, E.J. Process and characterization of reclaimed carbon fiber composites by pyrolysis and oxidation, assisted by thermal plasma to avoid pollutants emissions. *J. Compos. Mater.* **2018**, *52*, 1379–1398. [CrossRef]

30. Ghafoor, B.; Schrekker, H.S.; Morais, J.; Amico, S.C. Surface modification of carbon fiber with imidazolium ionic liquids. *Compos. Interfaces* **2022**, *29*, 915–927. [CrossRef]

31. Eyckens, D.J.; Servinis, L.; Scheffler, C.; Wölfel, E.; Demir, B.; Walsh, T.R.; Henderson, L.C. Synergistic interfacial effects of ionic liquids as sizing agents and surface modified carbon fibers. *J. Mater. Chem. A* **2018**, *6*, 4504–4514. [CrossRef]

32. Beggs, K.M.; Perus, M.D.; Servinis, L.; O'Dell, L.A.; Fox, B.L.; Gengenbach, T.R.; Henderson, L.C. Rapid surface functionalization of carbon fibres using microwave irradiation in an ionic liquid. *RSC Adv.* **2016**, *6*, 32480–32483. [CrossRef]

33. Prabhakara, M.; Maiti, B. Ionic liquid-immobilized proline (s) organocatalyst-catalyzed one-pot multi-component Mannich reaction under solvent-free condition. *Res. Chem. Intermed.* **2020**, *46*, 2381–2401. [CrossRef]

34. Zhou, J.; Li, Y.; Li, N.; Hao, X.; Liu, C. Interfacial shear strength of microwave processed carbon fiber/epoxy composites characterized by an improved fiber-bundle pull-out test. *Compos. Sci. Technol.* **2016**, *133*, 173–183. [CrossRef]

35. Zhang, F.-H.; Wang, R.-G.; He, X.-D.; Wang, C.; Ren, L.-N. Interfacial shearing strength and reinforcing mechanisms of an epoxy composite reinforced using a carbon nanotube/carbon fiber hybrid. *J. Mater. Sci.* **2009**, *44*, 3574–3577. [CrossRef]

36. He, D.; Soo, V.K.; Stojcevski, F.; Lipiński, W.; Henderson, L.C.; Compston, P.; Doolan, M. The effect of sizing and surface oxidation on the surface properties and tensile behaviour of recycled carbon fibre: An end-of-life perspective. *Compos. Part A Appl. Sci. Manuf.* **2020**, *138*, 106072. [CrossRef]

37. He, M.; Qi, P.; Xu, P.; Cai, Q.; Li, P.; Jia, X.; Yang, X. Establishing a phthalocyanine-based crosslinking interphase enhances the interfacial performances of carbon fiber/epoxy composites at elevated temperatures. *Compos. Sci. Technol.* **2019**, *173*, 24–32. [CrossRef]

38. Fonseca, E.; da Silva, V.D.; Klitzke, J.S.; Schrekker, H.S.; Amico, S.C. Imidazolium ionic liquids as fracture toughening agents in DGEBA-TETA epoxy resin. *Polym. Test.* **2020**, *87*, 106556. [CrossRef]

39. Soares, B.G.; Ferreira, S.C.; Livi, S. Modification of anionic and cationic clays by zwitterionic imidazolium ionic liquid and their effect on the epoxy-based nanocomposites. *Appl. Clay Sci.* **2017**, *135*, 347–354. [CrossRef]

40. Song, W.; Gu, A.; Liang, G.; Yuan, L. Effect of the surface roughness on interfacial properties of carbon fibers reinforced epoxy resin composites. *Appl. Surf. Sci.* **2011**, *257*, 4069–4074. [CrossRef]

41. Arnold, C.L.; Beggs, K.M.; Eyckens, D.J.; Stojcevski, F.; Servinis, L.; Henderson, L.C. Enhancing interfacial shear strength via surface grafting of carbon fibers using the Kolbe decarboxylation reaction. *Compos. Sci. Technol.* **2018**, *159*, 135–141. [CrossRef]

42. Matthews, R.P.; Ashworth, C.; Welton, T.; Hunt, P.A. The impact of anion electronic structure: Similarities and differences in imidazolium based ionic liquids. *J. Phys. Condens. Matter* **2014**, *26*, 284112. [CrossRef]

43. Deng, J.; Xu, L.; Zhang, L.; Peng, J.; Guo, S.; Liu, J.; Koppala, S. Recycling of carbon fibers from CFRP waste by microwave thermolysis. *Processes* **2019**, *7*, 207. [CrossRef]

44. Liu, Y.C.; Lu, D.N. Surface energy and wettability of plasma-treated polyacrylonitrile fibers. *Plasma Chem. Plasma Process.* **2006**, *26*, 119–126. [CrossRef]

45. Prasad, G.; Reddy, K.M.; Padamasuvarna, R.; Mohan, T.M.; Krishna, T.V.; Kumare, V.R. Thermophysical properties of 1-butyl-3-methylimidazolium bis (trifluoromethylsulfonyl) imide with 2-ethoxyethanol from T = (298.15 to 323.15) K at atmospheric pressure. *J. Mol. Liq.* **2018**, *251*, 335–344. [CrossRef]

46. Yu, L.; Pizio, B.S.; Vaden, T.D. Conductivity and spectroscopic investigation of bis (trifluoromethanesulfonyl) imide solution in ionic liquid 1-butyl-3-methylimidazolium bis (trifluoromethanesulfonyl) imide. *J. Phys. Chem. B* **2012**, *116*, 6553–6560. [CrossRef]

47. Akai, N.; Kawai, A.; Shibuya, K. First observation of the matrix-isolated FTIR spectrum of vaporized ionic liquid: An example of EmimTFSI, 1-Ethyl-3-methylimidazolium Bis (trifluoromethanesulfonyl) imide. *Chem. Lett.* **2008**, *37*, 256–257. [CrossRef]

48. Ou, R.; Xie, Y.; Shen, X.; Yuan, F.; Wang, H.; Wang, Q. Solid biopolymer electrolytes based on all-cellulose composites prepared by partially dissolving cellulosic fibers in the ionic liquid 1-butyl-3-methylimidazolium chloride. *J. Mater. Sci.* **2012**, *47*, 5978–5986. [CrossRef]

49. Zhu, H.; Li, X.; Han, F.; Dong, Z.; Yuan, G.; Ma, G.; Westwood, A.; He, K. The effect of pitch-based carbon fiber microstructure and composition on the formation and growth of SiC whiskers via reaction of such fibers with silicon sources. *Carbon* **2016**, *99*, 174–185. [CrossRef]

50. Dobiášová, L.; Starý, V.; Glogar, P.; Valvoda, V. Analysis of carbon fibers and carbon composites by asymmetric X-ray diffraction technique. *Carbon* **1999**, *37*, 421–425. [CrossRef]

51. Guimarães, C.J.B.; Aguiar, A.P.d.; Castro, A.T.d. Accurate measurement of pitch-based carbon fiber electrical resistivity. *Polímeros* **2021**, *31*. [CrossRef]

52. Osti, N.C.; Mamontov, E. Microscopic dynamics in room-temperature ionic liquids confined in materials for supercapacitor applications. *Sustain. Energy Fuels* **2020**, *4*, 1554–1576. [CrossRef]

53. Salanne, M. Ionic liquids for supercapacitor applications. In *Ionic Liquids II*; Springer: Cham, Switzerland, 2017; pp. 29–53.

54. Daguenet, C.; Dyson, P.J.; Krossing, I.; Oleinikova, A.; Slattery, J.; Wakai, C.; Weingärtner, H. Dielectric response of imidazolium-based room-temperature ionic liquids. *J. Phys. Chem. B* **2006**, *110*, 12682–12688. [CrossRef] [PubMed]

55. Kowsari, M.; Alavi, S.; Ashrafizaadeh, M.; Najafi, B. Molecular dynamics simulation of imidazolium-based ionic liquids. I. Dynamics and diffusion coefficient. *J. Chem. Phys.* **2008**, *129*, 224508. [CrossRef] [PubMed]

56. Xu, C.; Cheng, Z. Thermal stability of ionic liquids: Current status and prospects for future development. *Processes* **2021**, *9*, 337. [CrossRef]

MULTIFUNCTIONAL CHARACTERISTICS OF CARBON FIBERS MODIFIED WITH

IMIDAZOLIUM IONIC LIQUIDS

Bilal Ghafoor[1], Henri Stephan Schrekker[2], Sandro Campos Amico[1]

[1]PPGE3M, Federal University of Rio Grande do Sul, Porto Alegre/RS, 91501-970, Brazil

bilalghafoorist@hotmail.com, amico@ufrgs.br

[2]Laboratory of Technological Processes and Catalysis, Institute of Chemistry, Federal University of Rio Grande

do Sul, Porto Alegre/RS, 91501-970, Brazil

henri.schrekker@ufrgs.br

SUPPLEMENTARY MATERIAL
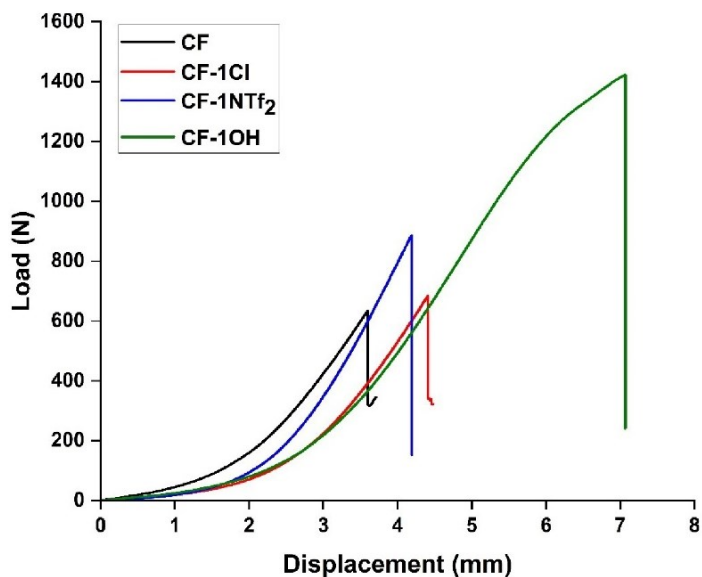
Figure S1. Load-displacement pull-out curves of CF, CF-1Cl, CF-1NTf$_2$ and CF-1OH.
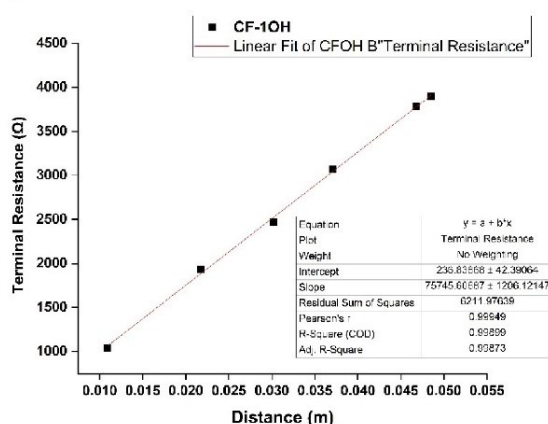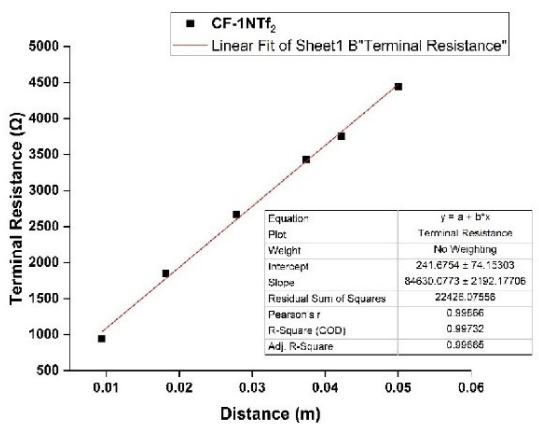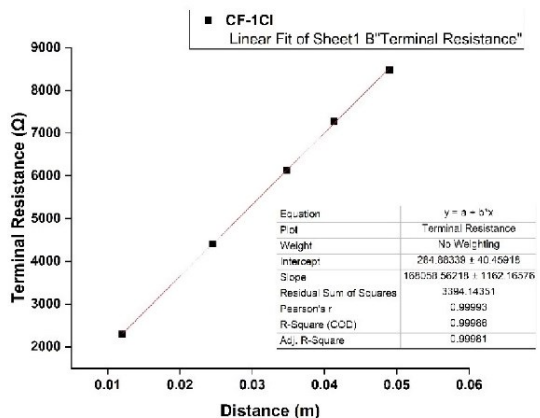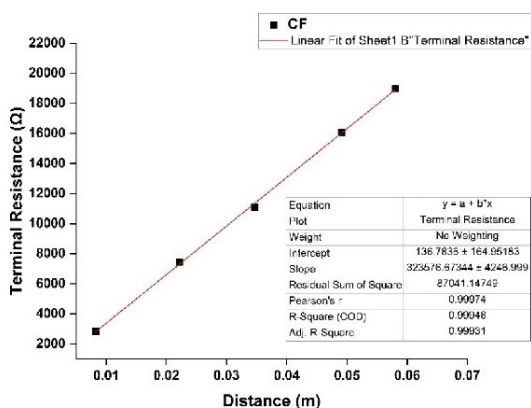
Figure S2. Curve fitting of two terminal electrical resistance vs distance for CF, CF-1Cl, CF-1NTf$_2$ and CF-1OH.
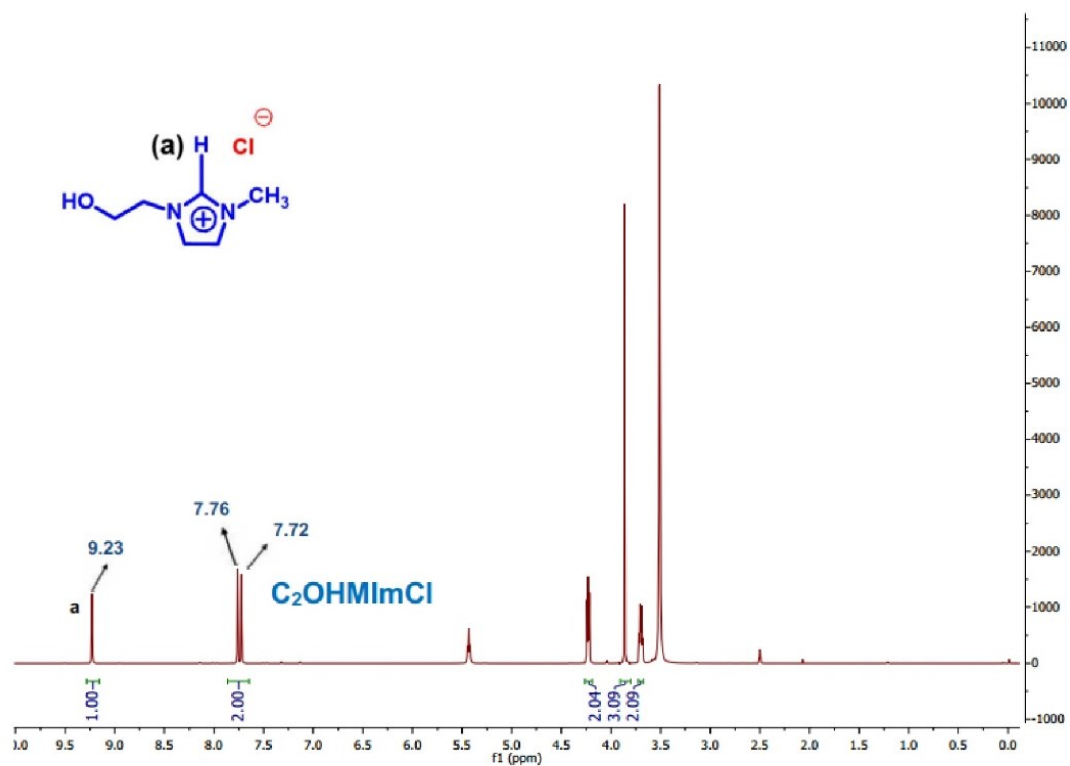
Figure S3. ^{1}H NMR spectrum of 1-(2-hydroxyethyl)-3-methylimidazolium chloride, C$_2$OHMImCl.

Table S1. FTIR transmittance peaks of C$_4$MImCl [5, 45-47].

Wavenumber of the bands	
Wave number (cm^{-1})	**Description**
3300	O-H (stretching)
2973, 2870	C-H (stretching-linear)
1635	C=C (stretching)
1600	N-H (bending)
1573	C–N (bending-aromatic)
1169	C-H (stretching-aromatic)
1166	C–H (bending-aromatic)
840	C-H (bending)

Table S2. FTIR transmittance peaks of $C_4MImNTf_2$ [45-47].

Wave number (cm^{-1})	Description
3121, 3158	C-H (stretching-aromatic)
2878, 2941, 2968	C-H (stretching-linear)
1571	C–N (bending-aromatic)
1466, 1437	C-C (stretch-aromatic), C-H (scissoring)
1349	O–S–O (stretching)
1186, 1138	C-N (stretching), C–H (scissoring)
1056	S-N-S (stretching)
790	C–H, -HC=CH- (bending)
883	C-H (bending)

Table S3. FTIR transmittance peaks of $C_2OHMImCl$ [5, 45-47]

Wave number (cm^{-1})	Description
3316	O-H stretching vibration
3148, 3097	C-H (stretching-aromatic)
2959, 2874	C-H (stretching-linear)
1568	C–N (bending-aromatic)
1450	C-C (stretch-aromatic)
1340	O-H (bending)
1258	C-N stretching (aromatic)
1167, 1069	C-H (bending), C-N (stretching)
868	C-H (bending)

Thermomechanical properties of imidazolium ionic liquid-modified mwcnt/ carbon fiber/epoxy hybrid composite laminates

Bilal Ghafoor[1] , Umar Farooq[2] , Henri Stephan Schrekker[3] and Sandro Campos Amico[1]

Abstract
Hybrid composite laminates with nanofillers are high performance materials for thermal and structural applications. In this work, multiwall carbon nanotubes (MWCNT) were non-covalently modified by treating them with 1 wt% or 5 wt% of ionic liquid (IL), 1-butyl-3-methylimidazolium chloride. The treated MWCNT were dispersed in epoxy resin (weight content: 0.2–2 wt% or 1 to 3 wt%, respectively) and used to obtain hybrid composite laminates based on carbon fibers (CF) molded by hand layup and vacuum bagging techniques. The hybrid composite laminate containing 1 wt% of MWCNT modified with 1 wt% of IL showed the best mechanical and thermomechanical properties, including an increase of 210% and 151% in flexural strength and modulus, and an increase of 101%, 116% and 29.3% in storage modulus, loss modulus and damping, respectively. Scanning and transmission electron micrographs showed the enhanced MWCNT dispersion and network at low IL content, justifying its improved mechanical properties. The application of a low amount of IL dispersant was found a promising approach to prepare MWCNT/CF/epoxy composites with enhanced properties.

Keywords
Hybrid composite, imidazolium ionic liquid, multiwalled carbon nanotube, vacuum bagging

Introduction

Carbon fiber reinforced composites (CFRC) are known for their high specific strength and modulus in longitudinal direction, which is not the case in through-the-thickness direction.[1] To improve that performance of CFRC, carbon based nanofillers such as single-wall carbon nanotubes (SWCNT), multi-wall carbon nanotubes (MWCNT), and carbon black are incorporated.[2] The presence of such nanofiller in composite structures provides resistance to mechanical loads and growth of cracks through physical interlocking in polymer matrices,[3] including the thickness direction.[4] Indeed, the combination of fiber, matrix, and nanofiller forming a three-component, or hybrid composite system can form a highly interconnected filler network that favors a multidimensional, high energy resistant structure.[5,6]

The effective transfer of nanofiller properties to obtain composites with improved performance is strongly dependent on its dispersion in the matrix, which can be predicted by the nanofiller surface characteristics.

Dispersion of MWCNT is challenging due to its non-polar nature and extended network of π-π attraction causing agglomeration in epoxy matrices. Methods applied to improve dispersion of MWCNT in epoxy include surface functionalization, mechanical mixing, and sonication.[7,8] Functionalized carbon nanotubes provide better dispersion, resulting in composites with better resistance to crack growth.[9,10] The optimum content of MWCNT in epoxy composites and the corresponding improvement in flexural

[1]PPGE3M, Federal University of Rio Grande do Sul, Porto Alegre, Brazil
[2]Department of Materials Science and Engineering, Institute of Space Technology, Islamabad, Pakistan
[3]Laboratory of Technological Processes and Catalysis, Institute of Chemistry, Federal University of Rio Grande do Sul, UFRGS IQ, Porto Alegre, Brazil

Corresponding author:
Bilal Ghafoor, PPGE3M, Federal University of Rio Grande do Sul, Av. Bento Gonçalves, 9500 - Setor 4 - Prédio 74 - Sala 211 Campus do Vale Porto Alegre/RS, Porto Alegre 90040-060, Brazil.
Email: bilalghafoorist@hotmail.com

strength and modulus are dependent on the dispersion method. Some of the works in the literature mention, respectively, 32% and 98% increase with ultrasonic dispersion of MWCNT (0.25 wt%),[11] 18.0% and 11.6% for high energy sonication of MWCNT (0.3 wt%),[12] 45% and 17% for mechanical mixing of MWCNT/carbon nanofibers (0.3 wt%),[13] 25% and 11% for mechanical mixing of MWCNT (2.4 wt%),[14,15] 15.4% and 7.15% for ultrasonic/high shearing of MWCNT (1 wt%),[1] 15.6% and 10.2% for mechanical mixing/sonication with amine-functionalized MWCNT (0.5 wt%),[16] and 28% and 19% for sonication with carboxyl-functionalized MWCNT (1.5 wt%).[17]

Recently, ionic liquids (IL) have emerged in the modification of carbon-based nanofillers as well as in the preparation of epoxy resins with improved properties. IL influences the curing kinetics of epoxy with the hardener and may also act as a hardener, affecting the overall properties of epoxy.[18] This can improve, for instance, toughness and viscoelastic properties, thus, under loading at high temperature.[19]

The cation and anion associated with the IL influence the properties of epoxy as well as the curing characteristics.[20] In particular, imidazolium-based IL provide a stronger interaction with carbon-based materials, promoting crosslinking in the epoxy resin, and causing a plasticizing effect. Imidazolium-based IL aid the dispersion of nanofillers due to the interaction of their cation π-electronic cloud with the nanofillers.[21,22] Previously, various imidazolium-based IL (1-ethyl-3-methyl-imidazolium acetate and 1-butyl-3-methylimidazolium hydrogen sulfate) have been applied to modify MWCNT for improved dispersion in polymer matrices.[23] In another case, imidazolium-based IL have been employed to modify carbon quantum dots and graphene oxide to obtain composites with reduced wear and friction rate. In both cases, the improvement in properties due to the IL was justified through secondary interactions with the nanofillers promoting better dispersion in polymers.[24,25] Since the IL enhanced two-component composites, this strategy could be extended to the manufacturing of three-component epoxy-based carbon fiber (CF) hybrid composites with improved overall properties. Even so, studies related to imidazolium IL-modified MWCNT incorporated into epoxy/CF composites are not easily found.

Considering that, the goal of the present study was to modify MWCNT with 1-butyl-3-methylimidazolium chloride (C_4MImCl) at various weight contents (1 and 5 wt%), disperse it in epoxy resin at various contents (up to 3 wt%) and to prepare cost effective improved-performance hybrid carbon fiber composites through a practical process.

Experimental

Materials

Epoxy resin (Araldite® 5052-Aerospace grade, Huntsman, USA), hardener (Aradur® 5052, Huntsman, USA), MWCNT (diameter 20–40 nm, length 5–15 μm, purity >95%, Chengdu Intl, China), polyacrylonitrile-based 3K-plain weave carbon fiber fabric (Toray, Taiwan), C_4MImCl (≥95% purity, Sigma-Aldrich, Brazil), acetone (99.5% purity, Sigma-Aldrich, Brazil) and ethanol (99.5% purity, Sigma-Aldrich, Brazil) were used as received.

Modification of MWCNT

MWCNT (3g) were treated with C_4MImCl (1 or 5 wt%). For that, C_4MImCl was added to 50 mL of anhydrous ethanol and stirred for 15 min at room temperature. The MWCNT were then added in the mixture and stirred for 15 min at room temperature and sonicated at 60°C and 60 Hz for 30 min. Subsequently, the ethanol was removed under vacuum at 60°C for 1 h. Commercial MWCNT and MWCNT modified with 1 wt% or 5 wt% of C_4MImCl were codified as MW, 1-MW and 5-MW, respectively, and the amount in weight of MWCNT added to epoxy is given as the last number, e.g., "0.2" in 1-MW-0.2.

Fabrication of hybrid composite laminates

The composite laminates were prepared by hand-lay-up followed by vacuum bagging (Figure 1). Initially, the treated MWCNT (with 1% of IL, or 5% of IL) were mechanically mixed with epoxy resin. The mixture was dispersed at 40 kHz for 15 min in an ultra-sonicator bath, followed by the addition of the hardener (100:38 (g:g), epoxy:hardener ratio). After mechanical mixing for 5 min, degassing at room temperature was done for 10 min, and the epoxy matrix with IL-modified MWCNT was applied to the carbon fabric by manual hand-lay-up. After complete impregnation of four fabric layers, the entire assembly was vacuum bagged. The laminates were demolded after 24 h of curing at room temperature followed by a post-curing at 100°C for 4 h, as suggested by the epoxy manufacturer. The approximate size of each composite laminate was 150 × 150 × 1 mm. The final hybrid carbon fiber composites are nominated using HCFC. So, the HCFC in which 1-MW-0.2 was used, is called as 1-HCFC-0.2. For comparison pure epoxy resin was also used to produce a CF composite, which is called EPCF.

Characterization

Fourier-transform infrared spectroscopy was performed with a Perkin Elmer Spectrum 1000 equipment. The transmission spectra were recorded with KBr pellets in the 400–4000 cm^{-1} range with 32 scans at a constant spectral resolution of 4 cm^{-1}, using a LiTaO$_3$ detector.

Dynamic mechanical analysis was performed according to ASTM D7028 for the determination of the epoxy glass transition temperature (T_g). The samples were cut to the
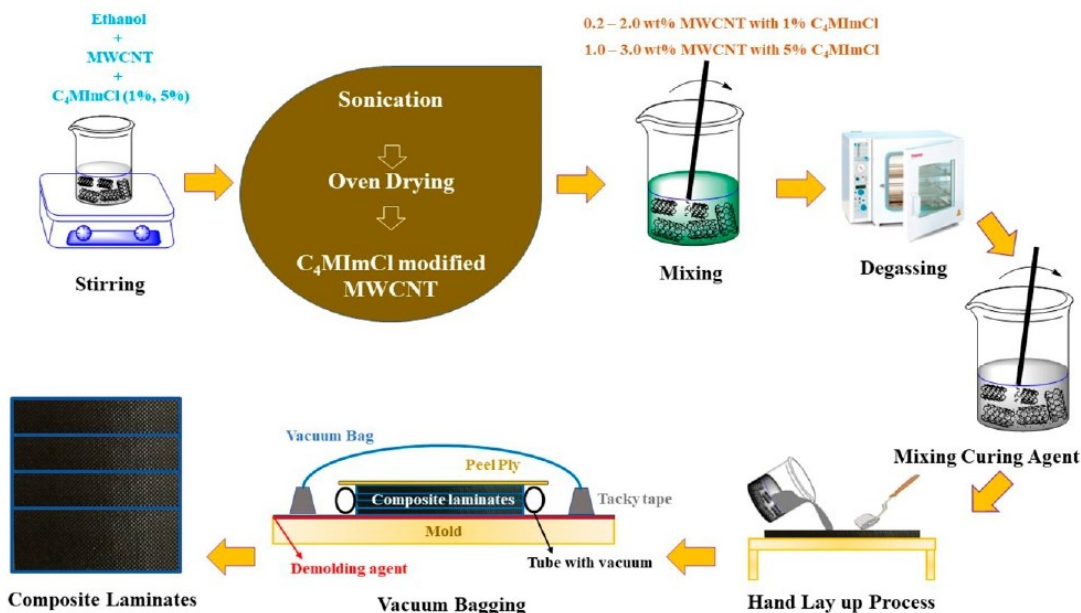
Figure 1. Schematic representation for the fabrication process of HCFC.

dimensions of 60 × 12 × 1 mm and analyzed with a DMA-2980 (TA instruments) equipment under dual cantilever mode and strain amplitude of 1 Hz. Temperature scan measurements were performed within 25–250°C at a heating rate of 10°C/min and a constant frequency of 1.0 Hz to determine storage modulus (E'), loss modulus (E'') and tan δ. The T_g was obtained from the storage modulus data.

Three-point flexural testing was performed using a universal testing machine Emic/Instron 23-5D with 10 kN load cell. Five specimens (60 × 13 × 1 mm) of each sample were tested at a constant speed of 2 mm/min according to ASTM D7264. ANOVA analysis was performed on the flexural strength and modulus results using commercial software Origin pro. The groups were compared using the Tukey test with 5% significance level.

Scanning electron microscopy was performed with a Carl Zeiss EVO MA10 electron microscope at an operating voltage of 20 kV. MW, 1-MW and fractured HCFC samples were gold coated and the images were acquired at various magnifications in secondary electron mode. EDS analysis was done for elemental compositional mapping of MW and 1-MW.

Transmission electron microscopy was performed with a Tecnai T20 microscope under an accelerating voltage of 200 kV. An ultramicrotome (Leica EM UC7) was used to obtain sectioned samples of ≈70 nm thickness, and deposited on a 200-mesh copper grid (EMS200-Cu). The dispersion of 1-MW and 5-MW in epoxy matrix was analyzed at different magnifications.

Results and discussion

The SEM micrograph and the EDS elemental maps of MW show an intermingled structure of nanotubes and the presence of carbon and oxygen, respectively (Figure 2(a)). In contrast, 1-MW exhibited a layered type of structure due to the presence of IL, as confirmed by the presence of chloride on its surface (Figure 2(b)). This presence of IL on the surface of 1-MW was also confirmed by FTIR analysis (Figure 3). The peak at around 1600 cm^{-1} corresponds to the aromatic C-C bond of MWCNT, and the one at 3429 cm^{-1} is related to the hydroxyl group of MW. 1-MW showed the characteristic IL peaks at 2973 and 2870 cm^{-1} corresponding to C-H linear stretching, and at 1573 cm^{-1} corresponding to C-N bending, whereas an enhanced OH peak indicates the presence of water. In general, MWCNT are not easily dispersed in common solvents due to their strong π-π interactions. Non-covalent functionalization of MWCNT is a facile way of modifying them without disrupting their extended π-conjugated structure and retaining the inherent electrical and mechanical properties. The interaction of the imidazolium IL cation-π cloud and the π-electronic surface of MWCNT leads to their disentanglement and the IL-epoxy interaction aids in their dispersion in epoxy matrices.[26] C$_4$MImCl favors the isolation of MWCNT bundles during the ultrasonic treatment which provides high shear to separates the bundles and, at the same time, promotes adsorption of IL onto the MWCNT surface.[27] Previous theoretical and spectroscopic studies have
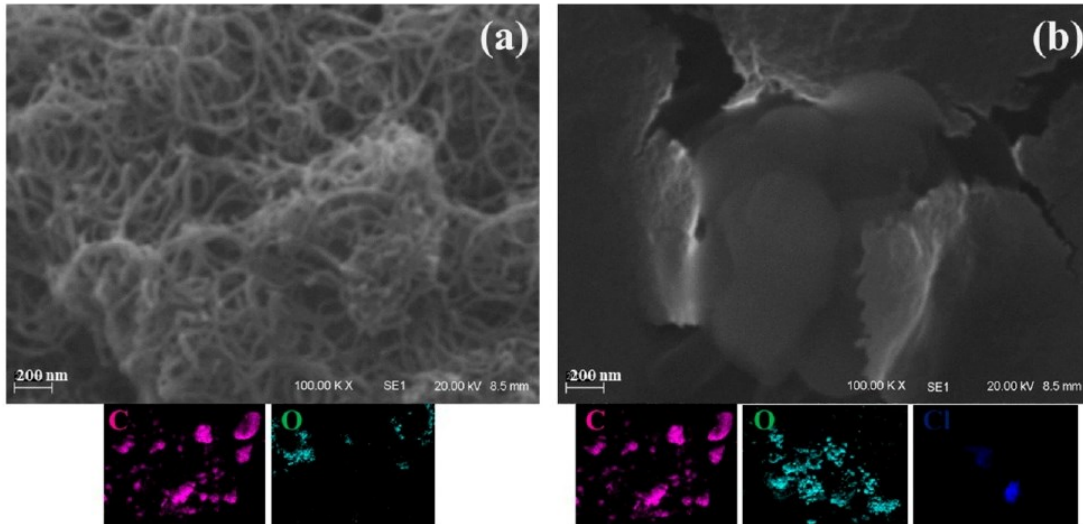
Figure 2. SEM micrographs and EDS elemental composition (carbon = pink; oxygen = cyan; chloride = blue) of: (a) MW, and (b) 1-MW.
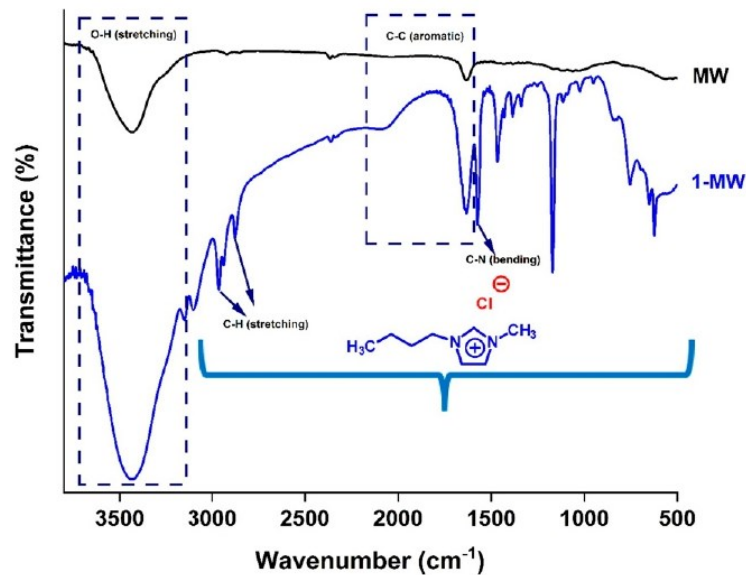
Figure 3. FTIR transmittance spectra of MW and 1-MW.

suggested that cation-π stacking or electrostatic shielding of MWCNT by IL are the reasons for those favorable interactions.[24]

The dispersion and adhesion in 1-MW and 5-MW, with the same MWCNT concentration (1 wt%), was analyzed by transmission electron microscopy (TEM). TEM images (Figure 4(a) and (b)) show well-dispersed 1-MW throughout the epoxy matrix, which is important for optimizing the mechanical properties of MWCNT/epoxy materials. These images shows low degree of entanglement between 1-MW and the epoxy matrix, enabling stronger bonding between them. This was most likely due to the interaction of IL, MWCNT and epoxy at a molecular level, which increased the mechanical strength due to the adhesion
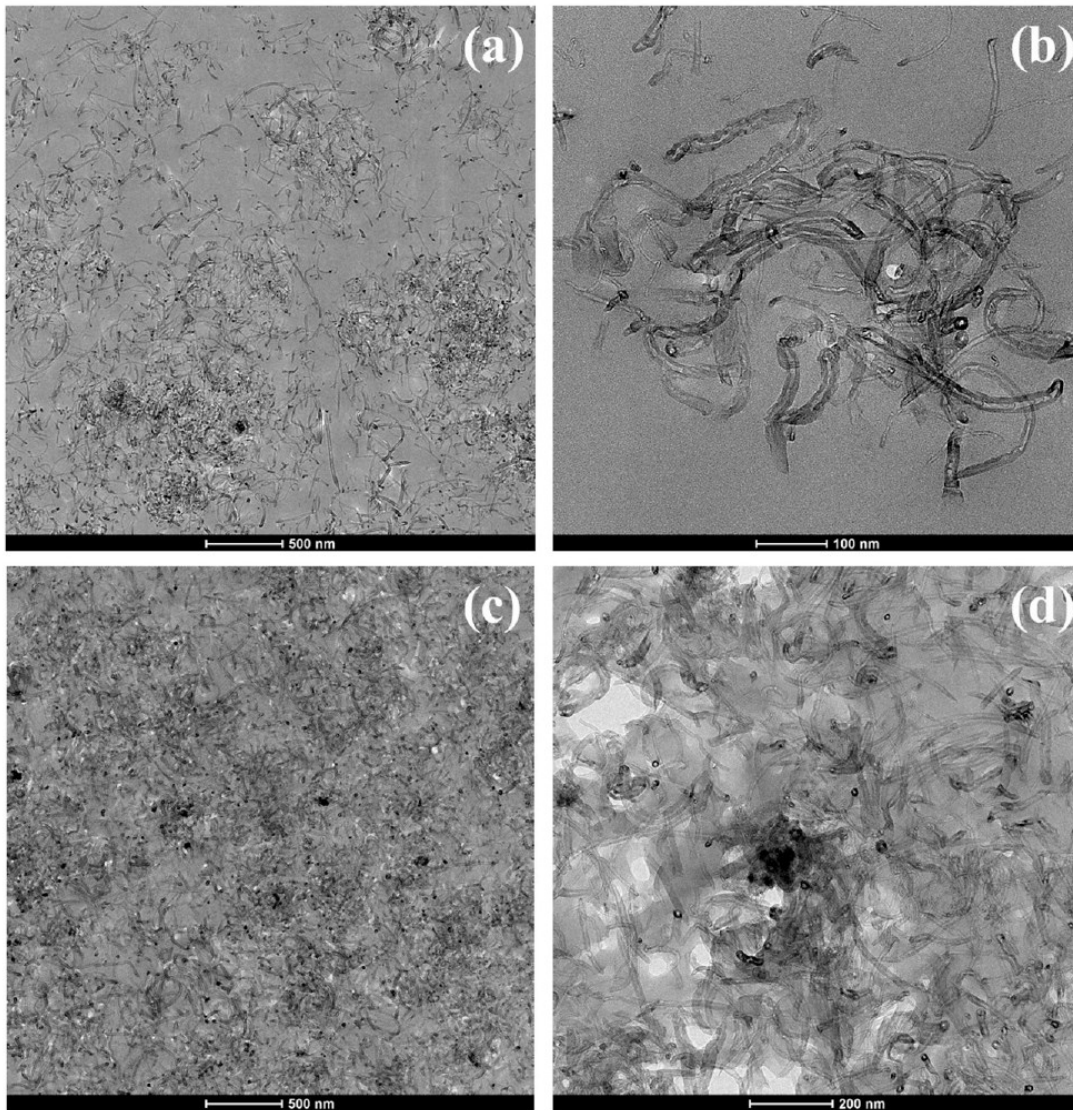
Figure 4. TEM micrographs of 1-MW (a), (b) and 5-MW (c), (d) in epoxy matrix.

of 1-MW nanotubes to the polymer matrix. The good dispersion and adhesion reduced self-agglomeration and contributed to overall properties.[28–30] This improved interfacial strength could be possibly due to the same behavior as IL-treated CF with epoxy matrix which has been explained in our previous studies through fiber pull out tests.[31] In the case of 5-MW (Figure 4(c) and (d)) at the same concentration in epoxy (1 wt%), a comparatively high agglomeration and concentration areas belonging to MWCNT were present. Such areas reduce the adhesion, form stress concentration points and the collective

effectiveness of these points cause a decrease in mechanical properties of the composite.

Scanning electron microscopy was performed in the fractured composite samples to analyze the dispersion behavior of IL-modified MWCNT (Figure 5). Composites without MWCNT showed a relatively smooth surface with less epoxy debris (Figure 5(a)) as compared to laminates with 1-MW/5-MW, suggesting a change in physical characteristics that could possibly promote brittle-to-ductile fracture with increased 1-MW/5-MW content (Figure 5(d)).[32] The 1-HCFC-0.8 sample, Figure 5(b), showed a slightly different
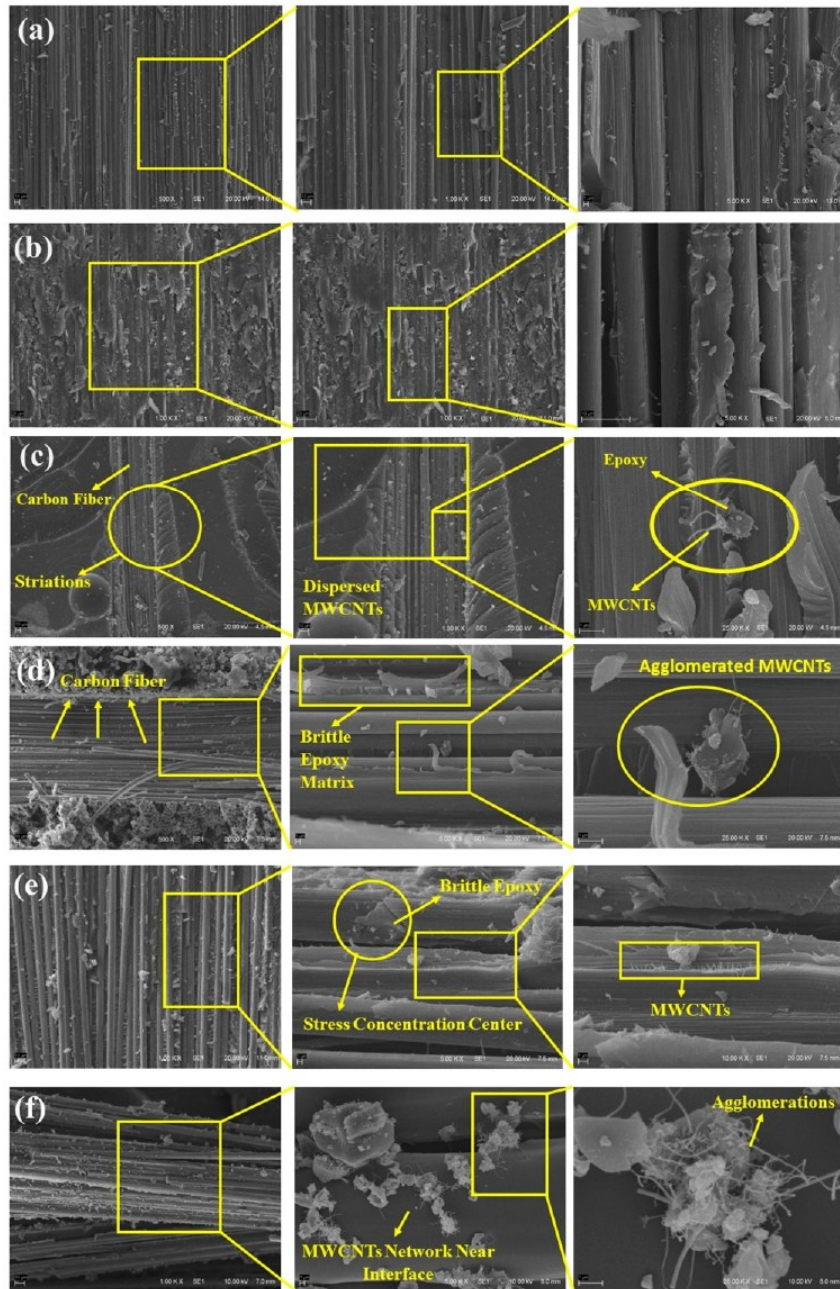
Figure 5. SEM micrographs of fractured composites: (a) EPCF, (b) 1-HCFC-0.8, (c) 1-HCFC-1.0, (d) 1-HCFC-2.0, (e) 5-HCFC-1.0, and (f) 5-HCFC-2.0.

surface, with more debris and a stepped fracture with relatively more roughness, depicting a more rigid structure. 1-HCFC-1.0 showed a surface morphology that reflects stress dispersion and restriction of crack movement through the

pinning effect maybe due to a three-dimensional MWCNT network (Figure 5(c)).[33,34] Higher contents of MWCNT caused inhomogeneous dispersion, agglomeration and originated stress concentration points. Intertwining of

MWCNT formed aggregates of micron size, increased wear debris, deep shallow grooves, cracks as well as adhesive wear phenomena.[35,36] The mentioned conditions, especially poor dispersion and agglomerate formation of MWCNT in epoxy negatively impact mechanical properties, which generally happens at high filler contents (Figure 5(d)).[37,38] The presence of a brittle second phase in HCFC, in a disordered manner, provided resistance to crack growth at certain critical content, above which it is expected to reduce performance.

The 5-HCFC-2.0 sample displayed an irregular curved formation of nanotubes, which are highly conductive, being visible as bright zones due to charge transport (Figure 5(f)).[39] Comparison of the fractured surfaces of 1-HCFC-1.0 and 5-HCFC-1.0, or 1-HCFC-2.0 and 5-HCFC-2.0, suggests that a higher concentration of IL (5 wt%) lead to the presence of MWCNT near the CF-epoxy matrix interface. Additionally, the HCFC with 1 wt% of MWCNT displayed a toothed protuberance, suggesting a reduction in mechanical strength (Figure 5(e)). Furthermore, the higher content of IL and MWCNT contributed to agglomeration at the CF-epoxy matrix interface (Figure 5(f)), which is expected to reduce performance.

Flexural mechanical testing was conducted to analyze the impact of IL-modified MWCNT on the mechanical performance of the composite. The flexural strength values are presented in Table 1 and the relative improvements are depicted in Figure 6(a). Increases in flexural strength, 57%–210% and 112%–144%, were obtained for HCFC with 1-MW and 5-MW, respectively. The maximum increase of 210% was obtained for 1-HCFC-1.0, a significant improvement in strength compared to the reported 32% increase,[11] and can be attributed to the combined effect of the MWCNT and IL at optimized content (both 1 wt%).

The flexural modulus of the composites was also obtained. The results are presented in Table 1 and the relative improvements in Figure 6(b). Increases in the range of 17.5%–151% and 68.4%–84.8% were achieved for HCFC with 1-MW (1-HCFC-1.0, 1-HCFC-2.0) and 5-MW (5-HCFC-1.0, 5-HCFC-2.0), respectively. The same HCFC (1-HCFC-1.0) that showed the highest flexural strength also presented the maximum increase in flexural modulus of 151%, which is higher than the reported increase of up to 92%.[11] The decrease in flexural properties for higher IL content may be due to a plasticizing effect of the epoxy, which increased flexibility of the polymer chain.[40]

The increase in flexural strength (210%) and flexural modulus (151%) is significantly higher compared to HCFC with the IL-free MWCNT.[14,41] Indeed, MWCNT in polymer matrices restrict the movement of polymer chains, which enhances the matrix's dominant load-bearing phenomena. A more dispersed filler provides more blocking points between polymer chains, increasing resistance to its movement contributing to stiffness.[16] High content of MWCNT also increases the viscosity of the resin, which is an

Table 1. Flexural strength and modulus of the studied composites (mean, standard deviation and percentage increase in relation to EPCF).

Sample ID	Flexural strength (MPa)[a]	Flexural modulus (GPa)*
EPCF	319.0±35.0	36.60±1.52
1-HCFC-0.2	518.5±88.8 (62%)	50.27±4.42 (37%)
1-HCFC-0.4	521.6±103.0 (63%)	45.93±3.57 (25%)
1-HCFC-0.6	537.7±92.0 (68%)	43.01±2.89 (17%)
1-HCFC-0.8	708.9±6.5 (122%)	73.73±11.43 (101%)
1-HCFC-1.0	987.8±109.4 (210%)	91.87±14.15 (151%)
1-HCFC-1.2	501.2±74.5 (57%)	50.74±7.68 (38%)
1-HCFC-1.4	601.9±71.0 (89%)	68.75±8.48 (87%)
1-HCFC-1.6	606.4±27.2 (90%)	48.29±3.57 (31%)
1-HCFC-2.0	634.2±41.6 (99%)	62.66±9.64 (71%)
5-HCFC-1.0	676.3±46.7 (112%)	61.64±5.21 (68%)
5-HCFC-2.0	777.0±46.6 (144%)	67.64±4.17 (84%)
5-HCFC-3.0	705.9±80.0 (121%)	62.35±4.22 (70%)

[a]% improvement in relation to EPCF in parenthesis.

important factor to consider for reduced effectiveness. Generally, flexural properties of epoxy composite laminates increase with the MWCNT content until a threshold value is achieved. After that, further increase of the MWCNT content results in a sudden decrease in properties indicating structural inhomogeneity and agglomeration or inhomogeneous distribution. In the current work, the limited content of IL and MWCNT in 1-HCFC-1.0 effectively contributed to a significant increase in mechanical strength.[14,15,42] Additionally, an increase in the IL content improved dispersion at higher MWCNT amount, showing a threshold level for 5-MW at higher filler content (Figure 6(a) and (b)). This is perhaps because at low amount of MWCNT with high IL content, self-agglomeration was dominant and did not provide enough interaction to contribute enough to disperse the MWCNT in epoxy. At comparatively higher amount of MWCNT, a balanced interaction has been achieved with the IL, shifting the threshold to a higher filler content. So, an increase in the IL content helps dispersing a higher amount of MWCNT in epoxy matrix and may be also beneficial for other properties of hybrid composites.[43]

The storage modulus, loss modulus and tan δ results from the dynamic mechanical analysis of the composites can be found in Figure 7 and are summarized in Table 2. The 1-MW has a significant positive effect on storage modulus (Figure 7(a)), increasing the capacity of HCFC to store energy and resist external loads in the elastic phase. The loss modulus (Figure 7(b)) followed the same tendency, whereas the glass transition temperature (Figure 7(c)) decreased. The 1-HCFC-1.0 presented the maximum percentual increase of 101% and 116% in storage modulus and loss modulus, respectively, bearing in mind that this sample also showed the highest flexural properties, and optimized MWCNT dispersion and MWCNT-IL-epoxy interactions. Improved
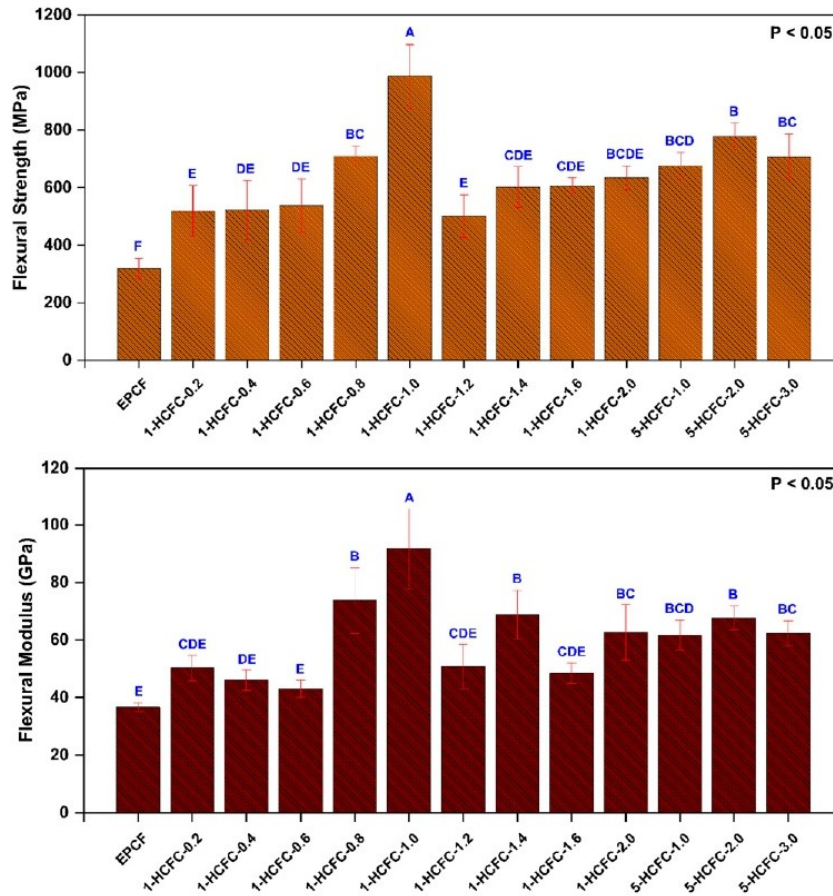
Figure 6. Flexural strength (a) and modulus (b) of the studied composites.

dispersion of and interactions through IL contributed to the enhancement in the viscoelastic properties, possibly due to better physical entanglement between MWCNT and polymer chains. Higher MWCNT content than 1 wt% reduced the viscoelastic properties, possibly related to the formation of agglomerates.

Previously, an increase in storage modulus of 94% at room temperature was reported for CF-epoxy composite with 1 wt% of carboxylic acid functionalized MWCNT (diameter: 5–10 nm). In the current case, the percentage increase in storage modulus is slightly higher (101%) and perhaps the MWCNT modification with IL showed high efficiency compared to previously used methods.[41]

Comparing the two IL treatments (at 1 wt% or 5 wt%) used for the modification of MWCNT, the viscoelastic properties are comparatively lower for 5 wt% of IL. Perhaps this could be justified considering that imidazolium-based IL may provide strong interactions with MWCNT through π–π stacking of the imidazolium nucleus' cation-π cloud

with the MWCNT π cloud, together with van der Waals forces. This imidazolium cation may interact with the MWCNT along with the epoxy by van der Waals forces with the N-alkyl chain, whereas the anion provides a bonding mechanism with the epoxy that will be intensified by its relative content.[44] This secondary involvement with the epoxy through the anion may influence the viscoelastic properties of composites.[45] As observed for loss modulus, the 1 wt% IL content was found to be most effective in improving these properties.

The damping curves of the composites are given in Figure 7(c). An increase in peak value of tan δ represents an improved damping response of the composite and 1-HCFC-1.0 showed an increase of 29.2%. This MWCNT content favored damping due to the formation of homogeneously dispersed and uniform MWCNT networks.[46] As the epoxy chain mobility decreases due to the presence of MWCNT and imparts stiffness, energy dissipation improves between the molecular chains due to internal friction. Also, the stick-
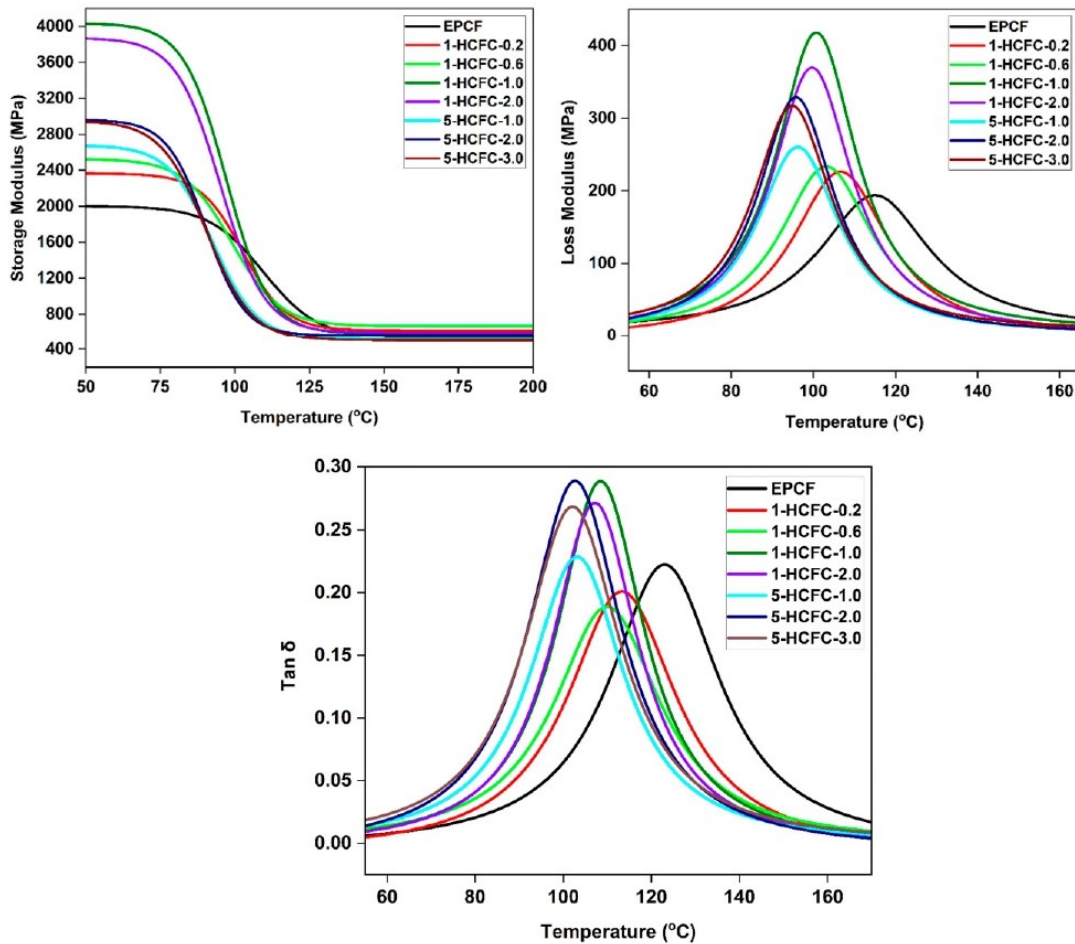
Figure 7. Storage modulus (a), loss modulus (b) and tan δ (c) of the studied composites.

Table 2. Storage modulus, loss modulus and tan δ values of the studied composites.

Sample ID	Storage modulus at 50°C (MPa)	Loss modulus (MPa)	Tan δ (°C)
EPCF	2003	193	123.0
1-HCFC-0.2	2360	226	113.2
1-HCFC-0.4	2300	213	113.7
1-HCFC-0.6	2518	232	109.7
1-HCFC-0.8	2490	310	105.3
1-HCFC-1.0	4036	417	108.5
1-HCFC-1.2	2480	305	106.0
1-HCFC-1.4	3248	364	105.5
1-HCFC-1.6	2560	252	104.6
1-HCFC-2.0	3856	369	107.4
5-HCFC-1.0	2677	260	103.0
5-HCFC-2.0	2962	328	102.7
5-HCFC-3.0	2950	317	101.9

slip mechanism is active between MWCNT and epoxy, causing an increase in damping, which decreased at higher MWCNT content due to aggregation.[46]

High damping properties of HCFC also indicate good interfacial characteristics, considering the fact of improved MWCNT/epoxy interaction due to the IL.[47] A decrease in glass transition temperature was observed with the addition of IL-modified MWCNT especially at higher IL content. This trend was the opposite of what is usually reported when nanofillers are added,[48] and perhaps is due to a decrease in surface tension of epoxy with IL, allowing the polymer to flow more easily and keeping a more plasticized state.[28]

Conclusions

The C_4MimCl ionic liquid has been successfully applied for the non-covalent modification of MWCNT and improvement in mechanical and thermomechanical properties of MWCNT/ carbon fiber/epoxy composites, retaining MWCNT's inherent properties. Application of 1 wt% of MWCNT treated with 1 wt% of IL yielded the best performing hybrid composite laminate showing enhanced strength and stiffness, as shown by flexural and DMA results. The simplicity of this MWCNT modification process, with good dispersion characteristics, has the potential of producing high performance multi-scale composites.

Declaration of conflict of interest

The author(s) declare no potential conflict of interest with respect to the research, authorship and publication of the article.

ORCID iDs

Bilal Ghafoor https://orcid.org/0000-0001-8232-9624
Umar Farooq https://orcid.org/0009-0003-1788-1211
Henri Stephan Schrekker https://orcid.org/0000-0002-8173-3841
Sandro Campos Amico https://orcid.org/0000-0003-4873-2238

References

1. Mirsalehi SA, Youzbashi AA and Sazgar A. Enhancement of out-of-plane mechanical properties of carbon fiber reinforced epoxy resin composite by incorporating the multi-walled carbon nanotubes. *SN Appl Sci* 2021; 3: 630–712.

2. Mehar K and Panda SK. Elastic bending and stress analysis of carbon nanotube-reinforced composite plate: experimental, numerical, and simulation. *Adv Polym Technol* 2018; 37: 1643–1657.

3. Singh BP, Saini K, Choudhary V, et al. Effect of length of carbon nanotubes on electromagnetic interference shielding and mechanical properties of their reinforced epoxy composites. *J Nanopart Res* 2014; 16: 2161–2211.

4. Ranjbar M and Feli S. Mechanical and low-velocity impact properties of epoxy-composite beams reinforced by MWCNTs. *J Compos Mater* 2019; 53: 693–705.

5. El Moumen A, Tarfaoui M, Lafdi K, et al. Dynamic properties of carbon nanotubes reinforced carbon fibers/epoxy textile composites under low velocity impact. *Composites Part B: Engineering* 2017; 125: 1–8.

6. Kim S-K, Kim JT, Kim H-C, et al. Thermal and mechanical properties of epoxy/carbon fiber composites reinforced with multi-walled carbon nanotubes. *Journal of Macromolecular Science, Part B* 2012; 51: 358–367.

7. Cysne Barbosa AP, P Fulco AP, SS Guerra E, et al. Accelerated aging effects on carbon fiber/epoxy composites. *Composites Part B: Engineering* 2017; 110: 298–306.

8. Godara A, Mezzo L, Luizi F, et al. Influence of carbon nanotube reinforcement on the processing and the mechanical behaviour of carbon fiber/epoxy composites. *Carbon* 2009; 47: 2914–2923.

9. Zhou Y, Pervin F, Lewis L, et al. Experimental study on the thermal and mechanical properties of multi-walled carbon nanotube-reinforced epoxy. *Materials Science and Engineering: A* 2007; 452: 657–664.

10. Quan D, Urdániz JL and Ivanković A. Enhancing mode-I and mode-II fracture toughness of epoxy and carbon fibre reinforced epoxy composites using multi-walled carbon nanotubes. *Materials & Design* 2018; 143: 81–92.

11. Tariq F, Shifa M and Baloch RA. Mechanical and thermal properties of multi-scale carbon nanotubes–carbon fiber– epoxy composite. *Arab J Sci Eng* 2018; 43: 5937–5948.

12. Kim M, Park Y-B, Okoli OI, et al. Processing, characterization, and modeling of carbon nanotube-reinforced multi-scale composites. *Composites Science and Technology* 2009; 69: 335–342.

13. Sui G, Zhong W, Liu M, et al. Enhancing mechanical properties of an epoxy resin using "liquid nano-reinforcements". *Materials Science and Engineering: A* 2009; 512: 139–142.

14. Kepple K, Sanborn G, Lacasse P, et al. Improved fracture toughness of carbon fiber composite functionalized with multi walled carbon nanotubes. *Carbon* 2008; 46: 2026–2033.

15. Azimpour-Shishevan F, Akbulut H and Mohtadi-Bonab M. Synergetic effects of carbon nanotube and graphene addition on thermo-mechanical properties and vibrational behavior of twill carbon fiber reinforced polymer composites. *Polymer Testing* 2020; 90: 106745.

16. Wu J, Guo J, Zhang Q, et al. Effect of different amino functionalized carbon nanotubes on curing behavior and mechanical properties of carbon fiber/epoxy composites. *Polym Compos* 2018; 39: E733–E744.

17. Soliman E, Kandil U and Taha MR. Improved strength and toughness of carbon woven fabric composites with functionalized MWCNTs. *Materials* 2014; 7: 4640–4657.

18. Zheng X, Li D, Feng C, et al. Thermal properties and non-isothermal curing kinetics of carbon nanotubes/ionic liquid/epoxy resin systems. *Thermochimica Acta* 2015; 618: 18–25.

19. Fonseca E, Silva VD, Amico SC, et al. Time-dependent properties of epoxy resin with imidazolium ionic liquid. *J Appl Polym Sci* 2021; 138: 51369.

20. Maka H, Spychaj T and Pilawka R. Epoxy resin/ionic liquid systems: the influence of imidazolium cation size and anion type on reactivity and thermomechanical properties. *Ind Eng Chem Res* 2012; 51: 5197–5206.

21. Muñoz B, del Bosque A, Sánchez M, et al. Epoxy resin systems modified with ionic liquids and ceramic nanoparticles as structural composites for multifunctional applications. *Polymer* 2021; 214: 123233.

22. Carvalho APA, Santos DF and Soares BG. Epoxy/imidazolium-based ionic liquid systems: the effect of the hardener on the curing behavior, thermal stability, and microwave absorbing properties. *J Appl Polym Sci* 2020; 137: 48326.

23. Ahmad A, Mansor N, Mahmood H, et al. Effect of ionic liquids on thermomechanical properties of polyetheretherketone-multiwalled carbon nanotubes nanocomposites. *J Appl Polym Sci* 2022; 139: 51788.

24. Liu C, Yin Q, Zhang W, et al. Tribological properties of graphene-modified with ionic liquids and carbon quantum dots/bismaleimide composites. *Carbon* 2021; 183: 504–514.

25. Kleinschmidt AC, Almeida JHS, Donato RK, et al. Functionalized-carbon nanotubes with physisorbed ionic liquid as filler for epoxy nanocomposites. *j Nanosci Nanotechnol* 2016; 16: 9132–9140.

26. Hameed N, Salim NV, Hanley TL, et al. Individual dispersion of carbon nanotubes in epoxy via a novel dispersion–curing approach using ionic liquids. *Phys Chem Chem Phys* 2013; 15: 11696–11703.

27. Kleinschmidt AC, Donato RK, Perchacz M, et al. Unrolling" multi-walled carbon nanotubes with ionic liquids: application as fillers in epoxy-based nanocomposites. *RSC Adv* 2014; 4: 43436–43443.

28. Lopes Pereira EC and Soares BG. Conducting epoxy networks modified with non-covalently functionalized multi-walled carbon nanotube with imidazolium-based ionic liquid. *J Appl Polym Sci* 2016; 133.

29. Chen C, Li X, Wen Y, et al. Noncovalent engineering of carbon nanotube surface by imidazolium ionic liquids: a promising strategy for enhancing thermal conductivity of epoxy composites. *Composites Part A: Applied Science and Manufacturing* 2019; 125: 105517.

30. Chen C, Liu J, Li X, et al. Epoxy/ionic liquid-like mwcnts composites with improved processability and mechanical properties. *Composites Communications* 2019; 15: 46–52.

31. Ghafoor B, Schrekker HS and Amico SC. Multifunctional characteristics of carbon fibers modified with imidazolium ionic liquids. *Molecules* 2022; 27: 7001.

32. Sheth D, Maiti S, Patel S, et al. Enhancement of mechanical properties of carbon fiber reinforced epoxy matrix laminated composites with multiwalled carbon nanotubes. *Fullerenes, Nanotubes and Carbon Nanostructures* 2021; 29: 288–294.

33. Dong L, Hou F, Li Y, et al. Preparation of continuous carbon nanotube networks in carbon fiber/epoxy composite. *Composites Part A: Applied Science and Manufacturing* 2014; 56: 248–255.

34. Kim HC, Kim EH, Lee I, et al. Fabrication of carbon nanotubes dispersed woven carbon fiber/epoxy composites and their damping characteristics. *Journal of Composite Materials* 2013; 47: 1045–1054.

35. Kim M, Rhee K, Lee J, et al. Property enhancement of a carbon fiber/epoxy composite by using carbon nanotubes. *Composites Part B: Engineering* 2011; 42: 1257–1261.

36. Kurien RA, Selvaraj DP, Sekar M, et al. Comparative mechanical, tribological and morphological properties of epoxy resin composites reinforced with multi-walled carbon nanotubes. *Arab J Sci Eng* 2022; 47: 8059–8067.

37. Song YS and Youn JR. Influence of dispersion states of carbon nanotubes on physical properties of epoxy nanocomposites. *Carbon* 2005; 43: 1378–1385.

38. Srivastava VK. Modeling and mechanical performance of carbon nanotube/epoxy resin composites. *Materials & Design* 2012; 39: 432–436.

39. Chang L, Friedrich K, Ye L, et al. Evaluation and visualization of the percolating networks in multi-wall carbon nanotube/epoxy composites. *J Mater Sci* 2009; 44: 4003–4012.

40. Therattil J, Anil KS, Pothan LA, et al. Cure acceleration and plasticizing effect of imidazolium ionic liquid on the properties of natural rubber/carbon nanotube composites. *Funct Compos Struct* 2020; 2: 035003.

41. Sarath Kumar P, Jayanarayanan K, Deeraj BDS, et al. Synergistic effect of carbon fabric and multiwalled carbon nanotubes on the fracture, wear and dynamic load response of epoxy-based multiscale composites. *Polym Bull (Berl)* 2022; 79: 5063–5084.

42. Ekrem M. The effects of carbon nanotubes added polyvinyl alcohol nanofibers on mechanical properties of carbon reinforced composite laminates. *Sādhanā* 2019; 44: 179–188.

43. Jain V, Jaiswal S, Dasgupta K, et al. Influence of carbon nanotube on interfacial and mechanical behavior of carbon fiber reinforced epoxy laminated composites. *Polymer Composites* 2022; 43: 6344–6354.

44. Fonseca E, Demétrio da Silva V, Klitzke JS, et al. Imidazolium ionic liquids as fracture toughening agents in DGEBA-TETA epoxy resin. *Polymer Testing* 2020; 87: 106556.

45. Lu Y, Xu Y, Lu L, et al. Interfacial interactions and structures of protic ionic liquids on a graphite surface: a first-principles study and comparison with aprotic ionic liquids. *Phys Chem Chem Phys* 2021; 23: 18338–18348.

46. Pan S, Dai Q, Safaei B, et al. Damping characteristics of carbon nanotube reinforced epoxy nanocomposite beams. *Thin-Walled Structures* 2021; 166: 108127.

47. Kamaraj M, Dodson EA and Datta S. Thermal and visco-elastic behaviour of graphene nanoplatelets/flax fibre/epoxy composites. *Plastics, Rubber and Composites* 2021; 50: 219–227.

48. Aziz I, Duran H, Saleem M, et al. The role of interface on dynamic mechanical properties, dielectric performance, conductivity, and thermal stability of electrospun carbon nanofibers reinforced epoxy. *Polymer Composites* 2021; 42: 4366–4379.

7   INTEGRATION OF THE ARTICLES

The objective of the doctorate study was to apply imidazolium-based IL for the modification of carbon-based structures to improve interfacial interactions and adhesion with epoxy matrix. During the development of this doctoral thesis, three research articles were published in high-impact factor journals in the field of polymers and composite materials:

ARTICLE I was published in Composite Interfaces, titled "Surface modification of carbon fiber with imidazolium ionic liquids". The main objective of this work was to evaluate the effect of non-covalent surface modification of carbon fiber (CF) using two different imidazolium ionic liquids (IL), 1-butyl-3-methyl imidazolium bis(trifluoromethylsulfonyl)imide (hydrophobic) and 1-butyl-3-methylimidazolium chloride (hydrophilic). Subsequently, the sizing of commercial CF was removed and the as obtained CF was treated with 10 wt% of IL. Contact angle measurements and fiber pull out tests were performed to evaluate the performance of the CF-epoxy interface due to the presence of IL.

ARTICLE II was published in Molecules, titled "Multifunctional characteristics of carbon fibers modified with imidazolium ionic liquids". After studying in ARTICLE I the effect of non-covalent modification of CF (without sizing) with 10 wt% of IL, the main objective of this study was to modify CF with lower contents of IL (0.25-3 wt%). 1-Butyl-3-methylimidazolium bis(trifluoromethylsulfonyl)imide, 1-butyl-3-methylimidazolium chloride and 1-(2-hydroxyethyl)-3-methylimidazolium chloride were used to treat the CF. Multifunctional properties of the CF were analyzed at the optimized IL percentage by studying electrical and mechanical properties at the interface.

ARTICLE III was published in Journal of Composite Materials, titled "Thermomechanical properties of imidazolium IL-modified MWCNT/carbon fiber/epoxy hybrid composite laminates". The main objective of this research was applying a similar strategy of non-covalent modification to modify MWCNT with an imidazolium IL, 1-butyl-3-methylimidazolium chloride, to improve adhesion and dispersion with and in epoxy matrix, respectively. The MWCNT treated with 1 or 5 wt% of IL were dispersed in epoxy resin (0.2-2 wt% or 1-3 wt%, respectively) and used to obtain hybrid composite laminates based on CF molded by hand layup and vacuum bagging techniques. Various characterization techniques such as microscopic, mechanical and thermomechanical were applied to test the performance of the hybrid composite laminates.

8   CONCLUSIONS

The present study provides a versatile and non-damaging route to modify the recycled CF surface to avoid waste and reduce climate problems, as well as providing a solution for waste management. The study demonstrated that IL can be used to modify the properties of carbon-based structures, such as CF and MWCNT, to improve their mechanical, electrical, and thermomechanical properties. The study also identified an optimized concentration of IL for the treatment of unfinished CF and demonstrated that a small amount of IL is practical for the modification process of carbon-based structures. The study has opened up new opportunities for the use of recycled CF in wider multifunctional applications. Furthermore, the study proposed a novel idea of modification of recycled CF, ensuring its sustainable use, which is aligned with the sustainable development goals defined by the United Nations Member States. Therefore, the present study is of great significance and has contributed to the development of efficient and sustainable methods for the modification of carbon-based structures.

The study demonstrated a practical method for surface functionalization of CF with imidazolium IL without chemical or structural modification of the CF. The presence of IL on the CF surface improved CF wettability and the IFSS with epoxy, indicating its potential for making high-strength polymer composites. The study identified an optimized concentration of 1% w/v IL for the treatment of unfinished CF. It was found that the polar functional group present on the alkyl chain of imidazolium ring of IL is more effective in providing the interactions and property enhancement.

Further, the study showed that a small amount of IL is practical for the modification process of carbon-based structures, considering the economic aspects of its use for industrial purposes. The use of IL for the modification of carbon-based structures presents an efficient alternative opportunity to be applied with alternative molecular structure, which is strongly supported by the present studies. The study demonstrated that IL can be used to modify recycled CF surface, which will ensure their sustainable use, reducing climate problems and providing a solution for waste management.

The study also analyzed the effect of IL on the electrical properties of CF surface and found that enhanced electrical conductivity on the fiber surface was obtained, allowing the design of composites with more electrically conductive interfaces. The good thermal stability of the IL on

the CF surface indicated its stable presence on the fiber surface. The obtained characteristics provided an opportunity to use CF, including recycled CF, in wider multifunctional applications.

Finally, the study demonstrated that using an imidazolium-based IL, specifically 1-butyl-3-methyl imidazolium chloride, for the modification of MWCNT is an effective way of dispersion in epoxy matrices. Being a good dispersing agent of MWCNT in composite lead to enhanced interfacial bonding with the polymer matrix. The study found that at a concentration of 1 wt% of MWCNT treated with 1 wt% of the IL, the maximum improvement in mechanical and thermomechanical properties was achieved. This suggests that the optimal concentration of both the MWCNT and IL to significantly impact the properties of the composite material.

The present findings are significant as they demonstrate the potential of imidazolium-based IL as a promising method for improving the properties of composite materials. By using an IL as a dispersing agent, the limitation of the agglomeration can be overcome and the improvement in the overall properties of the composites can be achieved. This could lead to the development of advanced composite materials with enhanced properties, making them suitable for a range of applications such as aerospace, automotive, and medical industries.

The IL in both cases provided an excellent and robust option to modify the carbon-based structures. Especially, the reuse of recycled CF, which is still in stage of infancy, this modification process will support sustainable use of CF in advanced structural and functional applications.

9   SUGGESTION FOR FUTURE STUDIES

➢ 1 wt% of the imidazolium-based IL with various functional groups for the modification of recycled CF for preparing recycled CF composites with improved strength.

➢ Imidazolium IL on the CF has the ability to directly attached carbon-based nanofillers on the surface of CF with the noncovalent bonding effect which will result in conductive interfaces which will be beneficial for the application of electromagnetic absorption panels.

➢ Applying various imidazolium IL with different alkyl chain length for the modification of carbon-based nanostructures (MWCNT, SWCNT, graphene) and incorporating these nanostructures in thermoplastic-based polymers to form multifunctional composite (SCHEME 1).

➢ Applying various imidazolium IL with different functional groups for the modification of carbon-based nanostructures (MWCNT, SWCNT, graphene) and incorporating these nanostructures in CF composites to form multifunctional hybrid composites considering its impact on the electrical properties (SCHEME 2).
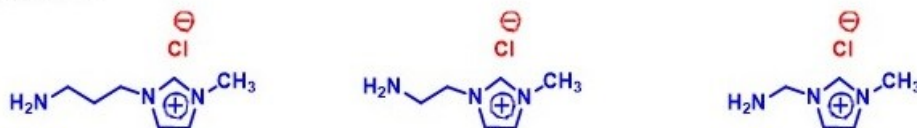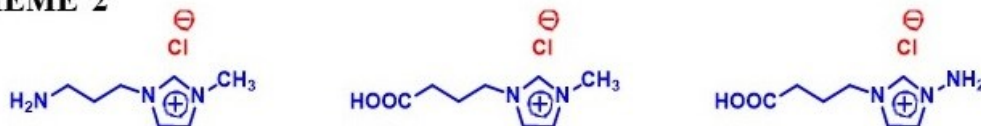
REFERENCES

[1]   G. Yang, M. Park, and S.-J. Park, "Recent progresses of fabrication and characterization of fibers-reinforced composites: A review," *Composites Communications,* vol. 14, pp. 34-42, 2019.

[2]   G. Jeevi, S. K. Nayak, and M. Abdul Kader, "Review on adhesive joints and their application in hybrid composite structures," *Journal of Adhesion Science and Technology,* vol. 33, no. 14, pp. 1497-1520, 2019.

[3]   Z. Wang, X. Huang, G. Xian, and H. Li, "Effects of surface treatment of carbon fiber: Tensile property, surface characteristics, and bonding to epoxy," *Polymer Composites,* vol. 37, no. 10, pp. 2921-2932, 2016.

[4]   S. Sharma *et al.*, "Enhanced thermomechanical and electrical properties of multiwalled carbon nanotube paper reinforced epoxy laminar composites," *Composites Part A: Applied Science and Manufacturing,* vol. 104, pp. 129-138, 2018.

[5]   Z. Xu *et al.*, "Wettability of carbon fibers modified by acrylic acid and interface properties of carbon fiber/epoxy," *European polymer journal,* vol. 44, no. 2, pp. 494-503, 2008.

[6]   E. Soliman, U. Kandil, and M. Reda Taha, "Improved strength and toughness of carbon woven fabric composites with functionalized MWCNTs," *Materials,* vol. 7, pp. 4640-4657, 2014.

[7]   M. S. A. Rahaman, A. F. Ismail, and A. Mustafa, "A review of heat treatment on polyacrylonitrile fiber," *Polymer degradation and Stability,* vol. 92, no. 8, pp. 1421-1432, 2007.

[8]   J. Liu, Y. Tian, Y. Chen, J. Liang, L. Zhang, and H. Fong, "A surface treatment technique of electrochemical oxidation to simultaneously improve the interfacial bonding strength and the tensile strength of PAN-based carbon fibers," *Materials Chemistry and Physics,* vol. 122, no. 2-3, pp. 548-555, 2010.

[9]   S. Corujeira Gallo, C. Charitidis, and H. Dong, "Surface functionalization of carbon fibers with active screen plasma," *Journal of Vacuum Science & Technology A: Vacuum, Surfaces, and Films,* vol. 35, no. 2, p. 021404, 2017.

[10]   S. Tiwari, J. Bijwe, and S. Panier, "Gamma radiation treatment of carbon fabric to improve the fiber–matrix adhesion and tribo-performance of composites," *Wear,* vol. 271, no. 9-10, pp. 2184-2192, 2011.

[11]   H. Maka, T. Spychaj, and R. Pilawka, "Epoxy resin/ionic liquid systems: the influence of imidazolium cation size and anion type on reactivity and thermomechanical properties," *Industrial & engineering chemistry research,* vol. 51, pp. 5197-5206, 2012.

[12]   V. Jain, S. Jaiswal, K. Dasgupta, and D. Lahiri, "Influence of carbon nanotube on interfacial and mechanical behavior of carbon fiber reinforced epoxy laminated composites," *Polymer Composites,* vol. 43, no. 9, pp. 6344-6354, 2022.

[13]   J. Eom *et al.*, "Highly conductive and stretchable fiber interconnections using dry-spun carbon nanotube fibers modified with ionic liquid/poly (vinylidene fluoride) copolymer composite," *Composites Science and Technology,* vol. 169, pp. 1-6, 2019.

[14]   D. J. Eyckens *et al.*, "Synergistic interfacial effects of ionic liquids as sizing agents and surface modified carbon fibers," vol. 6, no. 10, pp. 4504-4514, 2018.

[15]   K. M. Beggs *et al.*, "Rapid surface functionalization of carbon fibres using microwave irradiation in an ionic liquid," vol. 6, no. 39, pp. 32480-32483, 2016.

[16]   A. Kleinschmidt *et al.*, ""Unrolling" multi-walled carbon nanotubes with ionic liquids: application as fillers in epoxy-based nanocomposites," *RSC Advances,* vol. 4, no. 82, pp. 43436-43443, 2014.

[17]   C. Chen *et al.*, "Epoxy/ionic liquid-like mwcnts composites with improved processability and mechanical properties," *Composites Communications,* vol. 15, pp. 46-52, 2019.

[18]   X. Huang, "Fabrication and properties of carbon fibers," *Materials,* vol. 2, no. 4, pp. 2369-2403, 2009.

[19]   J.-j. Hao, C.-x. Lu, and D.-h. Li, "A comparative analysis of polyacrylonitrile-based carbon fibers:(II) Relationship between the microstructures and properties," *New Carbon Materials,* vol. 35, no. 6, pp. 802-809, 2020.

[20]   J. Lu, W. Li, H. Kang, L. Feng, J. Xu, and R. Liu, "Microstructure and properties of polyacrylonitrile based carbon fibers," *Polymer Testing,* vol. 81, p. 106267, 2020.

[21]   S. Tiwari and J. Bijwe, "Surface treatment of carbon fibers-a review," *Procedia Technology,* vol. 14, pp. 505-512, 2014.

[22]   M.-l. Wang and W.-f. Bian, "The relationship between the mechanical properties and microstructures of carbon fibers," *New Carbon Materials,* vol. 35, no. 1, pp. 42-49, 2020.

[23]   D. J. Johnson, "Structural studies of PAN-based carbon fibers," in *Chemistry and physics of carbon*: CRC Press, 2021, pp. 1-58.

[24]   S. G. Maxineasa and N. Taranu, "Life cycle analysis of strengthening concrete beams with FRP," in *Eco-efficient repair and rehabilitation of concrete infrastructures*: Elsevier, 2018, pp. 673-721.

[25]   P. Khorgade, M. Rettinger, A. Burghartz, and M. Schlaich, "A comparative cradle-to-gate life cycle assessment of carbon fiber-reinforced polymer and steel-reinforced bridges," *Structural Concrete,* 2022.

[26]   S. Karuppannan Gopalraj and T. Kärki, "A review on the recycling of waste carbon fibre/glass fibre-reinforced composites: Fibre recovery, properties and life-cycle analysis," *SN Applied Sciences,* vol. 2, no. 3, p. 433, 2020.

[27]   C. Peña *et al.*, "Using life cycle assessment to achieve a circular economy," *The International Journal of Life Cycle Assessment,* vol. 26, pp. 215-220, 2021.

[28]   R. J. Tapper, M. L. Longana, A. Norton, K. D. Potter, and I. Hamerton, "An evaluation of life cycle assessment and its application to the closed-loop recycling of carbon fibre reinforced polymers," *Composites Part B: Engineering,* vol. 184, p. 107665, 2020.

[29]   L. Mazzocchetti, T. Benelli, E. D'Angelo, C. Leonardi, G. Zattini, and L. Giorgini, "Validation of carbon fibers recycling by pyro-gasification: The influence of oxidation conditions to obtain clean fibers and promote fiber/matrix adhesion in epoxy composites," *Composites Part A: Applied Science and Manufacturing,* vol. 112, pp. 504-514, 2018.

[30]   J. A. Onwudili, N. Miskolczi, T. Nagy, and G. Lipóczi, "Recovery of glass fibre and carbon fibres from reinforced thermosets by batch pyrolysis and investigation of fibre re-using as reinforcement in LDPE matrix," *Composites Part B: Engineering,* vol. 91, pp. 154-161, 2016.

[31]   E. Pakdel, S. Kashi, R. Varley, and X. Wang, "Recent progress in recycling carbon fibre reinforced composites and dry carbon fibre wastes," *Resources, Conservation and Recycling,* vol. 166, p. 105340, 2021.

[32]   B. Rand, S. P. Appleyard, and M. F. Yardim, *Design and control of structure of advanced carbon materials for enhanced performance*. Springer Science & Business Media, 2012.

[33]   J. J. Andrew, S. M. Srinivasan, A. Arockiarajan, and H. N. Dhakal, "Parameters influencing the impact response of fiber-reinforced polymer matrix composite materials: A critical review," *Composite Structures,* vol. 224, p. 111007, 2019.

[34] J.-K. Kim and Y.-W. Mai, *Engineered interfaces in fiber reinforced composites*. Elsevier, 1998.

[35] P. Alam, D. Mamalis, C. Robert, C. Floreani, and C. M. Ó. Brádaigh, "The fatigue of carbon fibre reinforced plastics-A review," *Composites Part B: Engineering,* vol. 166, pp. 555-579, 2019.

[36] G. Wu, L. Ma, and H. Jiang, "The roles of surface wettability and roughness of carbon fibers in interfacial enhancement of silicone resin composites," *Polymer Composites,* vol. 40, no. S1, pp. E255-E264, 2019.

[37] M. Li *et al.*, "Improvements of adhesion strength of water-based epoxy resin on carbon fiber reinforced polymer (CFRP) composites via building surface roughness using modified silica particles," *Composites Part A: Applied Science and Manufacturing,* vol. 169, p. 107511, 2023.

[38] W. Song, A. Gu, G. Liang, and L. Yuan, "Effect of the surface roughness on interfacial properties of carbon fibers reinforced epoxy resin composites," *Applied surface science,* vol. 257, no. 9, pp. 4069-4074, 2011.

[39] M. Sharma, S. Gao, E. Mäder, H. Sharma, L. Y. Wei, and J. Bijwe, "Carbon fiber surfaces and composite interphases," *Composites Science and Technology,* vol. 102, pp. 35-50, 2014.

[40] E. P. Plueddemann, *Interfaces in Polymer Matrix Composites: Composite Materials, Vol. 6*. Elsevier, 2016.

[41] S. Y. Voronina, T. Shalygina, V. Voronchikhin, A. Y. Vlasov, A. Ovchinnikov, and N. Grotskaya, "Data for determining the surface properties of carbon fiber in contact interaction with polymeric binders," *Data in Brief,* vol. 35, p. 106847, 2021.

[42] G. Kola, M. Rahman, V. Vadlamudi, R. Raihan, and K. Reifsnider, "Effects of Surface Heterogeneity on Work of Adhesion of Carbon Fiber Reinforced Composites," 2021: The Composites and Advanced Materials Expo. CAMX Conference Proceedings ….

[43] A. Rehman, M. Park, and S.-J. Park, "Current progress on the surface chemical modification of carbonaceous materials," *Coatings,* vol. 9, no. 2, p. 103, 2019.

[44] J. Li, "Interfacial studies on the O3 modified carbon fiber-reinforced polyamide 6 composites," *Applied Surface Science,* vol. 255, no. 5, pp. 2822-2824, 2008.

[45]   H. Yuan, C. Wang, S. Zhang, and X. Lin, "Effect of surface modification on carbon fiber and its reinforced phenolic matrix composite," *Applied Surface Science,* vol. 259, pp. 288-293, 2012.

[46]   J. Yu, L. Meng, D. Fan, C. Zhang, F. Yu, and Y. Huang, "The oxidation of carbon fibers through K2S2O8/AgNO3 system that preserves fiber tensile strength," *Composites Part B: Engineering,* vol. 60, pp. 261-267, 2014.

[47]   D. Gao, H. Yang, G. Liu, C. Chen, J. Yao, and C. Li, "Effect of electrochemical oxidation degree of carbon fiber on the interfacial properties of carbon fiber–reinforced polyaryletherketone composites," *Journal of Reinforced Plastics and Composites,* p. 07316844221145763, 2022.

[48]   Y. Huang *et al.*, "Surface modification of activated carbon fiber by low-temperature oxygen plasma: Textural property, surface chemistry, and the effect of water vapor adsorption," *Chemical Engineering Journal,* vol. 418, p. 129474, 2021.

[49]   S. H. Han, H. J. Oh, and S. S. Kim, "Evaluation of fiber surface treatment on the interfacial behavior of carbon fiber-reinforced polypropylene composites," *Composites Part B: Engineering,* vol. 60, pp. 98-105, 2014.

[50]   J. Xie *et al.*, "Improving carbon fiber adhesion to polyimide with atmospheric pressure plasma treatment," *Surface and coatings technology,* vol. 206, no. 2-3, pp. 191-201, 2011.

[51]   K. Ma, P. Chen, B. Wang, G. Cui, and X. Xu, "A study of the effect of oxygen plasma treatment on the interfacial properties of carbon fiber/epoxy composites," *Journal of applied polymer science,* vol. 118, no. 3, pp. 1606-1614, 2010.

[52]   J. Sun, F. Zhao, Y. Yao, Z. Jin, X. Liu, and Y. Huang, "High efficient and continuous surface modification of carbon fibers with improved tensile strength and interfacial adhesion," *Applied Surface Science,* vol. 412, pp. 424-435, 2017.

[53]   H. Xiao, Y. Lu, M. Wang, X. Qin, W. Zhao, and J. Luan, "Effect of gamma-irradiation on the mechanical properties of polyacrylonitrile-based carbon fiber," *Carbon,* vol. 52, pp. 427-439, 2013.

[54]   J.-Q. Li, Y.-D. Huang, S.-Y. Fu, L.-H. Yang, H.-t. Qu, and G.-s. Wu, "Study on the surface performance of carbon fibres irradiated by γ-ray under different irradiation dose," *Applied Surface Science,* vol. 256, no. 7, pp. 2000-2004, 2010.

[55]   X. Cheng and Q. Shang-Guan, "Effect of rare earths on mechanical and tribological properties of carbon fibers reinforced PTFE composite," *Tribology Letters,* vol. 21, no. 2, pp. 153-160, 2006.

[56]   Q. SHANGGUAN and X. CHENG, "Effect of rare earths surface treatment on tribological properties of carbon fibers reinforced PTFE composite under oil-lubricated condition," *Journal of Rare Earths,* vol. 26, no. 4, pp. 584-589, 2008.

[57]   Z. Xu, Y. Huang, Y. Song, C. Zhang, and L. Liu, "Surface characteristics of rare earth treated carbon fibers and interfacial properties of composites," *Journal of rare earths,* vol. 25, no. 4, pp. 462-468, 2007.

[58]   Z. Xu, Y. Huang, C. Zhang, and G. Chen, "Influence of rare earth treatment on interfacial properties of carbon fiber/epoxy composites," *Materials Science and Engineering: A,* vol. 444, no. 1-2, pp. 170-177, 2007.

[59]   S. Tiwari, J. Bijwe, and S. Panier, "Role of nano-YbF3-treated carbon fabric on improving abrasive wear performance of polyetherimide composites," *Tribology Letters,* vol. 42, no. 3, pp. 293-300, 2011.

[60]   J. Liu, H. Ge, J. Chen, D. Wang, and H. Liu, "The preparation of emulsion type sizing agent for carbon fiber and the properties of carbon fiber/vinyl ester resin composites," *Journal of applied polymer science,* vol. 124, no. 1, pp. 864-872, 2012.

[61]   B. Fernandez, A. Arbelaiz, A. Valea, F. Mujika, and I. Mondragon, "A comparative study on the influence of epoxy sizings on the mechanical performance of woven carbon fiber-epoxy composites," *Polymer composites,* vol. 25, no. 3, pp. 319-330, 2004.

[62]   V. Martínez-Landeros, S. Vargas-Islas, C. E. Cruz-González, S. Barrera, K. Mourtazov, and R. Ramírez-Bon, "Studies on the influence of surface treatment type, in the effectiveness of structural adhesive bonding, for carbon fiber reinforced composites," *Journal of Manufacturing Processes,* vol. 39, pp. 160-166, 2019.

[63]   K. Olonisakin *et al.*, "Key improvements in interfacial adhesion and dispersion of fibers/fillers in polymer matrix composites; focus on pla matrix composites," *Composite Interfaces,* vol. 29, no. 10, pp. 1071-1120, 2022.

[64]   L. Yang, H. Xia, Z. Xu, Z. Lihua, and Q. Ni, "Influence of surface modification of carbon fiber based on magnetron sputtering technology on mechanical properties of carbon fiber composites," *Materials Research Express,* vol. 7, no. 10, p. 105602, 2020.

[65]   F. Liu *et al.*, "Reviews on interfacial properties of the carbon fiber reinforced polymer composites," in *Journal of Physics: Conference Series*, 2020, vol. 1637, no. 1: IOP Publishing, p. 012027.

[66]   D. J. Eyckens and L. C. J. F. i. c. Henderson, "A review of solvate ionic liquids: Physical parameters and synthetic applications," vol. 7, p. 263, 2019.

[67]   Z. Lei, B. Chen, Y.-M. Koo, and D. R. MacFarlane, "Introduction: ionic liquids," vol. 117, ed: ACS Publications, 2017, pp. 6633-6635.

[68]   K. Richards, E. Petit, Y. M. Legrand, and C. J. C. A. E. J. Grison, "Eco-Friendly Methodology for the Formation of Aromatic Carbon–Heteroatom Bonds by Using Green Ionic Liquids," vol. 27, no. 2, pp. 809-814, 2021.

[69]   J. M. Gomes, S. S. Silva, and R. L. J. C. S. R. Reis, "Biocompatible ionic liquids: fundamental behaviours and applications," vol. 48, no. 15, pp. 4317-4335, 2019.

[70]   C. Li, L. Gu, J. Tong, and J. J. A. N. Maier, "Carbon nanotube wiring of electrodes for high-rate lithium batteries using an imidazolium-based ionic liquid precursor as dispersant and binder: a case study on iron fluoride nanoparticles," vol. 5, no. 4, pp. 2930-2938, 2011.

[71]   M. Majidi, R. Baj, and A. J. O. C. Naseri, "Carbon nanotube-ionic liquid nanocomposite modified carbon-ceramic electrode for determination of dopamine in real samples," vol. 11, no. 7, pp. 1172-1186, 2013.

[72]   L. Urzúa, M. Pérez-Ortiz, and A. J. J. o. t. C. C. S. Álvarez-Lueje, "Electrocatalytic oxidation and voltammetric determination of sulfamethazine using a modified carbon electrode with ionic liquid," vol. 63, no. 1, pp. 3914-3917, 2018.

[73]   C. Song *et al.*, "High performance wire-type supercapacitor with Ppy/CNT-ionic liquid/AuNP/carbon fiber electrode and ionic liquid based electrolyte," vol. 144, pp. 639-648, 2019.

[74]   T. Y. Kim *et al.*, "High-performance supercapacitors based on poly (ionic liquid)-modified graphene electrodes," *ACS nano,* vol. 5, no. 1, pp. 436-442, 2011.

[75]   W. Wei, H.-H. Jin, and G.-C. J. M. A. Zhao, "A reagentless nitrite biosensor based on direct electron transfer of hemoglobin on a room temperature ionic liquid/carbon nanotube-modified electrode," vol. 164, no. 1, pp. 167-171, 2009.

[76]   X. Wang, C. Cheng, R. Dong, and J. J. J. o. S. S. E. Hao, "Sensitive voltammetric determination of rutin at a carbon nanotubes-ionic liquid composite electrode," vol. 16, no. 8, pp. 2815-2821, 2012.

[77]   V. V. Chaban, N. A. Andreeva, and E. E. J. N. J. o. C. Fileti, "Graphene/ionic liquid ultracapacitors: does ionic size correlate with energy storage performance?," vol. 42, no. 22, pp. 18409-18417, 2018.

[78]   C. Jiang, Y. Wang, H. Su, W. Li, W. Lou, and X. Wang, "Synthesis and evaluation of a protic ionic liquid as a multifunctional lubricant additive," *Friction,* vol. 8, no. 3, pp. 568-576, 2020.

[79]   T. Ichikawa, T. Kato, and H. J. C. C. Ohno, "Dimension control of ionic liquids," vol. 55, no. 57, pp. 8205-8214, 2019.

[80]   M. J. Park, J. K. Lee, B. S. Lee, Y.-W. Lee, I. S. Choi, and S.-g. Lee, "Covalent modification of multiwalled carbon nanotubes with imidazolium-based ionic liquids: effect of anions on solubility," *Chemistry of materials,* vol. 18, no. 6, pp. 1546-1551, 2006.

[81]   A. K. Dizaji, H. R. Mortaheb, and B. J. J. o. M. S. Mokhtarani, "Noncovalently functionalized graphene oxide/graphene with imidazolium-based ionic liquids for adsorptive removal of dibenzothiophene from model fuel," vol. 51, no. 22, pp. 10092-10103, 2016.

[82]   R. T. Kachoosangi *et al.*, "Carbon nanotube− ionic liquid composite sensors and biosensors," *Analytical chemistry,* vol. 81, no. 1, pp. 435-442, 2009.

[83]   R. Costa, C. M. Pereira, and A. F. J. E. A. Silva, "Insight on the effect of surface modification by carbon materials on the ionic liquid electric double layer charge storage properties," vol. 176, pp. 880-886, 2015.

[84]   T. Fukushima *et al.*, "Molecular ordering of organic molten salts triggered by single-walled carbon nanotubes," vol. 300, no. 5628, pp. 2072-2074, 2003.

[85]   T. Chatzimitakos and C. Stalikas, "Carbon-based nanomaterials functionalized with ionic liquids for microextraction in sample preparation," *Separations,* vol. 4, no. 2, p. 14, 2017.

[86]   Q. Lyu, H. Yan, L. Li, Z. Chen, H. Yao, and Y. Nie, "Imidazolium ionic liquid modified graphene oxide: as a reinforcing filler and catalyst in epoxy resin," *Polymers,* vol. 9, no. 9, p. 447, 2017.

[87] E. C. Lopes Pereira and B. G. Soares, "Conducting epoxy networks modified with non-covalently functionalized multi-walled carbon nanotube with imidazolium-based ionic liquid," *Journal of Applied Polymer Science,* vol. 133, no. 38, 2016.

[88] M. Qiu *et al.*, "Preparation of anion exchange membrane with enhanced conductivity and alkaline stability by incorporating ionic liquid modified carbon nanotubes," *Journal of Membrane Science,* vol. 573, pp. 1-10, 2019.

[89] H. Le *et al.*, "Selective wetting of carbon nanotubes in rubber compounds–Effect of the ionic liquid as dispersing and coupling agent," *European Polymer Journal,* vol. 75, pp. 13-24, 2016.

[90] R. Pamies, C. Espejo, F. Carrión, A. Morina, A. Neville, and M. J. J. o. R. Bermúdez, "Rheological behavior of multiwalled carbon nanotube-imidazolium tosylate ionic liquid dispersions," vol. 61, no. 2, pp. 279-289, 2017.

[91] C. N. De Castro, S. S. Murshed, M. Lourenço, F. Santos, M. M. Lopes, and J. França, "Enhanced thermal conductivity and specific heat capacity of carbon nanotubes ionanofluids," *International Journal of Thermal Sciences,* vol. 62, pp. 34-39, 2012.

[92] C. Chen *et al.*, "Noncovalent engineering of carbon nanotube surface by imidazolium ionic liquids: A promising strategy for enhancing thermal conductivity of epoxy composites," *Composites Part A: Applied Science and Manufacturing,* vol. 125, p. 105517, 2019.

[93] J. Jung *et al.*, "Ionic-liquid doping of carbon nanotubes with [HMIM][BF4] for flexible thermoelectric generators," *Chemical Engineering Journal,* vol. 438, p. 135526, 2022.

[94] O. Voigt, B. Krause, P. Pötschke, M. T. Müller, and S. Wießner, "Thermoelectric performance of polypropylene/carbon nanotube/ionic liquid composites and its dependence on electron beam irradiation," *Journal of Composites Science,* vol. 6, no. 1, p. 25, 2022.

[95] J. Abraham, P. Xavier, S. Bose, S. C. George, N. Kalarikkal, and S. Thomas, "Investigation into dielectric behaviour and electromagnetic interference shielding effectiveness of conducting styrene butadiene rubber composites containing ionic liquid modified MWCNT," *Polymer,* vol. 112, pp. 102-115, 2017.

[96] A. Ahmad, N. Mansor, H. Mahmood, T. Iqbal, and M. Moniruzzaman, "Effect of ionic liquids on thermomechanical properties of polyetheretherketone-multiwalled carbon

nanotubes nanocomposites," *Journal of Applied Polymer Science,* vol. 139, no. 11, p. 51788, 2022.

[97]   M. R. Zakaria, H. M. Akil, M. H. A. Kudus, F. Ullah, F. Javed, and N. Nosbi, "Hybrid carbon fiber-carbon nanotubes reinforced polymer composites: A review," *Composites Part B: Engineering,* vol. 176, p. 107313, 2019.

[98]   C. Su, X. Wang, L. Ding, and P. Yu, "Enhancement of mechanical behavior of resin matrices and fiber reinforced polymer composites by incorporation of multi-wall carbon nanotubes," *Polymer Testing,* vol. 96, p. 107077, 2021.

[99]   G. Bakis *et al.*, "Mechanical properties of the carbon nanotube modified epoxy–carbon fiber unidirectional prepreg laminates," *Polymers,* vol. 13, no. 5, p. 770, 2021.

[100]   G. Barra *et al.*, "Different methods of dispersing carbon nanotubes in epoxy resin and initial evaluation of the obtained nanocomposite as a matrix of carbon fiber reinforced laminate in terms of vibroacoustic performance and flammability," *Materials,* vol. 12, no. 18, p. 2998, 2019.

[101]   N. Yousefi, S. J. Fisher, C. Burgstaller, M. S. Shaffer, and A. Bismarck, "Hierarchical carbon fibre composites incorporating high loadings of carbon nanotubes," *Composites Science and Technology,* vol. 222, p. 109369, 2022.

[102]   A. Forcellese, M. Simoncini, A. Vita, A. Giovannelli, and L. Leonardi, "Performance analysis of MWCNT/Epoxy composites produced by CRTM," *Journal of Materials Processing Technology,* vol. 286, p. 116839, 2020.

[103]   P. Rahimi, H.-A. Rafiee-Pour, H. Ghourchian, P. Norouzi, M. R. J. B. Ganjali, and Bioelectronics, "Ionic-liquid/NH2-MWCNTs as a highly sensitive nano-composite for catalase direct electrochemistry," vol. 25, no. 6, pp. 1301-1306, 2010.

[104]   A. C. Kleinschmidt *et al.*, "Functionalized-carbon nanotubes with physisorbed ionic liquid as filler for epoxy nanocomposites," *Journal of Nanoscience and Nanotechnology,* vol. 16, no. 9, pp. 9132-9140, 2016.